NASA/TM-20240000755

Space Environmental Exposure of the MISSE 9-15 Polymers and Composites Experiment 1-4 (PCE 1-4)

Kim K. de Groh
Glenn Research Center, Cleveland, Ohio

Bruce A. Banks
Science Applications International Corporation, Cleveland, Ohio

February 2024

NASA STI Program . . . in Profile

Since its founding, NASA has been dedicated to the advancement of aeronautics and space science. The NASA Scientific and Technical Information (STI) Program plays a key part in helping NASA maintain this important role.

The NASA STI Program operates under the auspices of the Agency Chief Information Officer. It collects, organizes, provides for archiving, and disseminates NASA's STI. The NASA STI Program provides access to the NASA Technical Report Server—Registered (NTRS Reg) and NASA Technical Report Server—Public (NTRS) thus providing one of the largest collections of aeronautical and space science STI in the world. Results are published in both non-NASA channels and by NASA in the NASA STI Report Series, which includes the following report types:

- TECHNICAL PUBLICATION. Reports of completed research or a major significant phase of research that present the results of NASA programs and include extensive data or theoretical analysis. Includes compilations of significant scientific and technical data and information deemed to be of continuing reference value. NASA counter-part of peer-reviewed formal professional papers, but has less stringent limitations on manuscript length and extent of graphic presentations.

- TECHNICAL MEMORANDUM. Scientific and technical findings that are preliminary or of specialized interest, e.g., "quick-release" reports, working papers, and bibliographies that contain minimal annotation. Does not contain extensive analysis.

- CONTRACTOR REPORT. Scientific and technical findings by NASA-sponsored contractors and grantees.

- CONFERENCE PUBLICATION. Collected papers from scientific and technical conferences, symposia, seminars, or other meetings sponsored or co-sponsored by NASA.

- SPECIAL PUBLICATION. Scientific, technical, or historical information from NASA programs, projects, and missions, often concerned with subjects having substantial public interest.

- TECHNICAL TRANSLATION. English-language translations of foreign scientific and technical material pertinent to NASA's mission.

For more information about the NASA STI program, see the following:

- Access the NASA STI program home page at http://www.sti.nasa.gov

- E-mail your question to help@sti.nasa.gov

- Fax your question to the NASA STI Information Desk at 757-864-6500

- Telephone the NASA STI Information Desk at 757-864-9658

- Write to:
  NASA STI Program
  Mail Stop 148
  NASA Langley Research Center
  Hampton, VA 23681-2199

NASA/TM-20240000755

Space Environmental Exposure of the MISSE 9-15 Polymers and Composites Experiment 1-4 (PCE 1-4)

Kim K. de Groh
Glenn Research Center, Cleveland, Ohio

Bruce A. Banks
Science Applications International Corporation, Cleveland, Ohio

National Aeronautics and
Space Administration

Glenn Research Center
Cleveland, Ohio 44135

February 2024

Acknowledgments

We are grateful to the NASA Flight Opportunities program, the International Space Station Program Office and Aegis Aerospace for making these flight opportunities possible. We would also like to thank Diane Malarik of NASA Headquarters, along with Craig Robinson and Kelly Bailey of NASA Glenn Research Center for their long-term support of these MISSE-FF experiments. We would also like to thank Dorothy Lukco of HX5, LLC at NASA Glenn for conducting XPS analyses of the M13Z-S1 F AO Photo Monitor flight and control samples. And, Sadeq Malakooti of ORAU at NASA Glenn for his help with Zygo imaging of the M12R-S2 F flight sample. This work is supported by the Biological and Physical Sciences Division.

Level of Review: This material has been technically reviewed by technical management.

This report is available in electronic form at https://www.sti.nasa.gov/ and https://ntrs.nasa.gov/

Contents

Space Environmental Exposure of the MISSE 9-15 Polymers and Composites Experiment 1-4 (PCE 1-4)

Kim K. de Groh
National Aeronautics and Space Administration
Glenn Research Center
Cleveland, Ohio 44135

Bruce A. Banks
Science Applications International Corporation
Cleveland, Ohio 44135

Abstract

Spacecraft in low Earth orbit (LEO) are subjected to harsh environmental conditions, including radiation (cosmic rays, ultraviolet (UV), x-ray and charged particle radiation), micrometeoroids and orbital debris, temperature extremes, thermal cycling, and atomic oxygen (AO). These environmental exposures can result in erosion, embrittlement and optical property degradation of susceptible materials threatening spacecraft performance and durability. To increase our understanding of effects such as AO erosion and radiation induced embrittlement of spacecraft materials, NASA Glenn Research Center has developed a series of experiments that were flown as part of the Materials International Space Station Experiment (MISSE) missions on the exterior of the International Space Station (ISS). These experiments have provided critical space environmental durability data such as AO erosion data of polymers and composites, and radiation induced mechanical property degradation of spacecraft insulation materials, after long term space exposure. Recently, four Glenn experiments with 365 flight samples were flown on ISS's MISSE-Flight Facility (MISSE-FF). These experiments are the Polymers and Composites Experiment-1 (PCE-1) flown as part of the MISSE-9 mission, the PCE-2 flown as part of the MISSE-10 mission, the PCE-3 flown as part of the MISSE-12 and MISSE-15 missions, and the PCE-4 flown as part of the MISSE-13 mission. This paper provides details on the space environment exposure of Glenn's PCE 1-4 flight samples. Passive samples were flown in each flight orientation for post-flight AO fluence determination and on-orbit contamination analyses. Solar exposure estimates were computed by Aegis Aerospace, Inc. The environment exposure details include the total space vacuum duration, time on the MISSE-FF, the direct space exposure duration, the AO fluence and the computed mission Equivalent Sun Hours (ESH) solar exposure. Typical on-orbit temperatures are also provided along with a summary of analyses of PCE 1-4 contamination witness samples. Knowledge of the space environmental exposure of the PCE 1-4 flight samples is crucial for flight data interpretation.

1.0 Introduction

Materials used on the exterior of spacecraft are subjected to many environmental threats that can cause degradation. In low Earth orbit (LEO) these threats include visible light photon radiation, ultraviolet (UV) radiation, vacuum ultraviolet (VUV) radiation, x-rays, solar wind particle radiation (electrons, protons), cosmic rays, temperature extremes, thermal cycling, impacts from micrometeoroids and orbital debris (MMOD), on-orbit contamination, and atomic oxygen (AO). These environmental exposures can result in erosion, embrittlement and optical property degradation of susceptible materials threatening spacecraft performance and durability.

The flight orientation highly affects the environmental exposure. Ram facing surfaces (facing the direction of travel) receive a high flux of directed AO (ram AO) and sweeping (moderate) solar exposure. Zenith facing surfaces (direction facing away from Earth) receive a low flux of grazing arrival AO and the highest solar exposure. Wake facing surfaces (facing away from the direction of travel) receive essentially no AO flux and moderate solar radiation (levels similar to ram experiments). Finally, nadir facing surfaces (direction facing towards Earth) receive a low flux of grazing arrival AO and minimal solar radiation (albedo sunlight). All surfaces receive charged particle and cosmic radiation, which are omnidirectional. Figure 1 provides a diagram of the ram, wake, zenith and nadir flight orientations on the International Space Station (ISS).

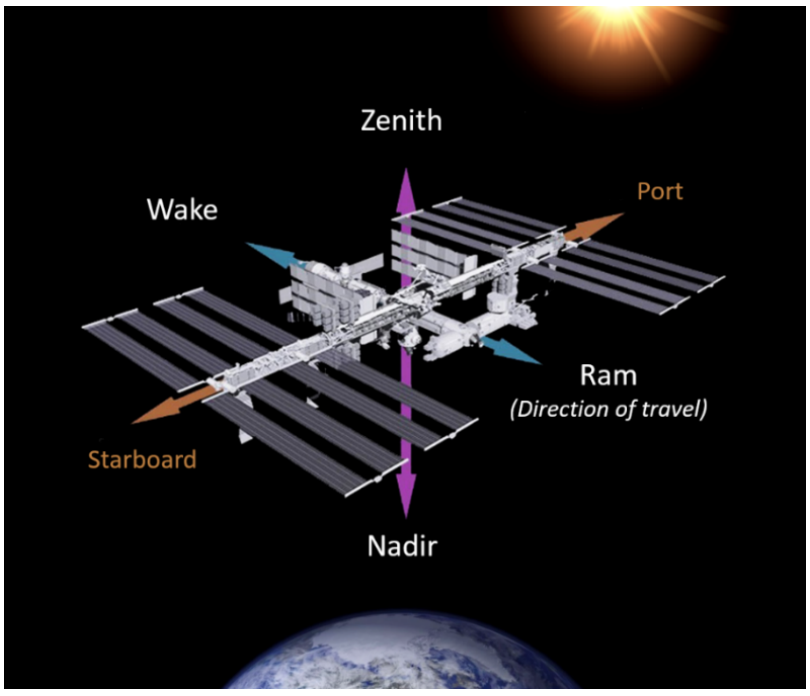

Figure 1. Diagram showing ram, wake, zenith, and nadir directions on the International Space Station.

Atomic oxygen is a particularly serious structural, thermal, and optical threat, especially to exterior oxidizable spacecraft components. Atomic oxygen is formed in the LEO environment through photodissociation of diatomic oxygen (O_2). Short-wavelength (< 243 nm) solar radiation has sufficient energy to break the 5.12-eV O_2 diatomic bond in an environment where the mean free path is sufficiently long (~10^8 m) so that the probability of re-association, or the formation of ozone (O_3), is small.[1,2] In LEO, between the altitudes of 180 and 650 km, AO is the most abundant species.[3]

A number of processes can take place when an oxygen atom strikes a spacecraft surface as a result of its orbital velocity and the thermal velocity of the atoms. These include chemical reaction with surface molecules, elastic scattering, scattering with partial or full thermal accommodation, and recombination or excitation of ram species, which consists predominantly of ground-state O(^{3}P) atomic oxygen atoms.[4] Atomic oxygen can react with polymers, carbon, and many metals to form oxygen bonds with atoms on the exposed surface. For most polymers, hydrogen abstraction, oxygen addition, or oxygen insertion can occur, with the oxygen interaction pathways eventually leading to volatile oxidation products.[5,6] This results in gradual erosion of hydrocarbon or halocarbon material, with the exception of silicone materials, which form a glassy silicate surface layer with AO exposure. Figure 2 shows AO erosion of Teflon™ fluorinated ethylene propylene (FEP) around a small protective particle after 5.8 years of space exposure on the Long Duration Exposure Facility (LDEF). An example of the complete loss of a Kapton® H thermal blanket insulation layer on the LDEF and degradation of other polymeric materials caused by AO erosion in LEO are provided in Figure 3.[2,7] AO scattering can cause oxidation of sensitive components not normally in direct line-of-site with LEO AO, such as within a telescope body. And, AO undercutting erosion at protective coating defect sites can also be a serious durability concern.

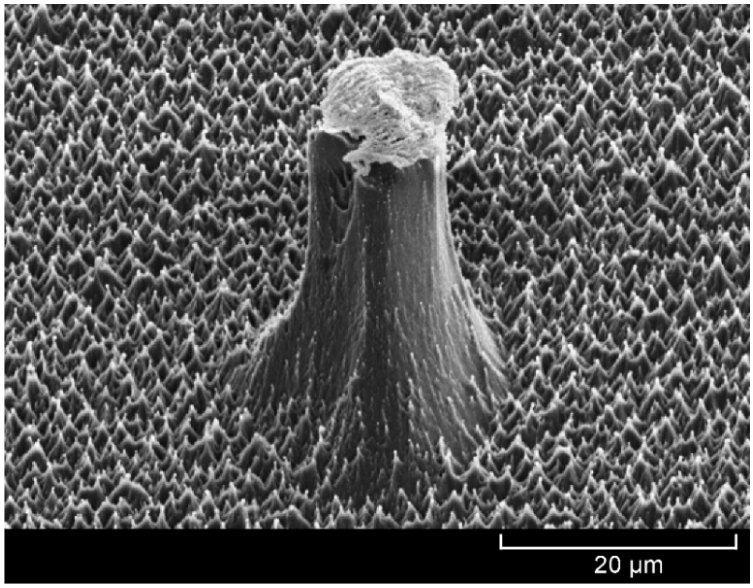

Figure 2. Atomic oxygen erosion of Teflon FEP after 5.8 years of space exposure.[2]

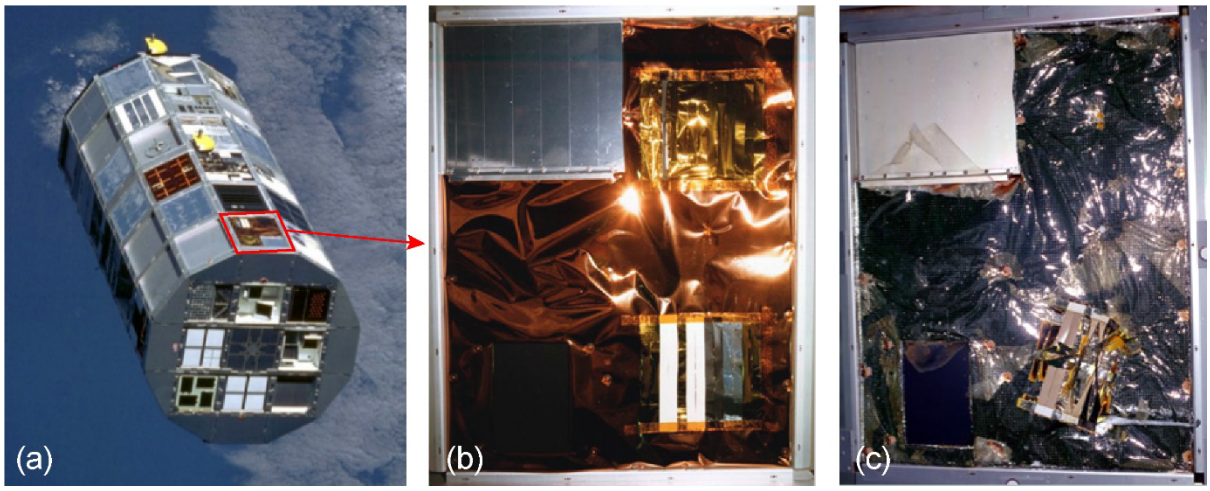

Figure 3. Atomic oxygen erosion of a Kapton insulation blanket from LDEF experiment Tray F-9, located on the leading edge and exposed to direct-ram AO for 5.8 years. (a) LDEF, (b) Tray F-9 pre-flight, and (c) Tray F-9 post-flight.[2,7]

In order to design durable high-performance spacecraft systems it is essential to understand the AO erosion yield (E_y) of materials being considered for spacecraft applications along with AO scattering characteristics. The E_y is the volume loss per incident oxygen atom (cm^3/atom). Materials spaceflight experiments for LEO E_y determination have been flown on the Shuttle, LDEF, the Russian space station Mir and other spacecraft. More recently, they have been flown as part of the Materials International Space Station Experiment (MISSE) missions on the exterior of the ISS.[8]

Another LEO threat to spacecraft materials is solar UV radiation. Air mass zero integrated solar irradiance in various wavelength ranges are provided in ASTM E490 and show that wavelengths shorter than approximately 120 nm represent a negligible portion of the solar spectrum.[9] Relevant to the study of space environment effects on materials, the UV range of wavelengths (100 to 400 nm) can be conveniently divided into two bands: Vacuum UV (VUV) as the 100 to 200 nm range and Near UV (NUV) as the 200 to 400 nm range.[6] Ultraviolet radiation is energetic enough to cause the breaking of organic bonds such as C=C, C=O, and C–H as well as bonds in other functional groups.[5] A molecule is raised to an excited state when an organic molecule absorbs a photon of UV radiation, and bond dissociation can occur if the molecule acquires enough energy at the excited state. Depending on the temperature and physical properties of the materials, the dissociated radical species are reactive intermediates, with the capability of diffusing several atomic distances from their point of origin and can participate in further reactions.[5] Solar radiation often results in bond breakage in materials as well as threats to functionality and stability of the materials. Therefore, solar radiation can impact the erosion of some materials along with AO.

Glass and ceramic materials have been observed to undergo UV radiation-induced darkening, also referred to as solarization.[6] UV-light interactions in glass and ceramic materials can cause formation of electrons or holes that are trapped in various defects. Some of these trapped species absorb light in specific wavelength ranges and are referred to as color centers.[6] Ultraviolet radiation darkening can be affected by purity of the material, particle shape and size, surface chemistry, and thermal history. Ultraviolet darkening can be detrimental to spacecraft materials such as white-paint coatings and solar-cell cover glass.[6] Examples of UV darkening of two types of polymers flown during the MISSE-7 mission in the zenith direction are provided in Figure 4.[10]

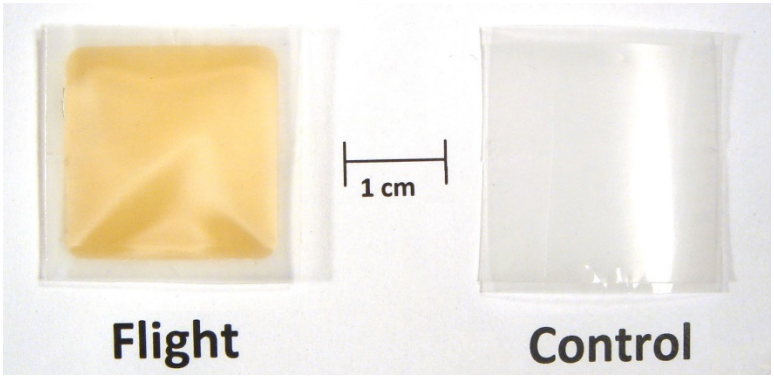

a.

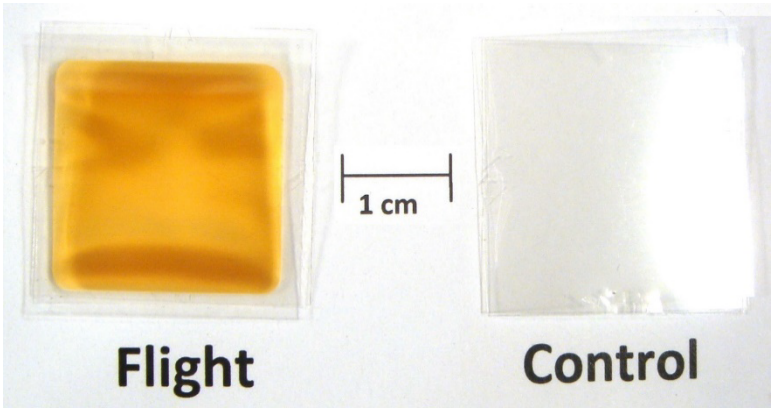

b.

Figure 4. Examples of UV darkening of polymers flown in the zenith direction as part of the MISSE-7A Zenith Polymers Experiment. (a) MISSE-7 Z-5 Polyvinylidene fluoride (PVDF, Kynar), and (b) MISSE-7 Z-6 Ethylene-chlorotrifluoroethylene (ECTFE, Halar).[10]

Space radiation, including solar UV, solar flare x-ray, and charged particle radiation, can also cause serious polymer embrittlement of spacecraft materials. For example, the metallized Teflon FEP multilayer insulation (MLI) blanket outer layer on the Hubble Space Telescope (HST) has become extremely embrittled in the space environment resulting in severe on-orbit through-thickness cracking. This became evident during the second servicing mission (SM2) after 6.8 years of space exposure where cracking of the 5 mil (127 μm) thick Al-FEP outer layer of the HST MLI blankets was observed on the light shield, forward shell and equipment bays.[11,12] Figure 5 shows large cracks in the outer layer of the solar facing Light Shield multilayer insulation (MLI) on the HST as observed during SM2 after 6.8 years of space exposure. By the time of the 5th servicing mission (SM4), there were hundreds of cracks in the Al-FEP outer layer of the HST MLI blankets. Figure 6 shows extensive crack of the MLI outer layer as observed during SM4 after 19 years of space exposure. MLI blanket sections were retrieved during the SM4 mission and the Al-FEP outer layer from Bay 8 was found to fracture like thin brittle glass.[13]

Figure 5. Large cracks in the outer layer of solar facing multilayer insulation (MLI) on the HST as observed during SM2 after 6.8 years of space exposure.[12]

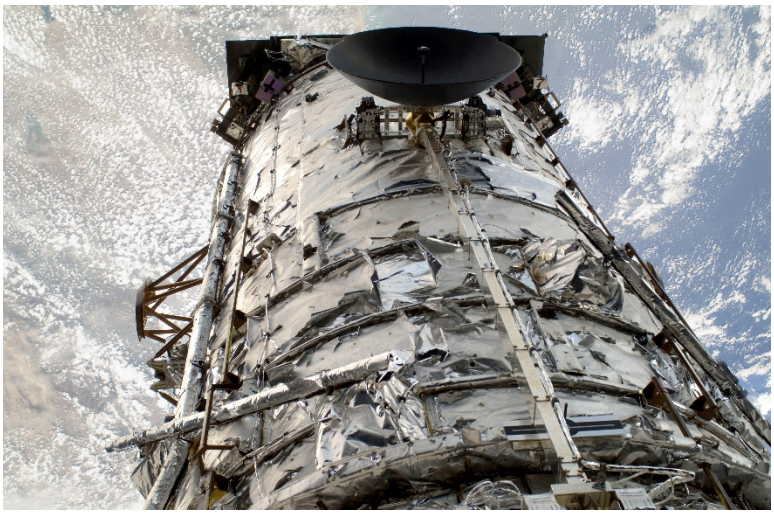

a.

b.

Figure 6. Severe cracking of the HST aluminized-Teflon outer layer of MLI after 19 years of space exposure. (a) Light Shield section with Earth in the back-ground,[14] and (b) Close-up image of the Light Shield MLI cracking.

Since 2001, NASA Glenn Research Center has flown a series of space exposure experiments as part of the Materials International Space Station Experiment (MISSE) missions on the exterior of the International Space Station (ISS).[15,16] Although Glenn's 44 MISSE experiments have numerous objectives, many of the experiments were flown to increase our understanding of AO erosion and radiation induced embrittlement of spacecraft materials.[15-20] The MISSE 1-8 missions were flown on the Shuttle (2001 to 2013). In the post-Shuttle era, the MISSE experiments (MISSE-9+) are launched on SpaceX Dragon or Northrop Grumman (NG) Cygnus spacecraft and robotically installed on ISS's external MISSE-Flight Facility (MISSE-FF).[21]

Four Glenn experiments with 365 flight samples were flown on ISS's MISSE-Flight Facility (MISSE-FF). These experiments are the 138 sample Polymers and Composites Experiment-1 (PCE-1) flown as part of the MISSE-9 mission, the 43 sample PCE-2 flown as part of the MISSE-10 mission, the 86 sample PCE-3 flown as part of the MISSE-12 and MISSE-15 missions, and the 98 sample PCE-4 flown as part of the MISSE-13 mission.[21] This paper provides details on the space environment exposure for the PCE 1-4 flight samples. The environment exposure details include the total space vacuum duration, the time on the MISSE-FF, the direct space exposure duration, the atomic oxygen fluence, and the calculated mission Equivalent Sun Hours (ESH) solar exposure. Also included are a summary of XPS analyses for contamination witness samples flown in each flight orientation for each experiment. The space environmental exposure details for the PCE 1-4 flight samples are necessary for flight data interpretation.

2.0 Atomic Oxygen Fluence

2.1 Atomic Oxygen Fluence Computation

The AO fluence (F) of a spaceflight mission is often determined based on the erosion of a passive Kapton H witness sample because Kapton H has a well characterized erosion yield, E_y (3.0×10^{-24} cm^3/atom) in the LEO environment (see the *Erosion Yield of Kapton in LEO* section below). The AO fluence is typically determined from mass loss of the Kapton H sample, but recession depth measurements can also be used.[22]

The mass loss based AO fluence can be calculated using the following equation:

$$F = \frac{\Delta M_K}{A_K \rho_K E_y} \tag{1}$$

where

F = *low Earth orbit AO fluence (atoms/cm^2)*
ΔM_K = *mass loss of Kapton H witness sample (g)*
A_K = *surface area of Kapton H witness sample exposed to AO (cm^2)*
ρ_K = *density of Kapton H witness sample (1.4273 g/cm^3)*[2,17]
E_y = *erosion yield of Kapton H witness sample (3.0×10^{-24} cm^3/atom)*[23-28]

It is important to calculate the AO fluence using dehydrated mass measurements before and after flight because Kapton is very hygroscopic and can fluctuate in mass with humidity and temperature.[29]

The recession depth based AO fluence can be calculated using the following equation:

$$F = \frac{T}{E_y} \tag{2}$$

where

F = *low Earth orbit AO fluence (atoms/cm^2)*
T = *thickness (cm)*
E_y = *erosion yield (cm^3/atom)*

2.2 Erosion Yield of Kapton H in LEO

The sensitivity of a hydrocarbon material to reaction with AO is quantified by the AO erosion yield (E_y) of the material. The AO E_y is the volume of a material that is removed (through oxidation) per incident oxygen atom and is measured in units of cm^3/atom. The AO E_y has been referred to as the recession rate, AO Reactivity and AO Reaction Efficiency (R_e) but the units of erosion (cm^3/atom) are the same.

As stated above, Kapton H has a well characterized E_y (3.0×10^{-24} cm^3/atom) in the LEO environment. The STS-8 Shuttle mission, flown in 1983 at 225 km, provided some of the first carefully characterized E_y values. Banks and Visentine both reported Kapton E_y values of 3.0×10^{-24} cm^3/atom from their STS-8 experiments.[23,24] Koontz determined the E_y of Kapton to be $3.05 \pm 0.1 \times 10^{-24}$ cm^3/atom based on the weight loss (and $3.16 \pm 0.1 \times 10^{-24}$ cm^3/atom based on profilometry) in his Evaluation of Oxygen Interaction with Materials-III (EOIM-III) experiment, which was flown on STS-46 in 1992 at an altitude of 230 km.[25]

The LDEF also provided important additional sources of Kapton LEO E_y data. The LDEF was deployed in April 1984 at 476 km and retrieved in January 1990 at 330 km.[30] Gregory reports the Kapton E_y from his leading edge (Row 9) A0114 experiment to be $2.89 \pm 0.06 \times 10^{-24}$ cm^3/atom.[26] LDEF received 75% of the total AO fluence within the last year of the mission, and the altitude for the last year ranged from ~449 to 334 km.[30] So, one could state that Gregory's 2.89×10^{-24} cm^3/atom was determined from a flight in the ~449 to 334 km range (the average (391 nm) is similar to ISS's altitude). LDEF experiment A0134, flown on the leading edge of LDEF, exposed its samples for the 1st 10 months of the LDEF mission in the Experiment Exposure Control Canister (EECC), when it was at the higher altitudes (481 to 470 km). The Kapton E_y for this experiment was determined to be 2.9×10^{-24} cm^3/atom.[27,28]

Silverman summarizes Kapton H E_y values from STS-5 (2.8×10^{-24} cm^3/atom) and STS-8 (3.0×10^{-24} cm^3/atom), and Kapton from LDEF A0134 (2.9×10^{-24} cm^3/atom) and LDEF A0114 ($2.89 \pm 0.06 \times 10^{-24}$ cm^3/atom) in his contract report "Space Environmental Effects on Spacecraft: LEO Materials Selection Guide."[28] He states that the Kapton E_y of 3.0×10^{-24} cm^3/atom should be used for spacecraft design considerations.

The neutral gas environment in LEO depends greatly on the altitude and solar activity.[31] It is worth noting that some researchers believe the E_y of Kapton may increase with decreasing altitude, particularly in very low Earth orbit (VLEO) where the ratio of N_2 to AO is significantly greater than in the higher altitude LEO. Although that may be true, the flight experiments mentioned above reported Kapton E_y values of 2.9 to 3.1 × 10^{-24} cm^3/atom for flight missions in the ~225 to 480 km altitude range. The altitude for ISS, and hence the MISSE PCE 1-4 experiments, is ~400 km.

3.0 Polymers and Composites Experiment 1-4 (PCE 1-4)

3.1 MISSE-9 Polymers and Composites Experiment-1 (PCE-1)

The Polymers and Composites Experiment-1 (PCE-1) was flown as part of the MISSE-9 inaugural mission of MISSE-FF. The MISSE-9 PCE-1 is a passive experiment with 138 samples that were flown in ram (39 samples), wake (52 samples) and zenith (47 samples) orientations. The primary objective of the PCE-1 is to determine the LEO AO E_y of spacecraft polymers, composites, and coated samples as a function of solar irradiation and AO fluence. Samples were also included to determine the mission AO fluence and on-orbit molecular contamination in the MISSE-9 ram, wake and zenith orientations. In addition, thin film polymer tensile samples were flown in the wake and zenith directions for studying space radiation induced embrittlement. A complete list of the PCE-1 samples is provided by de Groh in Reference 21 along with additional experiment objectives and pre-flight photos of select PCE-1 experiment samples.

Kapton H (E. I. du Pont de Nemours and Company) was used for the AO fluence witness samples for the PCE-1, and also for the PCE 2-4 experiments. Numerous PCE 1-4 materials, such as Kapton® HN, Teflon fluorinated ethylene propylene (FEP), polytetrafluoroethylene (PTFE), white Tedlar® (crystalline polyvinyl fluoride with white pigment), polyethylene (PE), Upilex-S®, and other polymers were also flown as part of Glenn's MISSE 2-8 experiments. The manufacturing information for these materials are provided in Reference 16.

Figure 7 shows a pre-flight photograph of the MISSE-9 PCE-1 samples loaded into the MISSE Sample Carrier (MSC) ram, wake and zenith flight mount-side (MS) decks. Each deck includes samples from two experiments, the PCE-1 and NASA Langley Research Center's Polymeric Materials Experiment. Figure 8 shows pre-flight photographs of the MISSE-9 decks with the PCE-1 samples outlined in red. Aluminum blocks with "RBF" ("remove before flight") written on them shown in the pre-flight photos were removed before flight. In addition, the blank tensile holder "bars" shown in Figures 7 and 8 were replaced with bars that include sample numbers prior to flight, so that the tensile sample ID could be seen in the on-orbit images. Figure 9 shows photographs of the zenith (Figure 9a) and wake (Figure 9b) tensile samples mounted on the decks with the tensile ID bars.

Figure 7. Pre-flight photograph of the MISSE-9 PCE-1 samples loaded into the MSC MS flight decks, from left to right: R2 MSC 3 (ram), W3 MSC 8 (wake), and Z3 MSC 5 (zenith).

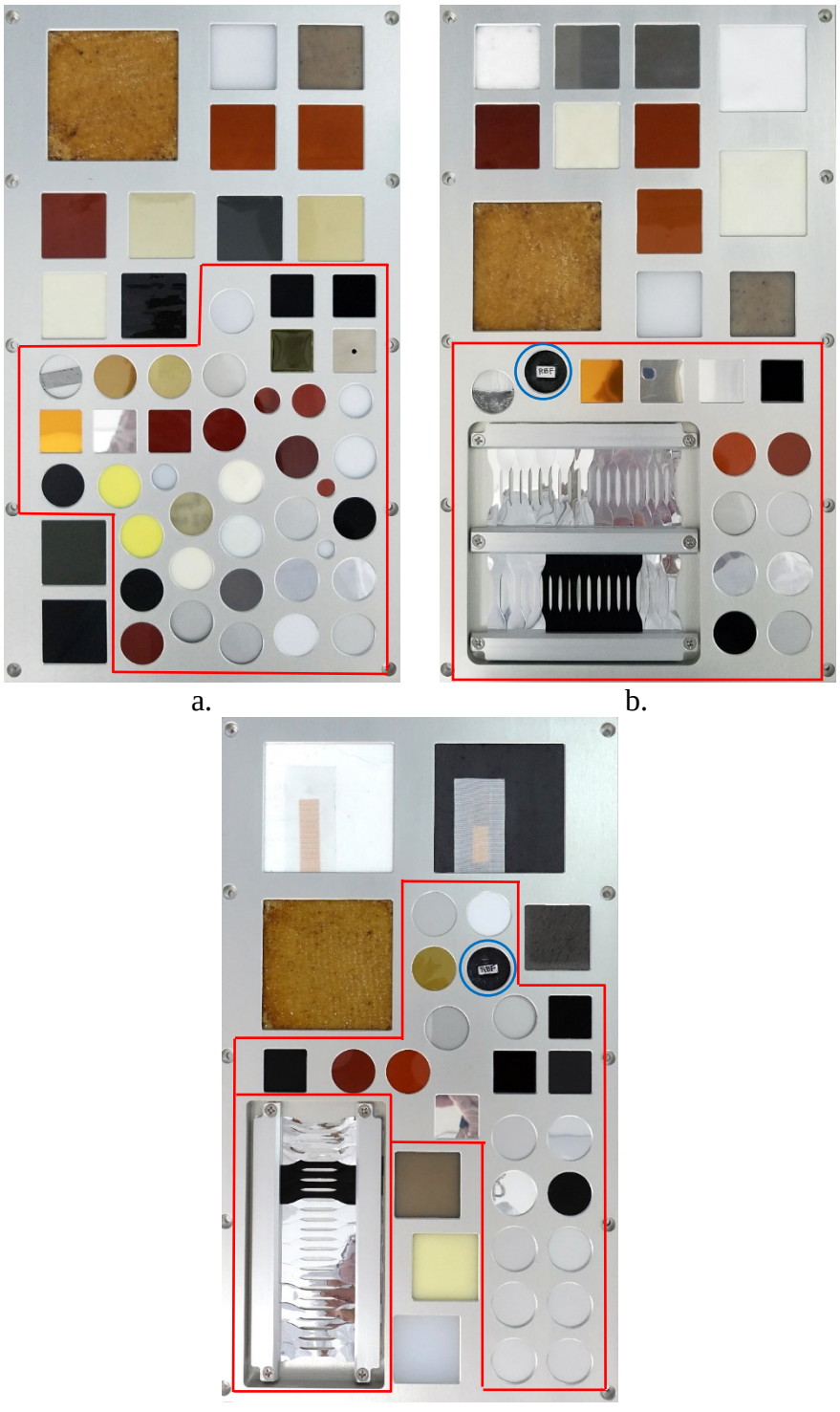

Figure 8. Pre-flight photographs of the MISSE-9 MSC decks with the PCE-1 samples outlined in red. (a). Ram samples in the R2 MSC 3 MS deck, (b) Wake samples in the W3 MSC 8 MS deck (the sample with the “RBF” block is circled in blue), and (c) Zenith samples in the Z3 MSC 5 MS deck (the sample with the “RBF” block is circled in blue).

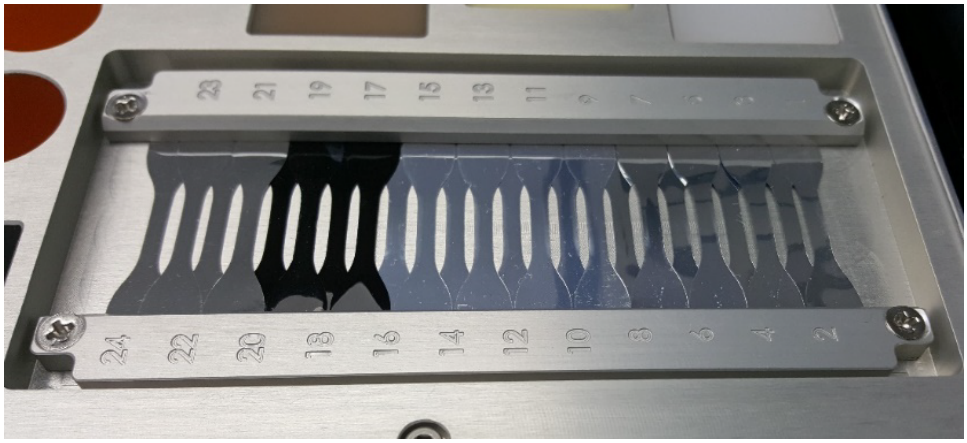

a.

b.

Figure 9. Pre-flight photographs of the MISSE-9 tensile samples. (a) Zenith samples with ID#s 1-24, and (b) Wake samples with ID#s 1-38.(Photo credit: Aegis Aerospace).

3.2 MISSE-10 Polymers and Composites Experiment-2 (PCE-2)

The MISSE-10 PCE-2 is a passive experiment with 43 samples that were flown in ram (21 samples), zenith (10 samples), and nadir (12 samples) directions. The objectives of the PCE-2 are similar to the PCE-1. The primary objective is to determine the LEO AO E_y of polymers, composites, and coated samples as a function of solar irradiation and AO fluence. Also like the PCE-1, samples were flown to determine the AO fluence for the mission and characterize molecular contamination in each flight direction. A complete list of the PCE-2 samples is provided in Reference 21 along with additional experiment objectives and pre-flight photos of select PCE-2 experiment samples.

One of the unique samples flown as part of the PCE-2 is the Photographic AO Fluence Monitor (M10R-R1, also called AO Photo Monitor). This sample has nine stepped layers of 0.3 mil thick Kapton over a white Tedlar substrate that is half coated with a very thin layer of carbon. A similar but smaller (1-inch square) Photographic AO Fluence Monitor (M19N-S1) with three layers of 0.3 mil Kapton was flown in the nadir direction (M10N-S1). The Photographic AO Fluence Monitors were designed to provide incremental AO fluence over time based on on-orbit images. Details on these samples are provided in the *Photographic AO Fluence Monitors* section below.

A pre-flight photograph of the PCE-2 samples loaded into the ram (R1 MSC 11), zenith (Z2 MSC 10), and nadir (N3 MSC 13) MS decks is shown in Figure 10. Figure 11 shows close-up pre-flight photographs of the PCE-2 samples in the ram, zenith and nadir decks.

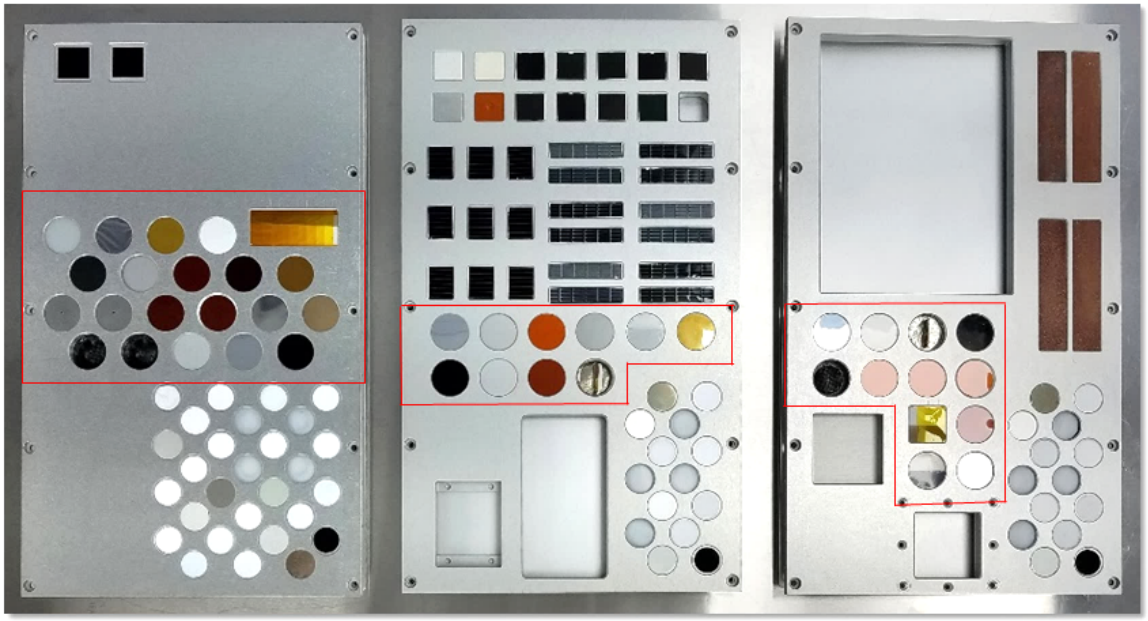

Figure 10. Pre-flight photograph of the MISSE-10 PCE-2 samples loaded into the MSC MS flight decks, from left to right: R1 MSC 11 (ram), Z2 MSC 10 (zenith), and N3 MSC 13 (wake). The PCE-2 samples are shown outlined in red.

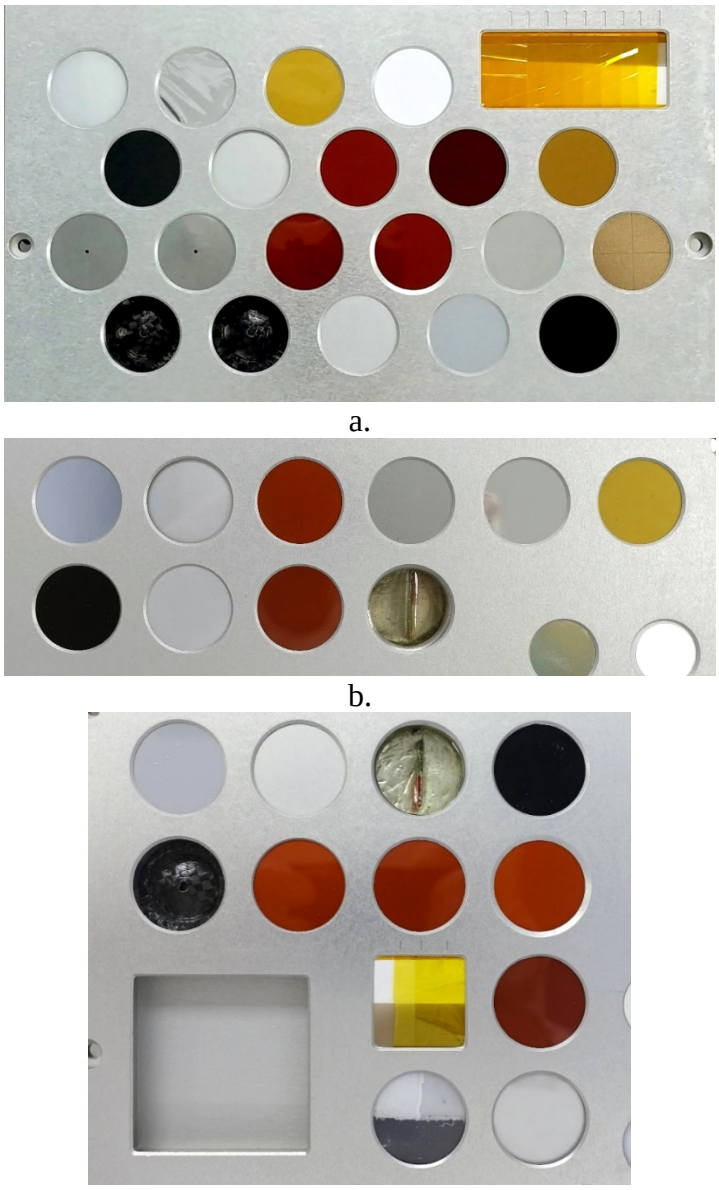

Figure 11. Pre-flight close-up photographs of the MISSE-10 PCE-2 samples. (a) ram samples, (b) zenith samples, and (c) nadir samples.

3.3 MISSE-12 and MISSE-15 Polymers and Composites Experiment-3 (PCE-3)

The PCE-3 is a passive experiment with 86 samples that was flown in ram (30 samples), wake (42 samples) and zenith (14 samples) directions as part of the MISSE-12 mission. The primary objective is to determine the LEO AO E_y of polymers, composites, and coated samples as a function of solar irradiation and AO fluence. Like the PCE 1-2, samples in the PCE-3 were included to determine the AO fluence for the mission and characterize any molecular contamination in each flight direction. The objectives of the PCE-3 are similar to the PCE-1 and PCE-2. A complete list of the PCE-3 samples is provided in Reference 21 along with additional experiment objectives and pre-flight photos of select PCE-3 experiment samples.

Photographic AO Fluence Monitors were also flown as part of the PCE-3 so that the AO fluence could be determined in a step-wise manner over the mission duration using on-orbit images. For the PCE-3, four Photographic AO Fluence Monitors were flown. Two in the ram direction (M12R-S1 and M12R-S2), one in the wake direction (M12W-S11) and one in the zenith direction (M12Z-S1). Details on the PCE-3 Photographic AO Fluence Monitors are provided in the *Photographic AO Fluence Monitors* section.

A pre-flight photograph of the PCE-3 samples loaded into the ram (R2 MSC 4 SS), zenith (Z1 MSC 18 MS), and wake (W3 MSC 6 MS) decks is shown in Figure 12. Figure 13 provides close-up photographs of the PCE-3 samples in the MSC decks. It should be noted that six wake samples and four zenith samples were moved to different MSC locations after the photographs in Figure 12 and Figure 13 were taken during sample integration. These 10 samples have two red boxes around them in Figure 12. The final flight positions are provided in the zenith and wake deck photos in Figure 14, with two red boxes around the samples in their new positions. The large yellow sample in Z1 MSC 18 MS shown in Figures 12 to 14 is not part of the PCE-3.

As discussed later, the MISSE-12 wake samples were not exposed to the space environment during the MISSE-12 mission. Thus, the 42 wake samples were re-flown (in the same sample holders) during the MISSE-15 mission in the wake direction. A pre-flight photograph of the PCE-3 wake samples in the MISSE-15 MSC deck is provided in Figure 14c.

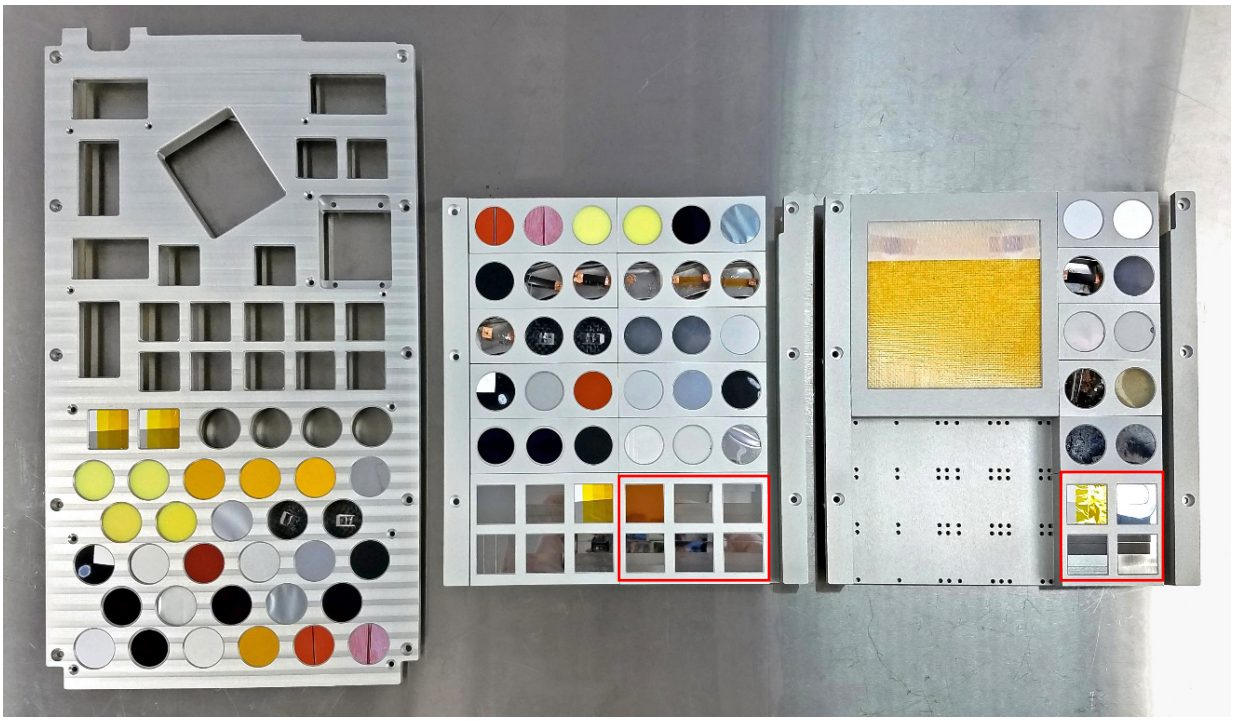

Figure 12. Pre-flight photograph of the MISSE-12 PCE-3 samples loaded into the MSC flight decks, from left to right: R2 MSC 4 SS (ram), W3 MSC 6 MS (wake), and Z1 MSC 18 MS (zenith). Samples in red boxes were moved to a different location on the deck prior to flight.

a.

b.

c.

Figure 13. Close-up photographs of the MISSE-12 PCE-3 samples loaded into the MSC flight decks, (a) R2 MSC 4 SS (ram), (b) W3 MSC 6 MS (wake), and (c) Z1 MSC 18 MS (zenith). The large yellow sample in Z1 MSC 18 MS is not part of the PCE-3.

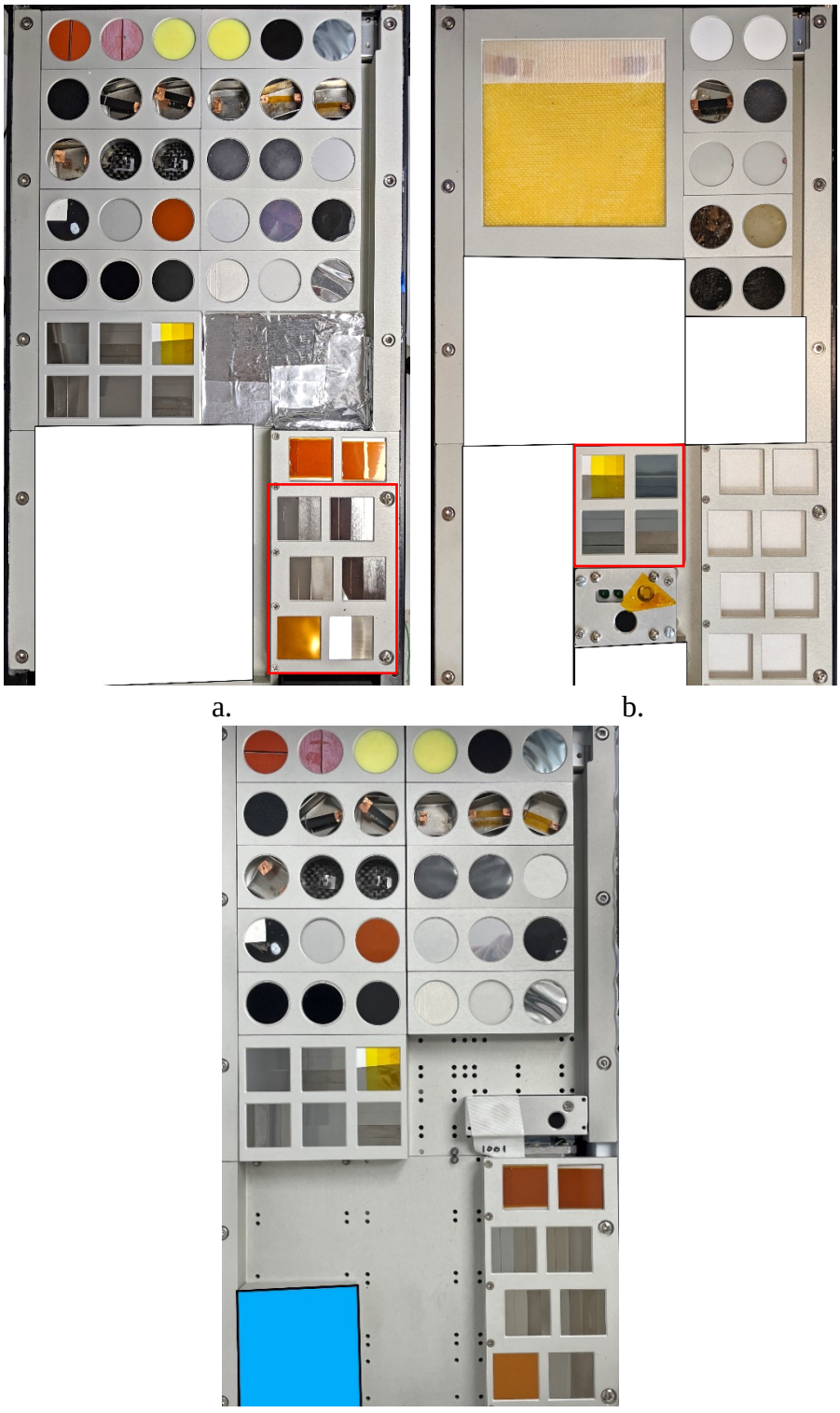

a. b. c.

Figure 14. Final pre-flight deck configurations of the MISSE-12 wake and zenith and MISSE-15 wake MSC flight decks. (a) MISSE-12 W3 MSC 6 MS (wake), (b) MISSE-12 Z1 MSC 18 MS (zenith), and (c) MISSE-15 W1 MSC 10 MS (wake). The moved samples are in the red-box areas in a and b. (Photo credit: Aegis Aerospace)

3.4 MISSE-13 Polymers and Composites Experiment-4 (PCE-4)

The MISSE-13 PCE-4 is a passive experiment with 98 samples that was flown in the wake (65 samples) and zenith (33 samples) directions. The primary objectives of the PCE-4 are to determine optical and mechanical property degradation of spacecraft materials, and to assess the functionality of shape memory alloys, shape memory polymer composites, melanin based composites and elastomer seal samples after radiation exposure in LEO. Like the PCE 1-3, samples in the PCE-4 were included to determine the AO fluence in each mission orientation. Teflon FEP samples were used for contamination studies. A complete list of the PCE-4 samples is provided in Reference 21 along with additional experiment objectives and pre-flight photos of select PCE-4 experiment samples.

Photographic AO Fluence Monitors were also flown as part of the PCE-4 in the wake (M13W-S1) and zenith (M13W-S2) directions flight samples. Because very little AO is expected in these directions, a modified design was used for the PCE-4 experiment. Details on the PCE-3 Photographic AO Fluence Monitors are provided in the *Photographic AO Fluence Monitors* section below.

A pre-flight photograph of the PCE-4 samples loaded into the zenith (Z2 MSC 19 MS), wake mount side (W1 MSC 5 MS) and wake swing side (W1 MSC 5 SS) decks is shown in Figure 15. The PCE-4 samples in the wake MS deck are outlined in red. The larger white and metallized square samples in MSC 5 MS are not part of the PCE-4. Figure 16 provides close-up photographs of the PCE-4 samples.

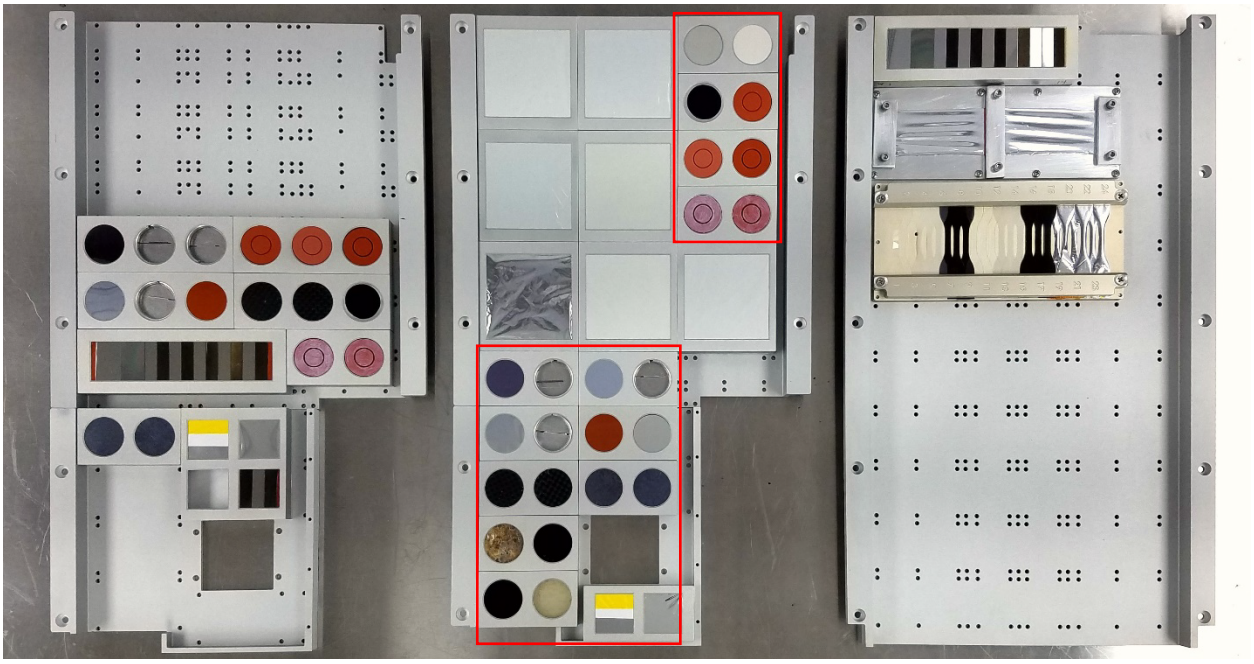

Figure 15. Pre-flight photograph of the MISSE-13 PCE-4 samples loaded into the MSC flight decks, from left to right: Z2 MSC 19 MS (zenith), W1 MSC 5 MS (wake) and W1 MSC 5 SS (wake). The PCE-4 samples in the wake MS deck are outlined in red.

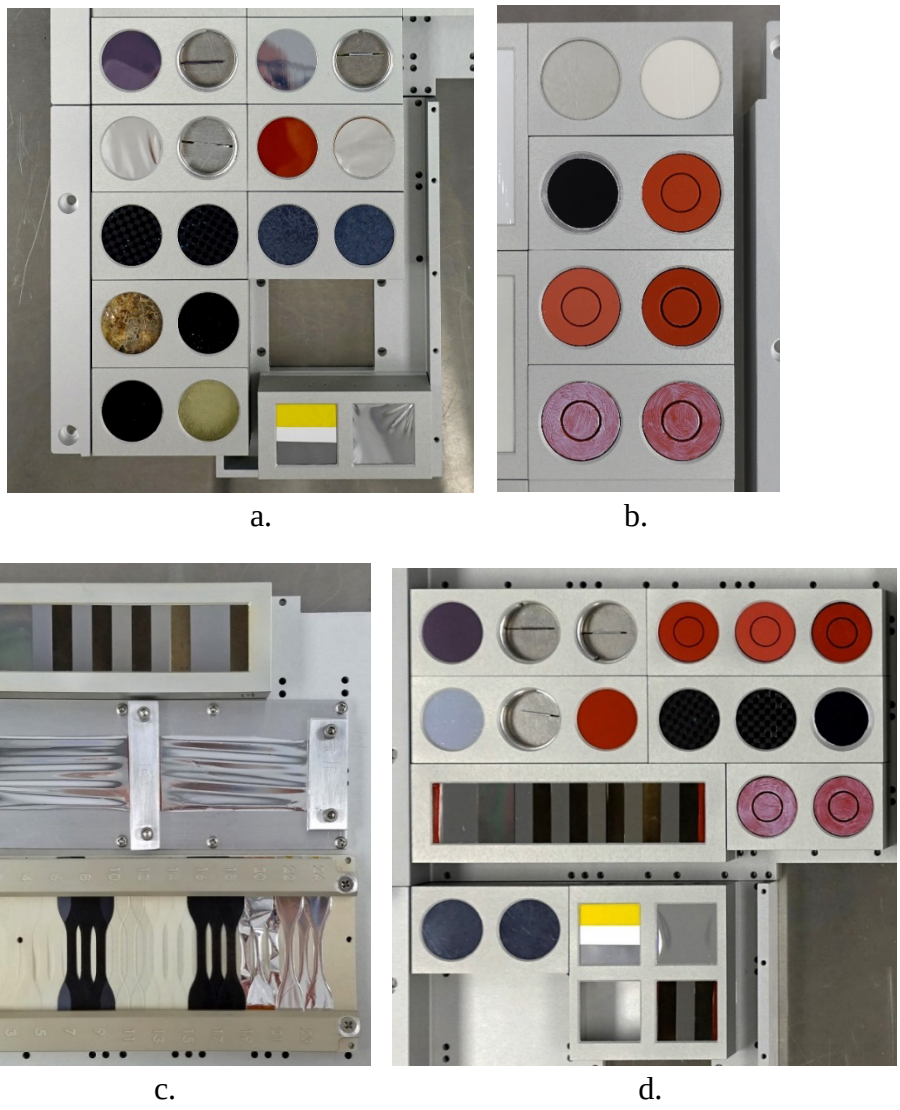

Figure 16. Close-up photographs of the MISSE-13 PCE-4 samples loaded into the MSC flight decks. (a) Lower section of samples in W1 MSC 5 MS (wake), (b) Upper section of samples in W1 MSC 5 MS (wake), (c). Samples in W1 MSC 5 SS (wake), and (d) Samples in Z2 MSC 19 MS (zenith).

4.0 PCE 1-4 AO Fluence Witness Samples

Two types of passive samples were flown as part of the PCE 1-4 experiments for AO fluence determination: 1) Kapton H samples, and 2) Photographic AO Fluence Monitors (also called AO Photo Monitors). The Kapton H AO fluence witness samples were in flown in most mission flight orientations for mass loss based fluence computation. These 12 samples are described in the *Kapton H AO Fluence Witness Samples* section below. Photographic AO Fluence Monitors were flown as part of the MISSE-10 PCE-2, MISSE-12 PCE-3 and MISSE-13 PCE-4 experiments. As stated previously, these unique samples were designed to determine incremental AO fluence versus mission time based on on-orbit images. These eight samples are described in the *Photographic AO*

Fluence Monitors section below. In addition, a simple thin carbon coated white Tedlar sample (M10Z-C2 F) was flown as part of the MISSE-10 PCE-2 experiment in the zenith direction for visual AO fluence determination. Table 1 provides a list of all 21 PCE 1-4 AO fluence witness samples.

Table 1. PCE 1-4 AO Fluence Witness Samples

MISSE-FF Mission	Flight Orientation	MISSE-FF MSC	Sample ID	Material
MISSE-9	Ram	R2 (MSC 3) MS	M9R-C1 F	Kapton H
	Ram	R2 (MSC 3) MS	M9R-C19 F	Kapton H
	Wake	W3 (MSC 8) MS	M9W-C1 F	Kapton H
	Zenith	Z3 (MSC 5) MS	M9Z-C1 F	Kapton H
MISSE-10	Ram	R1 (MSC 11) MS	M10R-C1 F	Kapton H
	Ram	R1 (MSC 11) MS	M10R-R1 F	AO Photo Monitor (0.3 mil Kapton H (9 layers))
	Zenith	Z2 (MSC 10) MS	M10Z-C1 F	Kapton H
	Zenith	Z2 (MSC 10) MS	M10Z-C2 F	Carbon (720 Å) coated White Tedlar
	Nadir	N3 (MSC 13) MS	M10N-C1 F	Kapton H
	Nadir	N3 (MSC 13) MS	M10N-S1 F	AO Photo Monitor (~0.1 mil Kapton H (3 layers))
MISSE-12	Ram	R2 (MSC 4) SS	M12R-C1 F	Kapton H
	Ram	R2 (MSC 4) SS	M12R-S1 F	AO Photo Monitor 1 (0.3 mil Kapton H (3 layers))
	Ram	R2 (MSC 4) SS	M12R-S2 F	AO Photo Monitor 2 (0.5 mil Kapton H (3 layers))
	Wake	W3 (MSC 6) MS	M12W-C1 F	Kapton H
	Zenith	Z1 (MSC 18) MS	M12Z-S1 F	AO Photo Monitor (0.3 mil Kapton H (3 layers))
MISSE-13	Wake	W1 (MSC 5) MS/SS	M13W-C1 F	Kapton H
	Wake	W1 (MSC 5) MS/SS	M13W-S1 F	AO Photo Monitor (0.3 mil Kapton H (1 layer))
	Zenith	Z2 (MSC 19) MS	M13Z-C1 F	Kapton H
	Zenith	Z2 (MSC 19) MS	M13Z-S1 F	AO Photo Monitor (0.3 mil Kapton H (1 layer))
MISSE-12/ MISSE-15	Wake	W1 (MSC 10) MS	M12W-C1 F	Kapton H
	Wake	W1 (MSC 10) MS	M12W-S11 F	AO Photo Monitor (0.3 mil Kapton H (3 layers))

MS: Mount side deck; SS: Swing side deck

4.1 Kapton H AO Fluence Witness Samples

Kapton H AO fluence samples for mass loss based fluence computation were 1-inch diameter (2.43 cm) samples. Typically, two 5 mil (0.005 inch, 0.127 mm) thick sample layers were stacked and flown together for each experiment in the ram direction: M9R-C1 F (Part A & Part B), M10R-C1 F (Part A & Part B) and M12R-C1 (Part A & Part B). There were no ram samples in the MISSE-13 missions. A second Kapton H AO fluence witness sample was flown in the ram direction on MISSE-9 (M9R-C19 (Part A & Part B)). A single 5 mil layer of Kapton H was flown in the zenith, nadir or wake direction: M9W-C1 F, M9Z-C1 F, M10Z-C1 F, M10N-C1 F, M12W-C1 F, M13W-C1 F and M13Z-C1 F. The exception was for MISSE-12 zenith, where only a Photographic AO Fluence Monitor sample was flown, not a Kapton H sample for mass loss.

Back-up (B), or control Kapton H samples, were prepared and characterized pre-flight identically to the Kapton H flight samples (F). Thus, if there was an issue loading the flight sample during integration into the flight decks, the back-up sample could be substituted and flown.

The sample ID provides the MISSE mission number (M#), the flight orientation (ram (R), wake (W), nadir (N) or zenith (Z)), the sample's shape (circular (C), square (S) or rectangular (R)), the ID number and the pre-flight sample designation of Flight (F) or Back-up (B). So, M9R-C1 F was a circular sample (#1) flown on the MISSE-9 mission in the ram direction and was designated pre-flight as the flight sample. For the two-layered ram samples, the Part A layer was the top, space exposed layer, and the Part B layer was stacked behind the Part A layer. The Part A and Part B layers were weighed individually pre-flight.

4.2 Photographic AO Fluence Monitors

The PCE 1-4 Photographic AO Fluence Monitors (abbreviated as AO Photo Monitors) are listed in Table 2. The Photographic AO Fluence Monitors are 1-inch square with the exceptions of M10R-R1 and M10Z-C2, which are rectangular and circular, respectively. All samples have a white Tedlar (crystalline polyvinyl fluoride with white pigment) substrate that is either 1 mil (0.001 inch (0.00254 cm)) or 2 mil (0.002 inch (0.00508 cm)) thick. Typically, half of the white Tedlar is coated with a thin layer of carbon (716-780 Å), with the exception of M10Z-C2 which has a thin carbon layer (720 Å) covering the entire white Tedlar substrate. The Photographic AO Fluence Monitors have very thin Kapton H layers (1, 3, or 9 layers) covering most of the white Tedlar and carbon-coated white Tedlar substrates. These layers are either ~0.1 mil, 0.3 mil or 0.5 mil thick (the actual thickness details for these materials are provided below). For the samples with 3 or 9 Kapton H layers, the various size layers are stacked in "stepped layers" so that different Kapton H thicknesses extend across the sample. Figure 17 shows a diagram of the design for the five Photographic AO Fluence Monitors with three layers of Kapton H: M10N-S1 F, M12S-S1 F, M12Z-S1 F, M12W-S11 F and M12R-S2 F.

Table 2. PCE 1-4 Photographic AO Fluence Monitors

MISSE-FF Mission	Flight Orientation	Sample ID	Material	Thickness			Number of Kapton H Layers
				White Tedlar (mils)	Carbon (Å)	Kapton H (mils)*	
MISSE-10	Ram	M10R-R1 F	AO Photo Monitor	1	720	0.3	9
	Zenith	M10Z-C2 F	Carbon coated White Tedlar	2	720	N/A	N/A
	Nadir	M10N-S1 F	AO Photo Monitor	1	720	~0.1	3
MISSE-12	Ram	M12R-S1 F	AO Photo Monitor 1	2	780	0.3	3
	Ram	M12R-S2 F	AO Photo Monitor 2	2	780	0.5	3
	Zenith	M12Z-S1 F	AO Photo Monitor	2	780	0.3	3
MISSE-13	Wake	M13W-S1 F	AO Photo Monitor	2	716	0.3	1
	Zenith	M13Z-S1 F	AO Photo Monitor	2	716	0.3	1
MISSE-12/ MISSE-15	Wake	M12W-S11 F	AO Photo Monitor	2	780	0.3	3

*The 0.3 mil Kapton is actually 0.38 mil thick and the 0.5 mil Kapton is actually 0.57 mil thick

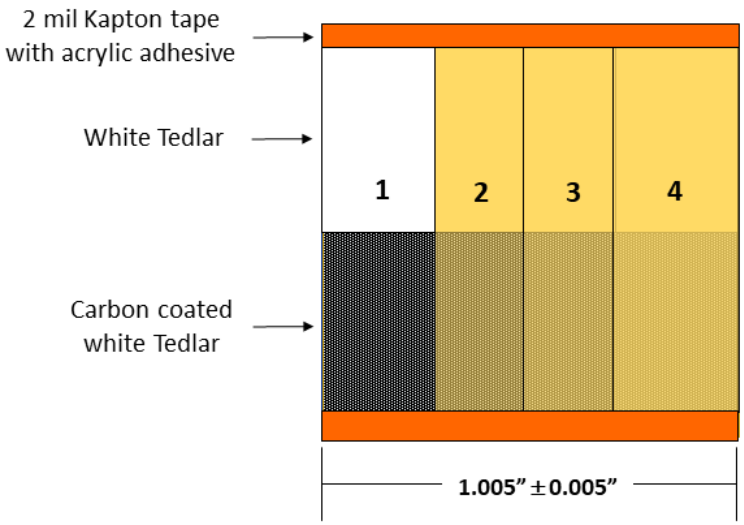

Layer 1 (base): 2 mil white Tedlar 1/2 coated with carbon (1.005" ± 0.005")
Layer 2: Kapton H* (0.700" ± 0.005", 0.6" exposed)
Layer 3: Kapton H* (0.500" ± 0.005", 0.4" exposed)
Layer 4 (top): Kapton H* (0.300" ± 0.005", 0.2" exposed)

*≈0.1 mil (M10N-S1), 0.3 mil (M12S-S1 F, M12Z-S1 F & M12W-S11 F) or 0.5 mil (M12R-S2 F)

Figure 17. Diagram showing the design for the Photographic AO Fluence Monitors with three layers of Kapton H.

Although the passive Photographic AO Fluence Monitors were designed to determine incremental AO fluence versus mission time based on on-orbit images, they also serve as low AO fluence witness samples post-flight. The first layer that would erode would be the thin carbon layer, which appears dark as compared to the bright white Tedlar. Once the layer of carbon is eroded away (and the carbon area appears white), the AO fluence can be computed based on recession depth. For these computations, we assume that the E_y of the carbon is the same as pyrolytic graphite (PG). A PG sample was exposed to four years of LEO ram AO as part of the MISSE 2 PEACE Polymers experiment, and the LEO E_y was determined to be 4.15×10^{-25} cm^3/atom.[17,32] Using the MISSE 2 LEO E_y for PG, the AO fluence to erode a 720 Å (7.2×10^{-6} cm) layer of carbon would be 1.73×10^{19} atoms/cm^2. After the carbon has eroded, the individual layers of Kapton H would erode with increasing AO fluence, based on the film thickness and number of sample layers.

The ~0.1 mil Kapton H was thinned with an AO plasma system from 0.3 mil thick Kapton H. The thicknesses of the thin Kapton H films, including the thinned ~0.1 mil Kapton H layers, were measured using a Heidenhain length gauge. For the thinned ~0.1 mil Kapton H layers, 10 measurements were made of each layer and the average was **0.103 mil** (2.616 µm). A total of 20 measurements were taken of three "0.3 mil" thick Kapton H film samples. Six of the measurements were considered outliners, and were not included in the average. The average of 14 measurements was 0.38 mil. A total of 15 measurements were taken of two "0.5 mil" thick Kapton H film samples. Two of the 0.5 mil measurements were considered outliners, and were not included in the average. The average of 13 measurements was 0.57 mil. Thus, **0.38 mil** (9.652 µm) and **0.57 mil** (14.478 µm) thickness was used as the actual thickness for these Kapton H films for determining the mission AO fluence.

Figure 18 provides pre-flight photographs of one of the five 1-inch square three layered Photographic AO Fluence Monitors. Figure 18a is a photograph of M12Z-S1 with 0.3 mil Kapton H layers. Figure 18b is a photograph of M12Z-S12 mounted in the M12 Z1 MS flight deck.

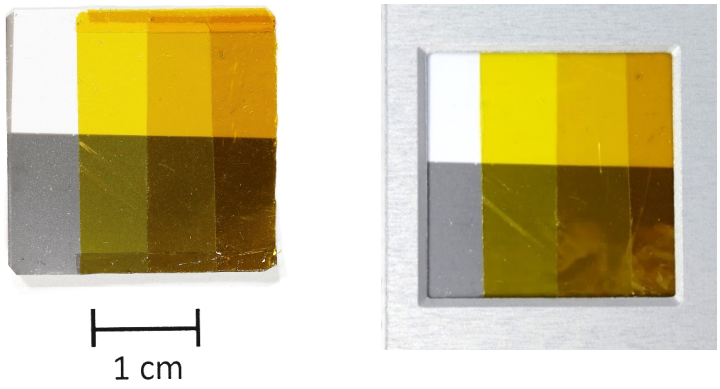

a. b.

Figure 18. Pre-flight photographs of the PCE-3 zenith Photographic AO Fluence Monitor. (a) M12Z-S1 F with 0.3 mil Kapton H layers and (b) M12Z-S1 F mounted in the Z1 (MSC 18) MS deck.

Figure 19 is pre-flight photograph of the PCE-2 MISSE-10 nine layered ram Photographic AO Fluence Monitor (M10R-R1). The rectangular sample (2.200” ± 0.005” × 1.005” ± 0.005”) has nine stepped layers of “0.3 mil” thick Kapton H. Thus, the Kapton H thicknesses range from 0.38 to 3.42 mil thick. As can be seen Figure 19b, the flight deck was designed to include tick marks every 0.2” to help identify the individual Kapton layers in on-orbit images.

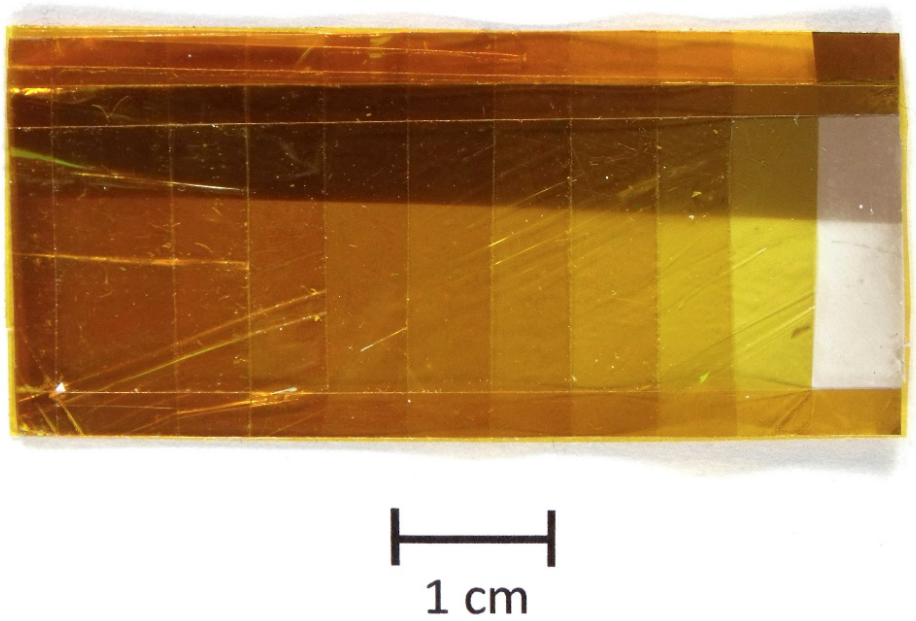

a.

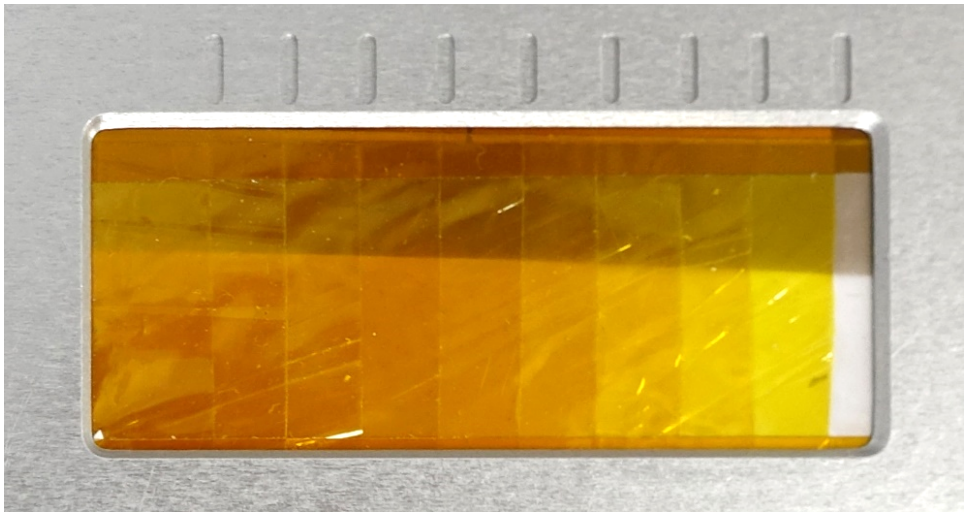

b.

Figure 19. Pre-flight photographs of the PCE-2 ram Photographic AO Fluence Monitor (M10R-R1). (a) Photo of the full sample and (b) Sample in the flight holder with tick marks every 0.2” to help identify individual Kapton H layers.

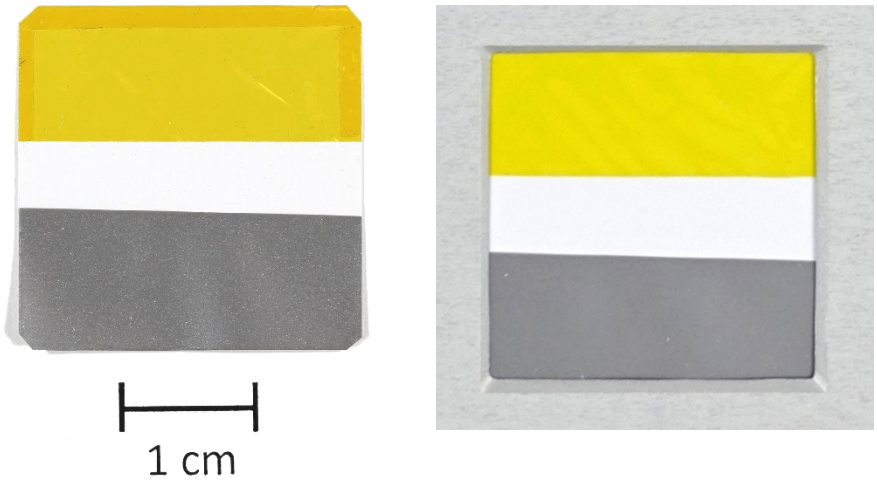

a. b.

Figure 20. Pre-flight photographs of the PCE-4 wake Photographic AO Fluence Monitor. (a) M13W-S1 F with a single 0.3 mil Kapton H layer and (b) M13W-S1 F mounted in the W1 (MSC 5) MS deck.

Photographic AO Fluence Monitors were also flown as part of the PCE-4 in the wake and zenith directions. Because very little AO is expected in these directions and the mission was planned to be 6 months, a modified design was used for the PCE-4 experiment. These samples include a thin vapor deposited layer of carbon, and one layer of 0.3 mil thick Kapton H, on white Tedlar. For the MISSE-13 samples, the Kapton layer does not overlap the carbon layer in the PCE-4 samples. Pre-flight photographs of the PCE-4 MISSE-13 wake sample are provided in Figure 20. Figure 20a is a photograph of M13W-S1 F with a single 0.3 mil Kapton H layer. Figure 20b is a photograph of M13W-S1 F mounted in the M13 Z2 MS flight deck.

5.0 Materials International Space Station Experiment-Flight Facility (MISSE-FF)

The MISSE-FF is operated by Aegis Aerospace, Inc. (previously called Alpha Space).[33] It is a modular and robotically serviceable external facility that is located on ISS Express Logistics Carrier-2 Site 3 (ELC-2 Site 3). Figure 21 provides an on-orbit photograph showing the location of the MISSE-FF on ELC-2. The MISSE-FF provides ram, wake, zenith, and nadir space exposures. The MISSE-FF supports both passive and active experiments, with downlink of data. It is designed to include active environmental sensors that provide environmental data over time in each flight orientation, including temperature, contamination and solar exposure (UV radiation). Arrangements can be made for sensors to be flown to provide AO fluence and total ionizing dose data. On-orbit facility cameras are typically scheduled to provide monthly sample images.

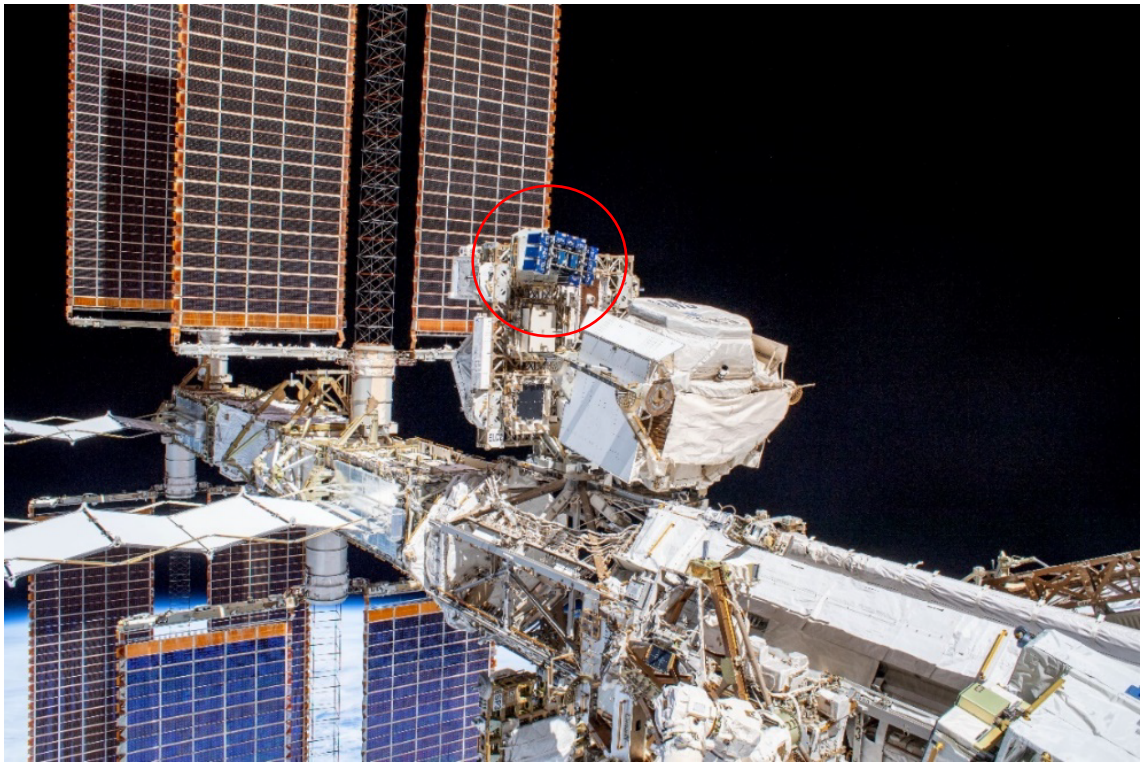

Figure 21. A view of the MISSE-FF on ELC-2 Site 3 as photographed during an EVA on November 15, 2019 (iss061e040917).

MISSE Sample Carriers, also called MISSE Science Carriers, house the material flight experiments. Each MSC has two sides, a mount-side (MS) and a swing-side (SS), with a central hinge. Materials and spacecraft components can be flown on either the MS or SS decks for direct space exposure, or they can be mounted on the underdecks. The MSCs are launched closed as pressurized cargo on either the Northrup Grumman Cygnus or SpaceX Dragon spacecraft, moved outside the ISS through the Kibo Japanese Experiment Module (JEM) Airlock on the MISSE Transfer Tray (MTT). They are then installed on the MISSE-FF structure via robotic arm. The SS decks are remotely opened to expose the experiments to space. The MSCs are closed during ship dockings to prevent contamination and minimize AO exposure of wake surfaces. The MSCs are typically closed during local EVAs and for on-demand images. Figure 22 provides a drawing of the MISSE-FF with MSCs closed. This image also shows the exposure direction and the MSC positions are labeled (R1, R2, R3, etc.). Figure 23 provides a drawing of the MISSE-FF with MSCs open. The MISSE-FF is rotated 8° “pitch up” such that the zenith direction is 8° away from ram and the nadir direction is 8° towards ram. Thus, the nadir samples will get slightly more grazing AO fluence and the zenith samples will get slightly less grazing AO fluence during the MISSE-FF missions. Additionally, the ram surface is offset 8° from true ram. This rotation “offset” can be seen in Figures 22 and 23.

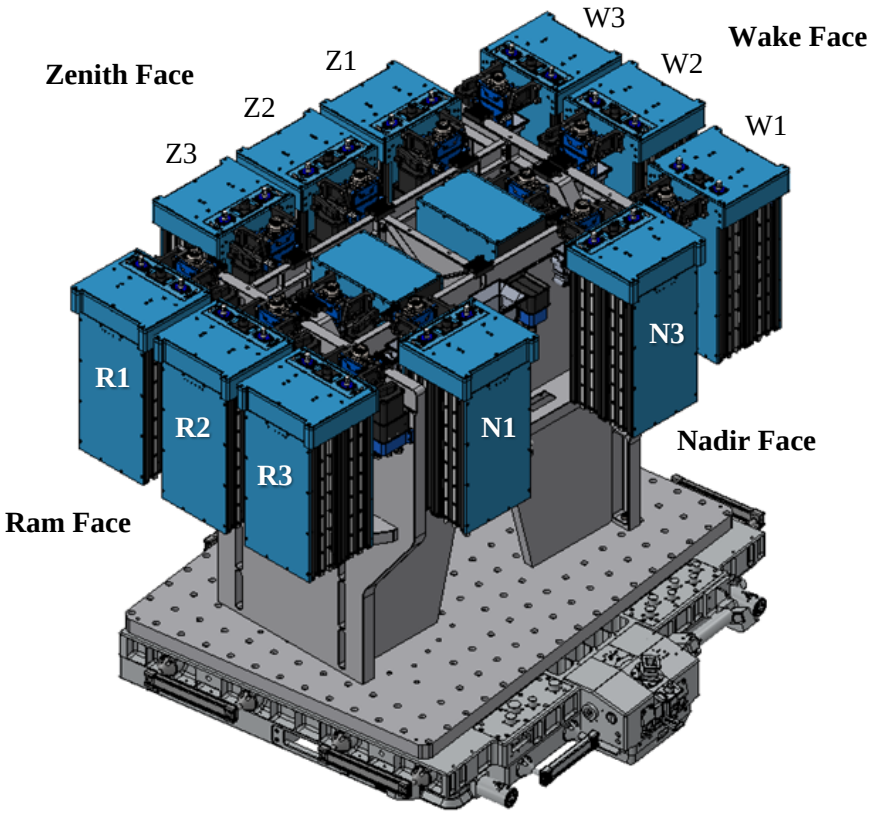

Figure 22. MISSE-FF with MSCs closed and the MSC positions labeled. The MISSE-FF 8° rotation can be seen in this image (Aegis Aerospace image).

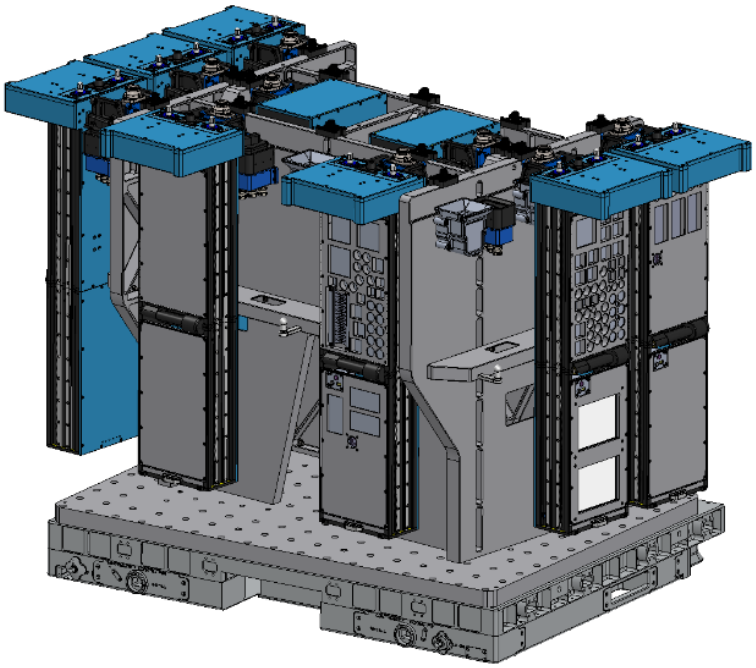

Figure 23. MISSE-FF with MSCs open (Aegis Aerospace image).

The MSCs get initial space vacuum exposure when the JEM airlock is put under vacuum and opened to space. Figure 24 shows astronauts Drew Morgan and Jessica Meir preparing MSCs for transfer through the JEM Airlock on the MTT. It can take several days to robotically move the MTT with the MSCs to ELC-2 and install the MSCs in the MISSE-FF. Figure 25 shows robotic translation of MSCs on the MTT using ISS's Special Purpose Dexterous Manipulator (SPDM) robotic arm. Figure 26 shows a close-up image of the robotic arm moving one of the MSCs (MSC 19) during Expedition 69.

Figure 24. Astronauts Drew Morgan and Jessica Meir preparing MSCs for transfer through the Japanese Experiment Module (JEM) Airlock using the MISSE Transfer Tray (MTT) on the ORU Transfer Interface (JOTI) in March 2020 (iss062e090043).

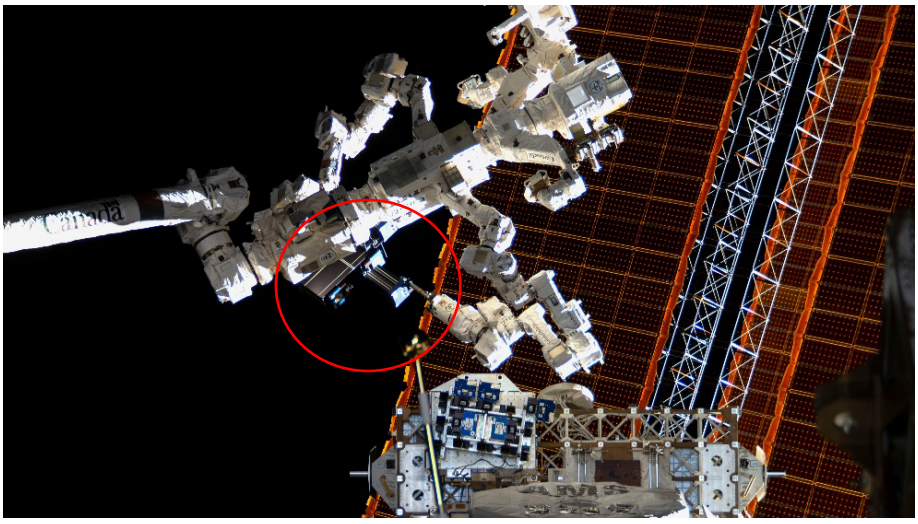

Figure 25. View of the Special Purpose Dexterous Manipulator (SPDM) robotic translation of MSCs on the MTT (iss069e000218). The red circle shows the SPDM attached to the MTT (the MISSE-FF is in the background).

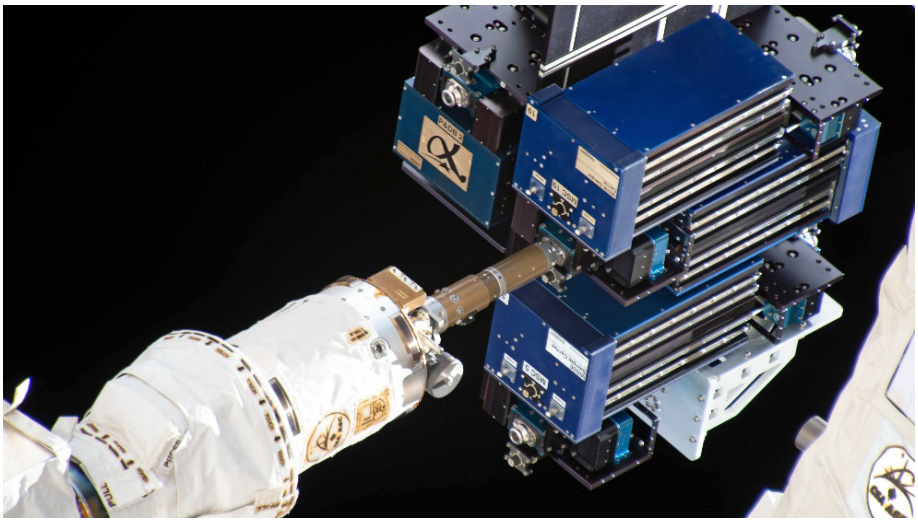

Figure 26. Close-up image of the robotic arm moving MSC 5 and MSC 19 during Expedition 69 (iss069e000575).

After insertion into the MISSE-FF, the MSC is then remotely “deployed” or opened to the space environment for the first time. As mentioned above, the MSCs are typically closed and re-opened numerous times during a mission. The MSCs are then closed for a final time, robotically retrieved from the MISSE-FF and placed back into the MTT, and the MTT is robotically moved back into the JEM airlock and repressurized. Thus, with respect to exposure durations, the space vacuum exposure is longest, then the duration installed on the MISSE-FF, then the “deployed duration” (first time opened to final time closed), and finally the actual time samples are directly exposed to space (accumulated open durations). These durations are discussed below for the various PCE 1-4 missions.

6.0 MISSE-FF Missions

The MISSE-FF and the inaugural set of experiments, called MISSE-9, were launched aboard the SpaceX Commercial Resupply Services-14 (CRS-14) Dragon, also called SpaceX-14, on April 2, 2018. The MISSE-FF was robotically installed on ELC-2 Site 3 on April 8, 2018. The MISSE-9 MSCs were installed in the MISSE-FF April 18-19, and the MISSE-9 PCE-1 samples were deployed on April 19, 2018 for a 1-year space exposure mission.

The PCE 1-4 flight experiments were flown as part of the MISSE-9, MISSE-10, MISSE-12, MISSE-13 and MISSE-15 missions. The last flown PCE 1-4 MSC (MISSE-15 wake) was closed for the final time on July 18, 2022 and retrieved from the MISSE-FF on August 2, 2022. The MISSE-15 MSCs were returned in the SpaceX-25 Dragon capsule on August 20, 2022. Thus, the PCE 1-4 experiments were flown on the MISSE-FF from April 2018 to August 2022. Details of the mission exposures for each MSC are provided in the *PCE 1-4 Environmental Exposure* section.

Figure 27 provides an on-orbit photograph of the MISSE-FF with the MISSE-9 and MISSE-10 MSCs installed. As seen from this top perspective, the ram MSCs are on the left (partially hidden in this image), the zenith MSCs are at the top, the wake MSCs are on the right and the nadir MSCs (two) are at the bottom. The MSC numbers (i.e., R1, R2, and R3) are in numerical order going counter-clockwise (i.e., R1 is near the zenith direction (top ram MSC in Figure 27) and R3 is near the nadir direction (bottom ram MSC in Figure 27). Figures 28 and 29 provide on-orbit images of the MISSE-FF with the MISSE-10 PCE-2 and MISSE-12 PCE-3 MSCs installed.

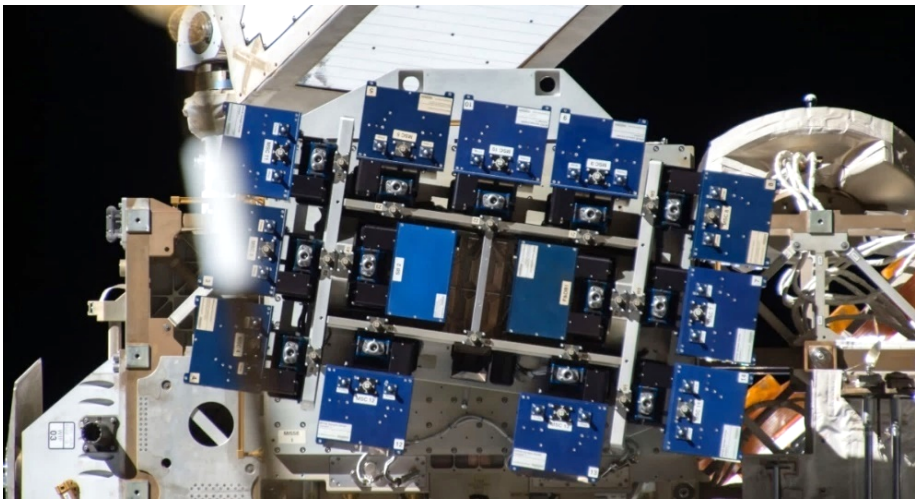

Figure 27. An on-orbit image taken on January 16, 2019 showing the top of the MISSE-FF with the MISSE-9 and MISSE-10 MSCs installed (iss058e003972).

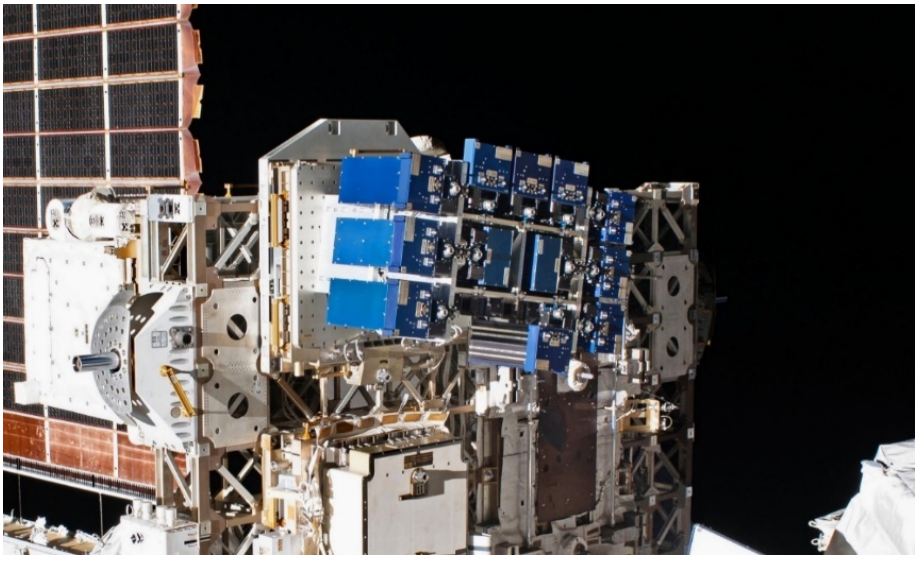

Figure 28. Close-up image of the MISSE-FF with the MISSE-10 PCE-2 and MISSE-12 PCE-3 MSCs as photographed during an EVA on January 25, 2020. The front surface of the blue ram MSCs can be seen in the closed position (iss061e142772).

Figure 29. The wake side of the MISSE-FF with the MISSE-10 PCE-2 and MISSE-12 PCE-3 MSCs as photographed on January 25, 2020 during an EVA. The MSCs are closed, except for the central wake MSC which is open (iss061e143021).

It should be noted that while MSCs are installed on the MISSE-FF and are closed, the samples on those MSCs are exposed to the vacuum of space, thermal cycling (different levels than when the MSCs are open) and energetic radiation, such as galactic cosmic rays. But, when the MSCs are closed the samples are not exposed to visible, UV and VUV radiation, x-rays, solar wind particle radiation (electrons, protons), impacts from MMOD and atomic oxygen (AO). For these experiments, “space exposure” means the MSCs are open and the samples are directly exposed to the space environment.

7.0 PCE 1-4 Environmental Exposure

7.1 PCE-1 Mission Overview and Exposure Durations

As stated previously, the MISSE-9 PCE-1 experiment was launched aboard SpaceX-14 along with the MISSE-FF and the PCE-1 MSCs (ram R2 MSC 3, zenith Z3 MSC 5, and wake W3 MSC 8) were deployed on April 19, 2018. The PCE-1 MSCs were closed December 26, 2018 in preparation for the MISSE-10 installation and remained closed, with the exception of the MISSE-9 ram MSC as discussed below.

The MISSE-9 PCE-1 wake and zenith MSCs were retrieved from the MISSE-FF during the MISSE-11 installation ops on April 26, 2019 and brought back inside ISS and stowed. The MSCs were returned to Earth in the SpaceX-17 Dragon capsule on June 3, 2019. The MSCs were exposed to the vacuum of space for 1.07 years (April 13, 2018 to May 9, 2019) and installed on the MISSE-FF for 1.02 years. The MSCs had an 8.3 month (0.69 year) deployed mission between the first time the MSCs were opened to space (April 19, 2018) to the last time they were closed (December 26, 2018). During that time, the MSCs were closed 21% of the time to protect against

contamination from visiting vehicles, EVAs, etc. Therefore, the MISSE-9 PCE-1 zenith and wake samples were directly exposed to the space environment for a total of **0.54 years**.

Because the MISSE-9 MSCs were closed from December 26, 2018 until the planned retrieval in April 2019 and the LEO AO flux was low during the MISSE-9 mission due to the 11-year solar cycle period, NASA MISSE-9 principal investigators (PIs) were concerned that the ram samples would not receive the AO fluence necessary to obtain meaningful flight data. Therefore, the NASA PIs with samples on MISSE-9 R2 MSC 3 requested that the MSC be left on-orbit for additional AO exposure. Aegis Aerospace agreed to this mission extension request and the MISSE-9 MSC was re-deployed on April 26, 2019 along with the MISSE-10 PCE-2 MSCs. The MISSE-9 ram MSC was closed for a final time on October 2, 2019 and retrieved on November 11, 2019 during the MISSE-12 deployment ops and brought inside ISS on November 13, 2019. The PCE-1 ram MSC was exposed to the vacuum of space for 1.59 years (April 13, 2018 to November 13, 2019) and had a deployed mission duration of 1.46 years. The MSC was returned in the SpaceX-19 Dragon after 1.57 years on the MISSE-FF with a total of **0.77 years** of direct space exposure.

7.2 PCE-2 Mission Overview and Exposure Durations

The MISSE-10 PCE-2 experiment MSCs were launched aboard the Northrop Grumman (NG) Cygnus cargo ship (NG-10) on November 17, 2018, and were transferred for storage inside the ISS. The PCE-2 MSCs (ram R1 MSC 11, zenith Z2 MSC 10 and nadir N3 MSC 13) were robotically installed on the MISSE-FF on January 4, 2019. The MISSE-10 (and MISSE-9) MSCs remained closed after the MISSE-10 installation operations due to an anomaly which occurred in the communication system during the MISSE-10 installation. A new Power and Data Box (PDB) was launched along with the MISSE-11 MSCs on April 17, 2019 as part of the NG-11 mission. The new MISSE-FF PDB resolved the communication issue and the MISSE-10 PCE-2 MSCs were deployed on April 26, 2019, exposing the samples to the space environment.

The MISSE-10 zenith and nadir MSCs were closed for the final time on March 12, 2020 and retrieved from the MISSE-FF on March 18, 2020. The MSCs were exposed to the vacuum of space for 1.25 years (December 26, 2018 to March 25, 2020) and had a deployed mission duration of 0.88 years. The MSCs were returned to Earth in the SpaceX-20 Dragon on April 7, 2020 after 1.20 years on the MISSE-FF during which time the MISSE-10 zenith MSC had **0.69 years** of direct space exposure and the MISSE-10 nadir MSC had **0.48 years** of direct space exposure.

The MISSE-10 MSCs were closed a significant amount of time during the MISSE-10 mission due to required safety and contamination control closures. Similar to MISSE-9 ram samples, NASA PIs were concerned that the MISSE-10 ram samples had not received enough AO fluence to obtain meaningful science at the time of the planned retrieval. Therefore, NASA MISSE-10 PIs requested an on-orbit mission extension for the MISSE-10 ram MSC. Once again, the mission extension request was approved by Aegis Aerospace and the MISSE-10 ram MSC remained on-orbit for additional AO exposure. The MISSE-10 PCE-2 ram MSC was robotically closed and retrieved on November 25, 2020. It was brought back inside the ISS JEM Airlock and

repressurized on December 1, 2020. It was returned as part of the SpaceX-21 mission in January 2021. The MISSE-10 ram MSC was exposed to the vacuum of space for 1.93 years (December 26, 2018 to December 1, 2020). It was on the MISSE-FF facility for 1.90 years and had a deployed mission duration of 1.59 years. During the deployed duration, the PCE-2 ram samples had a total of **1.17 years** of direct space exposure.

7.3 PCE-3 Mission Overview and Exposure Durations

The MISSE-12 PCE-3 experiment was launched aboard Cygnus NG-12 on November 2, 2019 and the MSCs were installed on the MISSE-FF on November 11, 2019. The MISSE-12 ram R2 MSC 4 carrier was deployed on December 3, 2019. The PCE-3 wake (W3 MSC 6) and zenith (Z1 MSC 18) carriers were installed in the wrong flight orientations (i.e., swapped) and thus were left closed until MISSE-13 installation operations. The carriers were moved to the correct locations (switched) during the MISSE-13 ops on March 16 and March 17, 2020, respectively. The MISSE-12 zenith MSC was deployed on March 20, 2020. The **wake MSC was never deployed** and hence those samples were not directly exposed to the space environment during the MISSE-12 mission.

On April 28, 2020, Aegis Aerospace lost communications with the MISSE-FF and the MSCs could not be remotely opened or closed, and images and active data could not be taken or downlinked. Fortunately, all the PCE 2-4 on-orbit MSCs were open at the time, with the exception of the MISSE-12 wake MSC. The PCE 2-4 on-orbit MSCs remained open receiving uninterrupted space exposure from April 28, 2020 until the final robotic closure. The MISSE-12 PCE-3 ram MSC was robotically closed and retrieved from the MISSE-FF on November 25, 2020. MISSE-12 PCE-3 zenith MSC was closed for the final time on September 2, 2020 and retrieved on November 26, 2020. MISSE-12 wake MSC (never opened) was retrieved on November 27, 2020. The MSCs were brought back inside the ISS JEM Airlock on the MTT and repressurized on December 1, 2020 and returned as part of the SpaceX-21 mission.

The MISSE-12 ram MSC was exposed to the vacuum of space for 1.07 years (November 7, 2019 to December 1, 2020). It was on the MISSE-FF facility for 1.04 years and had a deployed mission duration of 0.98 years. During the deployed duration, the PCE-3 ram samples had a total of **0.89 years** of direct space exposure.

MISSE-12 PCE-3 zenith MSC was exposed to the vacuum of space for 1.07 years (November 7, 2019 to December 1, 2020). It was on the MISSE-FF facility for 1.05 years and had a deployed mission duration of 0.45 years. During the deployed duration, the PCE-3 zenith samples had a total of **0.45 years** of direct space exposure.

MISSE-12 PCE-3 wake MSC was exposed to the vacuum of space for 1.07 years (November 7, 2019 to December 1, 2020) during the MISSE-12 mission. It was on the MISSE-FF facility for 1.05 years, but it was **never deployed** (i.e., opened). Thus, the PCE-3 wake samples were re-flown as part of the MISSE-15 mission.

The MISSE-15 experiment MSCs were launched aboard SpaceX-23 on August 29, 2021. The MISSE-15 wake W1 MSC 10 was robotically installed on the MISSE-FF on December 28, 2021, and was deployed on January 6, 2022 for a 6 month mission. The MSC was closed for the final time on July 18, 2022 and retrieved from the MISSE-FF on August 2, 2022. The MISSE-15 MSCs were returned as part of the SpaceX-25 Dragon mission. The MISSE-15 PCE-3 wake W1 MSC 10 was exposed to the vacuum of space for 0.71 years (November 20, 2021 to August 5, 2022). It was on the MISSE-FF facility for 0.60 years and had a deployed mission duration of 0.53. During the deployed duration, the PCE-3 wake samples had a total of **0.44 years** of direct space exposure.

7.4 PCE-4 Mission Overview and Exposure Durations

The MISSE-13 PCE-4 experiment was launched aboard SpaceX-20 on March 6, 2020 and the MSCs were installed on the MISSE-FF on March 18, 2020. The MISSE-13 wake W1 MSC 5 and zenith Z2 MSC 19 carriers were deployed on March 20, 2020 for a 6 month mission. The wake MSC was robotically closed for the final time on September 2, 2020 and the zenith MSC was closed for the final time on September 3, 2020. These MSCs had constant space exposure from April 28, 2020 until September 2-3, 2020. The MISSE-13 MSC was retrieved on November 26, 2020 and MISSE-13 MSC was retrieved on November 27, 2020. The MSCs were brought back inside the ISS JEM Airlock on the MTT and re-pressurized on December 1, 2020. The PCE-4 MSCs were returned as part of the SpaceX-21 mission.

MISSE-13 PCE-4 wake W1 MSC 5 was exposed to the vacuum of space for 0.72 years (March 12, 2020 to December 1, 2020). It was on the MISSE-FF facility for 0.70 years and had a deployed mission duration of 0.46 years. During the deployed duration, the PCE-4 wake samples had a total of **0.44 years** of direct space exposure.

MISSE-13 PCE-4 zenith Z2 MSC 19 was exposed to the vacuum of space for 0.72 years (March 12, 2020 to December 1, 2020). It was on the MISSE-FF facility for 0.70 years and had a deployed mission duration of 0.46 years. During the deployed duration, the PCE-4 zenith samples had a total of **0.46 years** of direct space exposure.

Table 3 provides a detailed summary of Glenn's PCE 1-4 mission durations including launch, installation, deploy, closure, retrieval and return dates for each MSC. It also includes each MSC's time on the MISSE-FF, the space vacuum exposure durations and the direct space exposure durations. A couple minor up-dates have been made from the mission duration table published by de Groh in Reference 21. The MISSE-12 zenith direct space exposure duration has been up-dated from 0.44 to 0.45 years. And, the MISSE-13 wake swing and mount-side sample decks have been corrected (39 samples were flown in SS (not MS) and 26 samples were flown in MS (not SS)).

Table 3. Polymers and Composites Experiment 1-4 (PCE 1-4) Mission Duration Summary

MISSE-FF Expt.	Flight Direction	# of Samples	MISSE Sample Carrier (MSC)	Launch Mission	Installed on MISSE-FF	Deployed	Final Time Closed	Retrieved from MISSE-FF	Return Mission	Space Vacuum Duration (Years)	Time on MISSE-FF (Years)	Direct Space Exposure Duration (Years)
MISSE-9 PCE-1	Ram	39	R2 (MSC 3) MS	SpaceX-14 April 2, 2018	April 18, 2018	April 19, 2018	Oct. 2, 2019	Nov. 11, 2019	SpaceX-19 Jan. 7, 2020	1.59	1.57	0.77
	Wake	52	W3 (MSC 8) MS		April 18, 2018		Dec. 26, 2018	April 26, 2019	SpaceX-17 June 3, 2019	1.07	1.02	0.54
	Zenith	47	Z3 (MSC 5) MS		April 19, 2018					1.07	1.02	0.54
MISSE-10 PCE-2	Ram	21	R1 (MSC 11) MS	NG-10 Nov. 17, 2018	Jan. 4, 2019	April 26, 2019	Nov. 25, 2020	Nov. 25, 2020	SpaceX-21 Jan. 13, 2021*	1.93	1.90	1.17
	Zenith	10	Z2 (MSC 10) MS				March 12, 2020	March 18, 2020	SpaceX-20 April 7, 2020	1.25	1.20	0.69
	Nadir	12	N3 (MSC 13) MS							1.25	1.20	0.48
MISSE-12 PCE-3	Ram	30	R2 (MSC 4) SS	NG-12 Nov. 2, 2019	Nov. 11, 2019	Dec. 3, 2019	Nov. 25, 2020	Nov. 25, 2020	SpaceX-21 Jan. 13, 2021*	1.07	1.04	0.89
	Wake	42	W3 (MSC 6) MS			N/A	N/A	Nov. 27, 2020		1.07	1.05	0**
	Zenith	14	Z1 (MSC 18) MS			March 20, 2020	Sept. 2, 2020	Nov. 26, 2020		1.07	1.05	0.45
MISSE-13 PCE-4	Wake	39	W1 (MSC 5) SS	SpaceX-20 March 6, 2020	March 18, 2020	March 20, 2020	Sept. 2, 2020	Nov. 27, 2020	SpaceX-21 Jan. 13, 2021*	0.72	0.70	0.44
		26	W1 (MSC 5) MS									
	Zenith	33	Z2 (MSC 19) MS				Sept. 3, 2020	Nov. 26, 2020		0.72	0.70	0.46
MISSE-15 PCE-3 Wake Re-flight**	Wake	42	W1 (MSC 10) MS	SpaceX-23 Aug. 29, 2021	Dec. 28, 2021	Jan. 6, 2022	July 18, 2022	Aug. 2, 2022	SpaceX-25 Aug. 20, 2022	0.71	0.60	0.44

MS: Mount side deck; SS: Swing side deck

*January 13, 2021 EST (January 14, 2021 UTC)

**The PCE-3 wake samples were re-flown as part of the MISSE-15 mission

8.0 Post-Flight Atomic Oxygen Fluence Analyses

8.1 Kapton H AO Fluence Witness Samples

8.1.1 Mass Loss

One of the critical issues with using mass loss for obtaining AO fluence (or E_y) values is that dehydrated mass measurements are needed. Many polymer materials, including Kapton H, are very hygroscopic (absorbing up to 2% of their weight in moisture) and can fluctuate in mass with humidity and temperature.[29] Therefore, for accurate mass loss measurements to be obtained, it is necessary that the samples be fully dehydrated (i.e., in a vacuum desiccator) immediately prior to measuring the mass both pre-flight and post-flight. Thus, dehydrated mass of the PCE 1-4 Kapton H AO fluence flight samples was obtained pre- and post-flight for AO fluence determination.

To obtain the pre- and post-flight mass, the PCE 1-4 Kapton H samples were dehydrated at room temperature in a vacuum desiccator maintained at a pressure of 5.3 to 13.3 Pa (40 to 100 mtorr) with a mechanical roughing pump. Typically, ten samples were placed in a vacuum desiccator, in a particular order (i.e., order of weighing), and left under vacuum for a minimum of 72 to 96 hours. The PCE 1-4 Kapton H AO fluence samples were dehydrated with other mission samples being flown for *Ey* determination. But, the Kapton H AO fluence flight samples were typically placed in the "first mass position" and were the first samples weighed after dehydration.

Once a sample was removed for weighing, the vacuum desiccator was immediately put back under vacuum to keep the other samples under vacuum. Previous tests showed that the mass of a dehydrated sample was not adversely affected if the desiccator was opened and quickly closed again and pumped back down to approximately 20 Pa (150 mtorr) prior to that sample being weighed. This process allows multiple samples to be dehydrated together. The time at which the sample was first exposed to air was recorded along with the times at which it was weighed. A total of three mass readings were obtained and averaged. The total time it took to obtain the three readings, starting from the time air was let into the desiccator, was typically 5 min. The samples were weighed pre-flight using a Sartorius ME5 Microbalance (±0.005 mg sensitivity). Records of the following were kept: the sequence of sample weighing, the number of samples in each set, the time under vacuum prior to weighing, the temperature and humidity in the room, the time air was let into the desiccator, and the time a sample was taken out of the desiccator, the time of each weighing and the mass. The same procedure and sequence was repeated as best as possible with the samples post-flight.

8.1.2 Density

The density of the Kapton H samples (1.4273 g/cm^3*)* was based on density gradient column measurements of Kapton H film made for the MISSE 2 Polymers experiment.[2,17] The MISSE 2 density gradient columns were created in 50-mL burets either with solvents of cesium chloride (CsCl, density $\rho \approx 2$ g/cm^3) and water (H_2O, $\rho = 1.0$ g/cm^3). A quadratic calibration curve was developed for the columns based on the equilibrium vertical position of three to four standards of

known density (±0.0001 g/cm^3). Subsequently, density values of samples were calculated based on the vertical positions of small (<2 mm) pieces placed into the column and allowed to settle for 2 hours. Where possible, the same batch of material was used for all the Glenn MISSE polymers experiments.

8.1.3 Exposed Surface Area

The exposed surface area of the circular Kapton H flight samples was determined post-flight by taking a minimum of four diameter measurements of the MSC deck sample openings for each flight sample using electronic digital calipers.

8.2 Photographic AO Fluence Monitors

The AO fluences of the Photographic AO Fluence Monitors were computed using recession depth measurements as described in Equation (2) in the *AO Fluence Section* above. Depending on the level of erosion, the AO fluence was computed based on either erosion of the carbon layer or the Kapton H layer(s). The specific analysis for each Photographic AO Fluence Monitor is provided in the *Post-Flight Atomic Oxygen Fluence Results* section below.

9.0 Post-Flight Atomic Oxygen Fluence Results

9.1 MISSE-9 PCE-1

9.1.1 Kapton H AO Fluence Witness Samples

Four Kapton H AO fluence witness samples were flown as part of the MISSE-9 PCE-1: M9R-C1 F and M9R-C19 F in ram, M9W-C1 F in wake and M9Z-C1 F in zenith. The PCE-1 did not include any Photographic AO Fluence Monitors. Both of the ram Kapton H samples had two 5 mil thick (0.0127 cm) layers stacked together for flight: Part A and Part B. Erosion only occurred in the top layer (Part A). Because the layers were weighed separately pre-flight, only the mass loss of the Part A layer was used for computing the AO fluence for the ram flight samples.

Figure 30 provides post-flight photographs of the PCE-1 ram M9R-C1 F (flight) and M9R-C1 B (control) samples. Figure 30a shows both the Part A (top) and Part B (bottom) layers. And, Figure 30b shows the M9R-C1 F Part A and M9R-C1 B Part A samples on a dark background. The exposed eroded area of the M9R-C1 F Part A sample shows clearly in Figure 30b. The Kapton H samples were also examined, and imaged, with a 365 nm UV light source. The eroded area of the ram flight sample was clearly visible under the UV light as shown in Figure 30c.

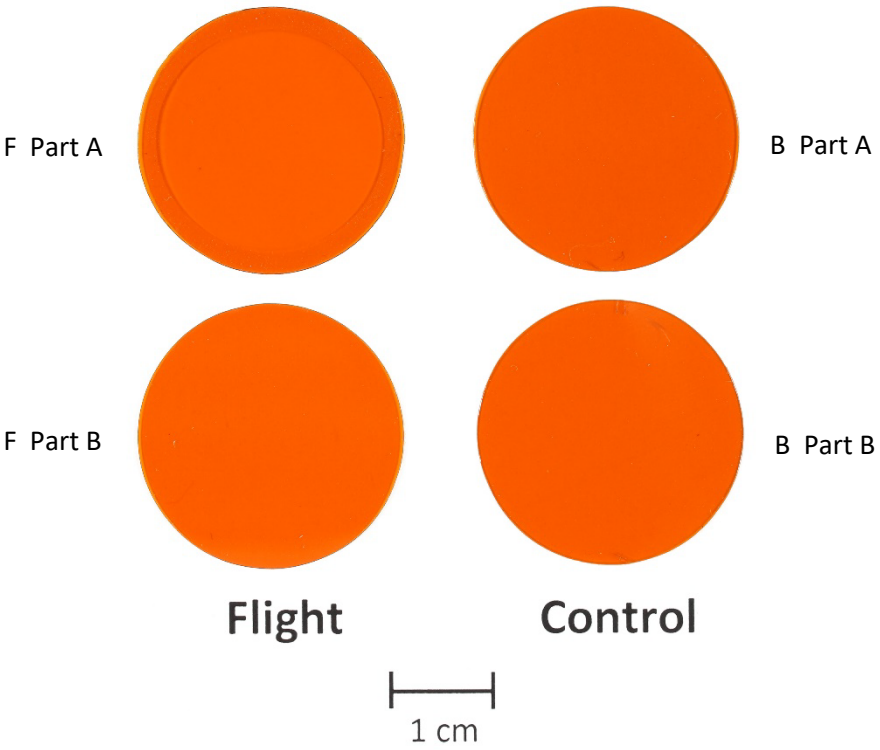

a.

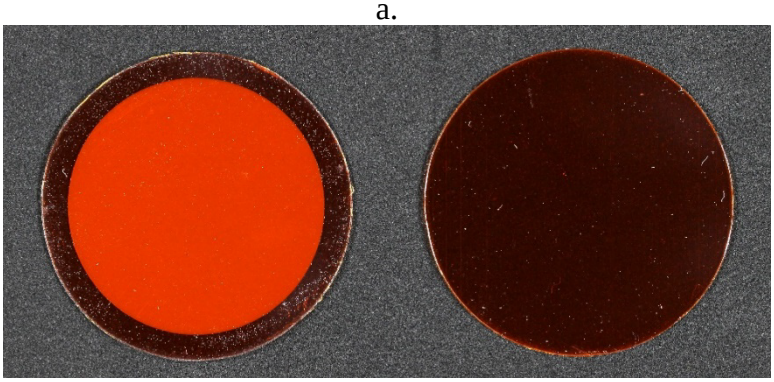

b.

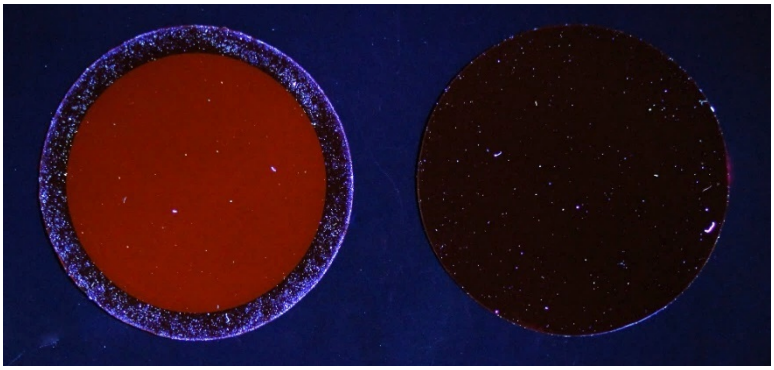

c.

Figure 30. Post-flight photographs of M9R-C1 F and M9R-C1 B. (a) Visible light image with both Part A (top layer) and Part B (bottom layer), (b) Visible light image (M9R-C1 F Part A on left and M9R-C1 B Part A on the right), and (c) UV light (365 nm) image with M9R-C1 F Part A on left and M9R-C1 B Part A on the right.

Figure 31 provides post-flight photographs of the PCE-1 ram M9R-C19 F (flight) and M9R-C19 B (control) samples. Figure 31a shows both the Part A (top) and Part B (bottom) layers. And, Figure 31b shows the M9R-C19 F Part A and M9R-C19 B Part A samples on a dark background. Similar to M9R-C1 F, the exposed eroded area of the M9R-C19 F Part A sample shows clearly in the dark background image.

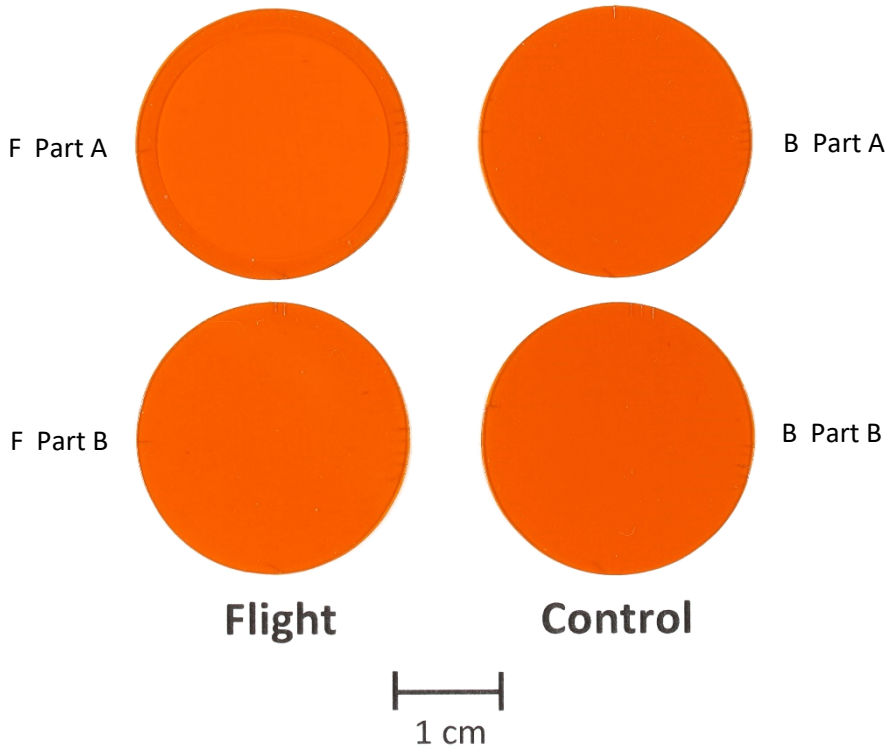

a.

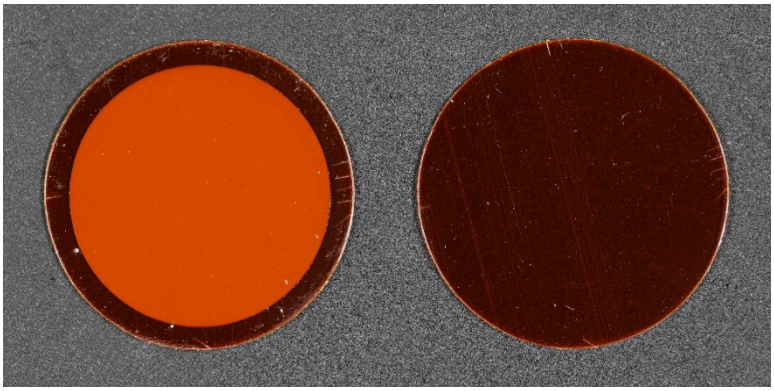

b.

Figure 31. Post-flight photographs of M9R-C19 F and M9R-C19 B. (a) With both Part A (top layer) and Part B (bottom layer), and (b) M9R-C19 F Part A on left and M9R-C19 B Part A on the right.

Figure 32 provides post-flight photographs of the PCE-1 wake M9W-C1 F (flight) and M9W-C1 B (control) samples. Figure 32a shows the samples on a white background and Figure 32b shows the samples on a dark background (M9W-C1 F on the left and M9W-C1 B on the right). There was no visual erosion or texturing of the flight sample. The only visible effects on the flight sample are holder marks on the perimeter. This is noticeable in the image on the dark background (Figure 32b) when zoomed in. Interestingly, the exposed area of the M9W-C1 F flight sample was slightly enhanced under the UV light, as shown in Figure 32c, although there was no visual erosion or texturing of the flight sample.

Figure 33 provides post-flight photographs of the PCE-1 zenith M9Z-C1 F (flight) and M9Z-C1 B (control) samples. Figure 33a shows the samples on a white background and Figure 33b shows the samples on a dark background (M9Z-C1 F on the left and M9Z-C1 B on the right). There was no visual erosion of the flight sample. The only visible effects on the flight sample are holder marks on the perimeter. This is very noticeable in the image on the dark background in the upper left area of the sample (Figure 33b). The exposed area of the M9Z-C1 F flight sample looked only a slight bit different under UV light, and the difference was only noticeable when the UV image was brightened significantly.

Table 4 provides a list of the MISSE-9 PCE-1 Kapton H AO Fluence Witness samples along with the sample film thickness, the dehydrated sample mass loss, LEO exposed surface area, Kapton H density and LEO E_y, and the computed MISSE-9 AO fluence for each flight sample. As can be seen, the AO fluence for the two ram samples were very similar: 3.44×10^{20} atoms/cm^2 for M9R-C1 F and 3.43×10^{20} atoms/cm^2 for M9R-C19 F. Thus, the AO fluence for the MISSE-9 ram direction is the average of these two values, which is 3.436×10^{20} atoms/cm^2 or **3.44×10^{20} atoms/cm^2**. It should be noted that the mass loss for the wake sample (M9W-C1 F) was 0.001 mg with a computed AO fluence of 4.46×10^{16} atoms/cm^2. This is *within error* of the Sartorius ME5 Microbalance (±0.005 mg sensitivity). And, the mass loss for the zenith sample (M9Z-C1 F) was 0.057 mg with a computed AO fluence of 3.19×10^{18} atoms/cm^2.

9.2 MISSE-10 PCE-2

Three Kapton H AO fluence witness samples were flown as part of the MISSE-10 PCE-2: M10R-C1 F in ram, M10Z-C1 F in zenith and M10N-C1 F in nadir. The PCE-2 also included two Photographic AO Fluence Monitors: M10R-R1 F flown in ram and M10N-S1 F flown in nadir. The PCE-2 also included a carbon coated white Tedlar sample, M10Z-C2 F, flown in the zenith direction for visual AO fluence determination.

9.2.1 Kapton H AO Fluence Witness Samples

The ram Kapton H sample (M10R-C1 F) had two 5 mil thick (0.0127 cm) layers stacked together for flight: Part A and Part B. Erosion only occurred in the top layer (Part A). Because the layers were weighed separately pre-flight, only the mass loss of the Part A layer was used for computing the AO fluence for the ram flight samples. The zenith and nadir Kapton H samples only had one 5 mil layer flown.

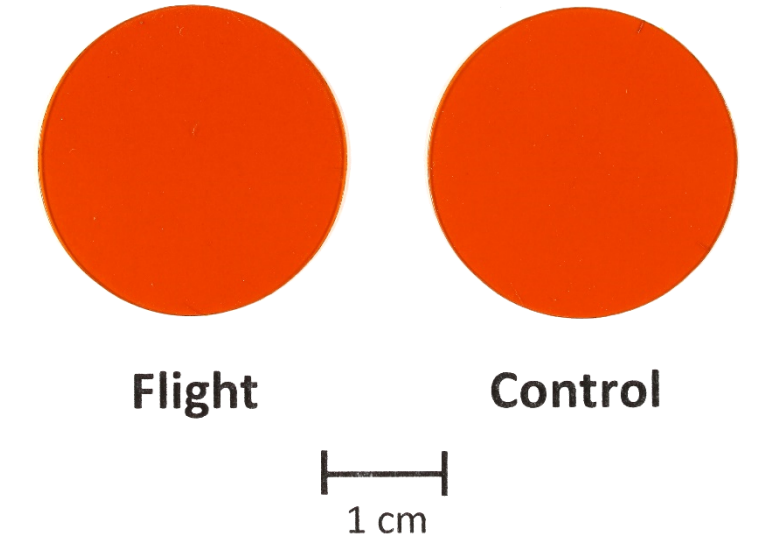

a.

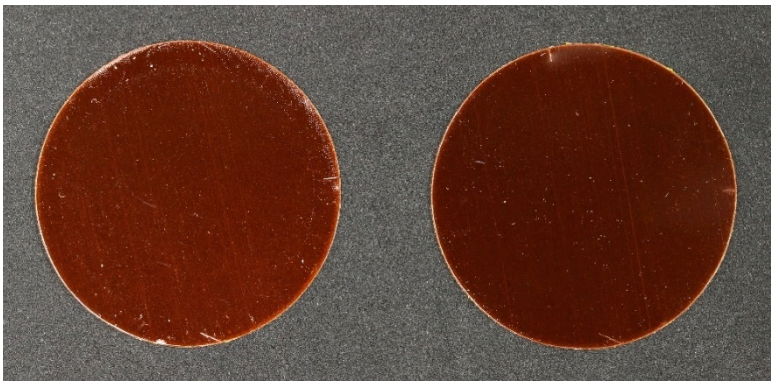

b.

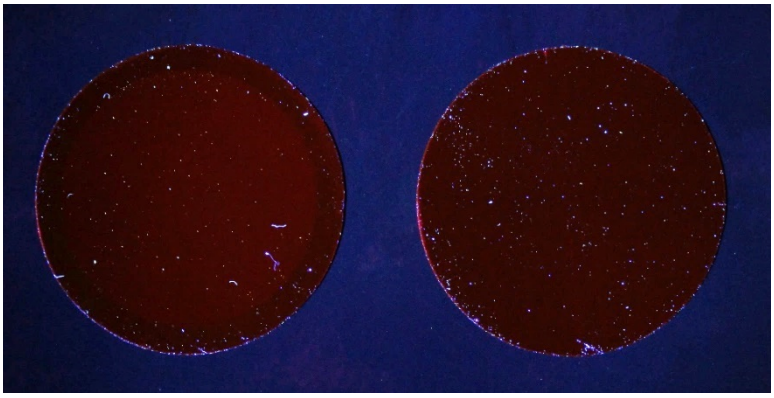

c.

Figure 32. Post-flight photographs of M9W-C1 F and M9W-C1 B. (a) Visible light image with a white background, (b) Visible light image with a dark background (M9W-C1 F on the left and M9W-C1 B on the right), and UV light (365 nm) image with M9W-C1 F on left and M9W-C1 B on the right.

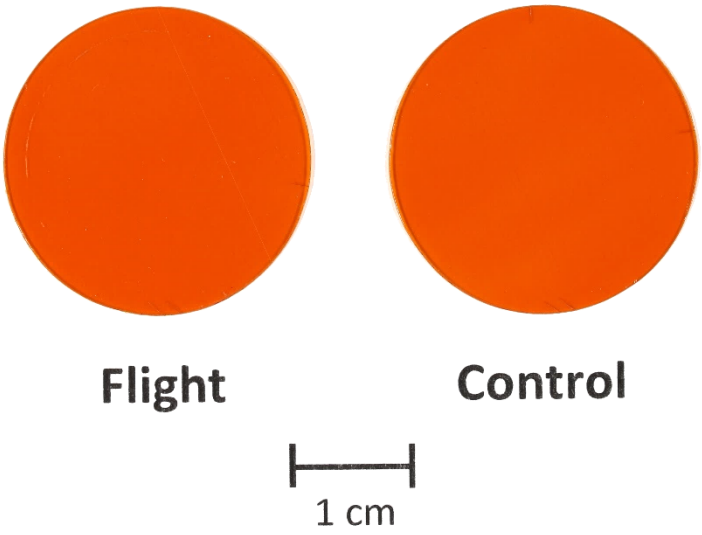

a.

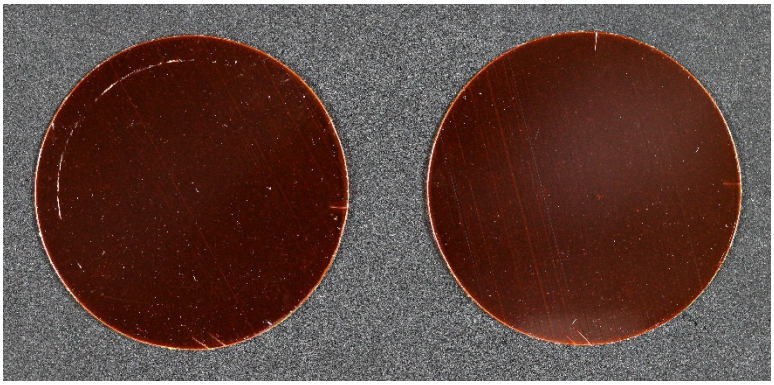

b.

Figure 33. Post-flight photographs of M9Z-C1 F and M9Z-C1 B. (a) Samples on a white background, and (b) Samples on a dark background (M9Z-C1 F on the left and M9Z-C1 B on the right).

Table 4. MISSE-9 PCE-1 Kapton H AO Fluence Witness Samples

Flight Orientation	**Sample ID**	**Thickness (inch)**	**Mass Loss (g)**	**Surface Area (cm^2)**	**Density (g/cm^3)**	**LEO AO E_y (cm^3/atom)**	**MISSE-9 AO Fluence (atoms/cm^2)**
Ram	M9R-C1 F Part A	0.005	0.005265	3.569	1.4273	3.00E-24	3.44E+20
Ram	M9R-C19 F Part A	0.005	0.005350	3.646	1.4273	3.00E-24	3.43E+20
Wake	M9W-C1 F	0.005	0.000001	3.488	1.4273	3.00E-24	4.46E+16
Zenith	M9Z-C1 F	0.005	0.000057	3.612	1.4273	3.00E-24	3.19E+18

Figure 34 provides post-flight photographs of the PCE-2 ram M10R-C1 F (flight) and M10R-C1 B (control) samples. Figure 34a shows both the Part A (top) and Part B (bottom) layers. Figure 34b shows the M10R-C1 F Part A and M10R-C1 B Part A samples on a dark background. The exposed eroded area of the M10R-C1 F Part A sample shows clearly in the dark background image. As can be seen in Figure 34c, under UV light the space exposed area of the flight sample is clearly defined, similar to the M9R-C1 F and M9R-C19 F samples.

Figure 35 provides post-flight photographs of the PCE-2 zenith M10Z-C1 F (flight) and M10Z-C1 B (control) samples. Figure 35a shows the samples on a white background. Figure 35b shows the samples on a dark background (M10Z-C1 F on the left and M10Z-C1 B on the right). And, Figure 35c shows the samples under UV light. There was no visual erosion or texturing of the flight sample. The only visible effects on the flight sample are holder marks on the perimeter. This is noticeable in the image on the dark background (Figure 35b). Under 365 nm UV light, the space exposed area of the flight sample is enhanced as shown in Figure 35c, even though there was no visible erosion or texturing of the flight sample.

Figure 36 provides post-flight photographs of the PCE-2 nadir M10N-C1 F (flight) and M10N-C1 B (control) samples. Figure 36a shows the samples on a white background. Figure 36b shows the samples on a dark background (M10N-C1 F on the left and M10N-C1 B on the right). And, Figure 36c shows the samples under UV light. There was no visual erosion or texturing of the flight sample. The only visible effects on the flight sample are holder marks on the perimeter. This is noticeable in the image on the dark background (Figure 36b). Under 365 nm UV light, only the flight sample's perimeter damage is shown (see Figure 36c). This is different than the zenith flight sample that shows a difference in the space exposed area as compared to the protected area under UV light, as shown in Figure 35c.

Table 5 provides a list of the MISSE-10 PCE-2 Kapton H AO Fluence Witness samples along with the sample film thickness, the dehydrated sample mass loss, LEO exposed surface area, Kapton H density and LEO E_y, and the computed MISSE-10 AO fluence for each flight sample. The AO fluence for the ram sample was 3.93×10^{20} atoms/cm^2. The MISSE-10 ram AO fluence (1.17 year direct space exposure) is a little higher than the AO fluence for the MISSE-9 ram mission (0.77 year direct space exposure). The AO fluence for the zenith sample was 4.84×10^{18} atoms/cm^2 based on a 0.075 mg mass loss. And, the AO fluence for the nadir sample was 6.94×10^{18} atoms/cm^2 based on a 0.106 mg mass loss. This slight increase in the AO fluence for the nadir sample as compared to the zenith sample is consistent with the MISSE-FF 8° "pitch up" rotation discussed in the *MISSE-FF Section* above. The MISSE-10 zenith AO fluence (0.69 year direct space exposure) is similar to the MISSE-9 zenith AO fluence (0.54 year direct space exposure).

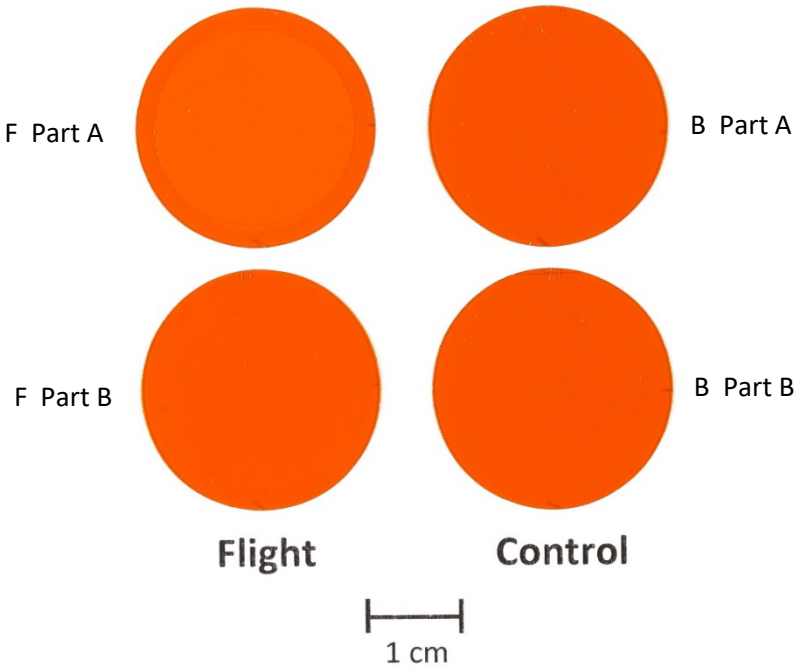

a.

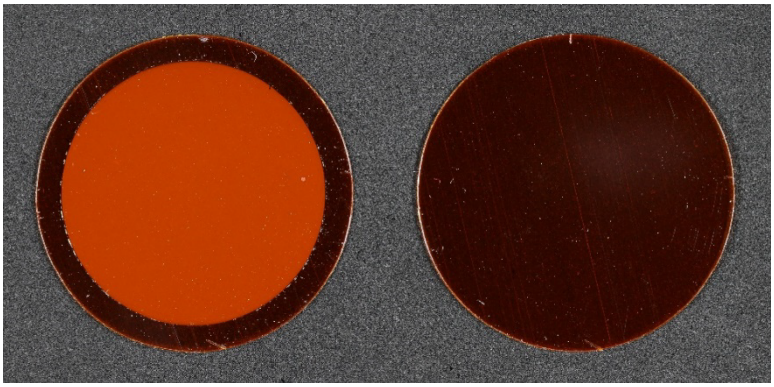

b.

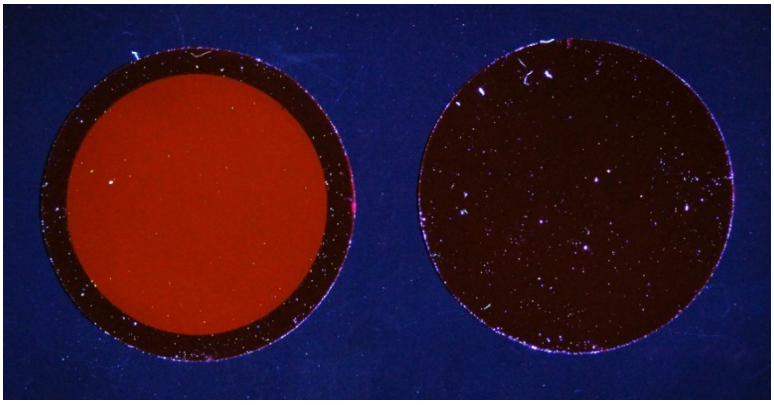

c.

Figure 34. Post-flight photographs of M10R-C1 F and M10R-C1 B. (a) Visible light image with both Part A (top layer) and Part B (bottom layer), (b) Visible light image (M10R-C1 F Part A on left and M10R-C1 B Part A on the right), and (c) UV light (365 nm) image with M10R-C1 F Part A on left and M10R-C1 B Part A on the right.

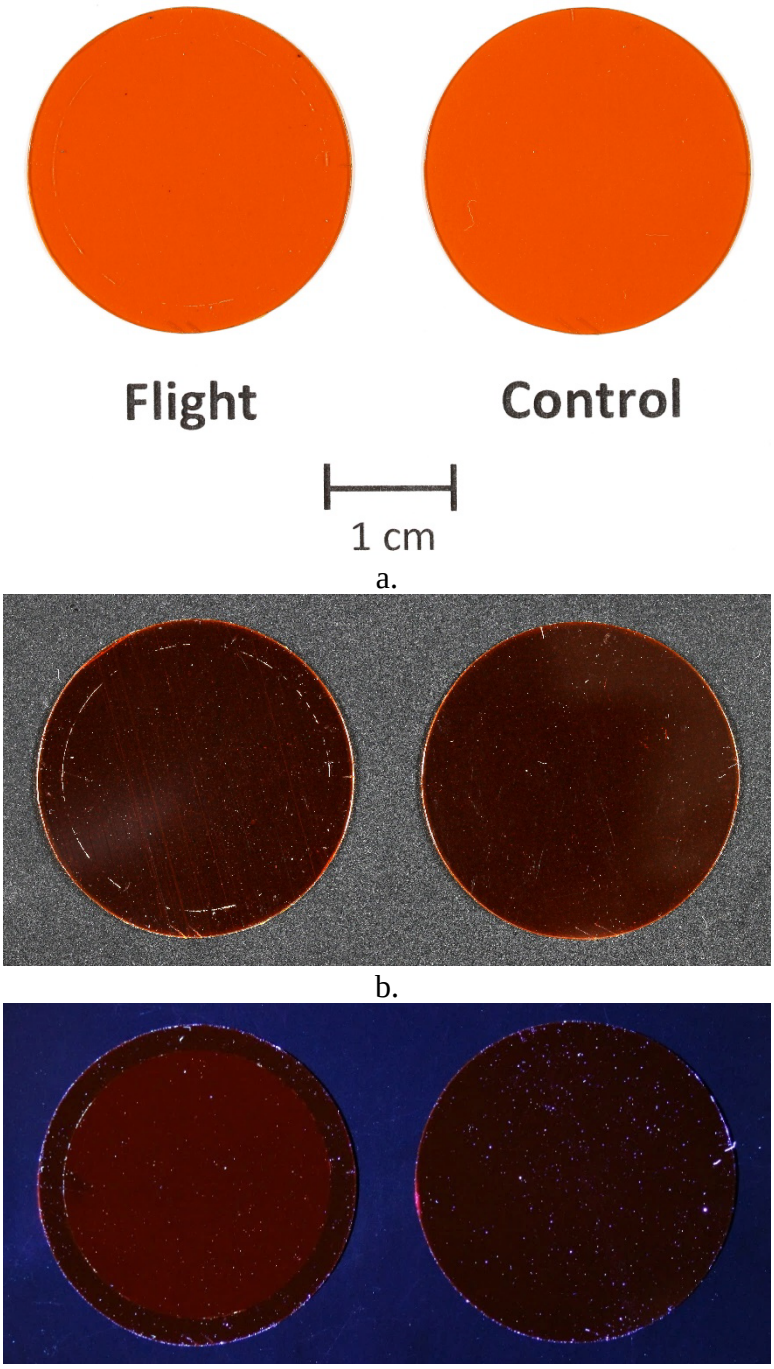

Figure 35. Post-flight photographs of M10Z-C1 F and M10Z-C1 B. (a) Samples on a white background, (b) Visible light image of samples on a dark background (M10Z-C1 F on the left and M10Z-C1 B on the right), and (c) UV light (365 nm) image with M10Z-C1 F on the left and M10Z-C1 B on the right.

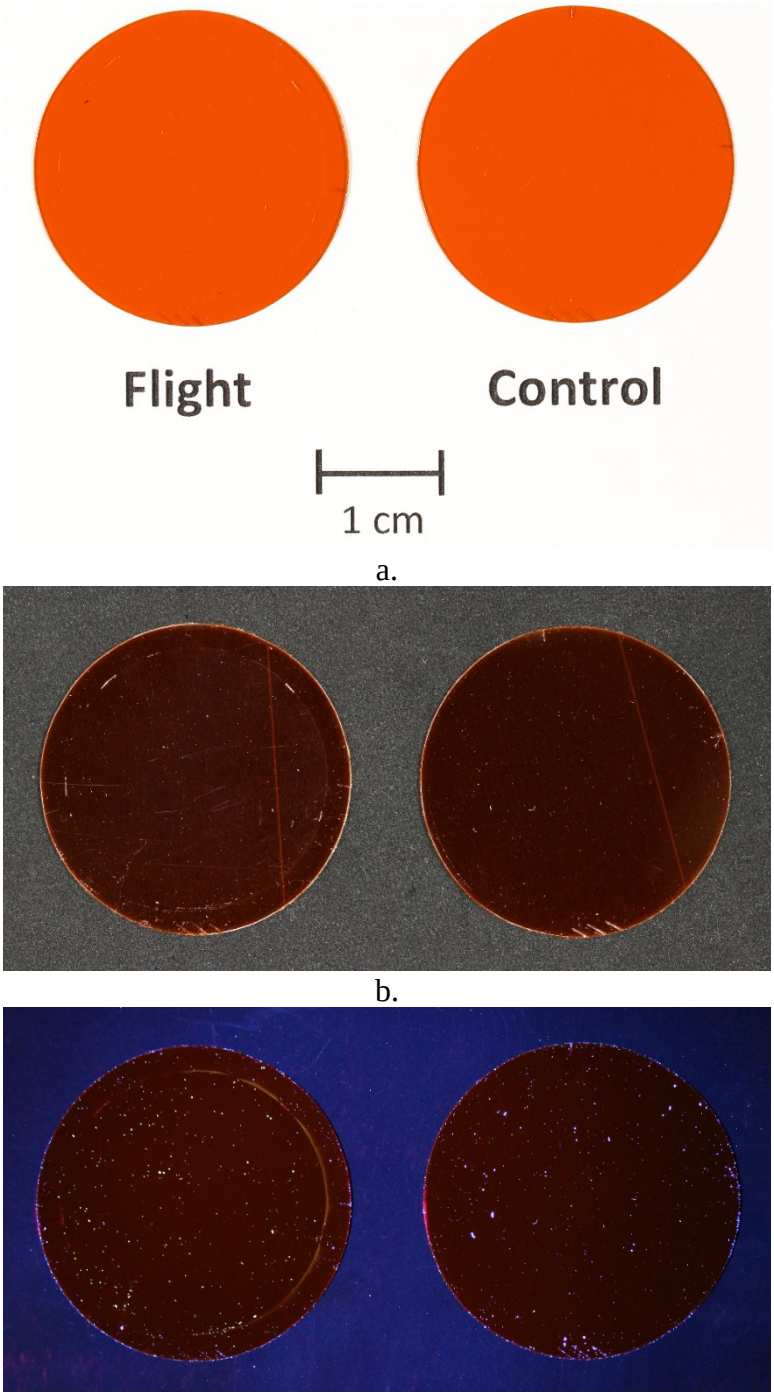

a.

b.

c.

Figure 36. Post-flight photographs of M10N-C1 F and M10N-C1 B. (a) Samples on a white background, (b) Visible light image of samples on a dark background (M10N-C1 F on the left and M10N-C1 B on the right), and (c) UV light (365 nm) image with M10N-C1 F on the left and M10N-C1 B on the right.

Table 5. MISSE-10 PCE-2 Kapton H AO Fluence Witness Samples

Flight Orientation	Sample ID	Thickness (inch)	Mass Loss (g)	Surface Area (cm^2)	Density (g/cm^3)	LEO AO *Ey* (cm^3/atom)	MISSE-10 AO Fluence (atoms/cm^2)
Ram	M10R-C1 F	0.005	0.005964	3.540	1.4273	3.00E-24	3.93E+20
Zenith	M10Z-C1 F	0.005	0.000075	3.602	1.4273	3.00E-24	4.84E+18
Nadir	M10N-C1 F	0.005	0.000106	3.567	1.4273	3.00E-24	6.94E+18

9.2.2 Photographic AO Fluence Monitors

Figure 37 provides post-flight images of the M10R-R1 F Photographic AO Fluence Monitor sample. As mentioned previously, this sample had a thin layer of carbon along with nine layers of 0.38 mil Kapton H. The carbon film thickness is assumed to be 720 Å, which is the thickness for the M10Z-C2 F film thickness witness sample. As can be seen in Figure 37a, the 1st Kapton H layer is completely eroded away (0.38 mil), and the 2nd layer is thinned significantly (compare to Figure 19). The 365 nm UV light image (Figure 37b) did not show anything significant. The AO fluence for erosion of 0.38 mil Kapton H (9.652 µm) is 3.22×10^{20} atoms/cm^2. The AO fluence for erosion of two 0.38 mil Kapton H layers (0.76 mils, 19.304 µm) is 6.43×10^{20} atoms/cm^2. Thus, the AO fluence based on visual erosion of the M10R-R1 F Photographic AO Fluence Monitor is between 3.22 to 6.43×10^{20} atoms/cm^2. The AO fluence for the ram Kapton H witness sample was 3.93×10^{20} atoms/cm^2, which is consistent. Because of the relatively low AO fluence and corresponding erosion of only one 0.38 mil Kapton layer, the intermittent AO fluence over time on-orbit (based on on-orbit images) was not determine for this, or any, of the PCE 2-4 Photographic AO Fluence Monitors.

Figure 38 provides post-flight images of the M10Z-C2 F sample (Carbon coated White Tedlar). This sample had a 720 Å thick carbon layer fully covering the white Tedlar substrate. There was no visible carbon erosion, as can be seen in Figures 38a and 38b, although the carbon appears to be slightly darkened. The 365 nm UV light image shown in Figure 38c shows a different in appearance in the exposed versus protected areas. It is difficult to tell if this is due to very slight erosion of the carbon or a possible contamination film (see the *Contamination Section* below), or both. The AO fluence for this sample was determined to be $<<1.73 \times 10^{19}$ atoms/cm^2 based on no visual erosion of the 720 Å carbon film. This is consistent with the AO fluence for the zenith Kapton H witness sample, which is 4.84×10^{18} atoms/cm^2.

Figure 39 provides post-flight images of the M10N-S1 F Photographic AO Fluence Monitor. As mentioned previously, this sample had a thin layer of carbon along with three layers of 0.103 mil (2.616 µm) Kapton H. The carbon film thickness is assumed to be 720 Å. As can be seen in Figure 39a, the carbon layer has some erosion but is not completely gone, and the first Kapton H layer is still intact (and is shiny), indicating very little erosion. The 365 nm UV light image (Figure 39b) did not show anything significant. The AO fluence for this sample was determined

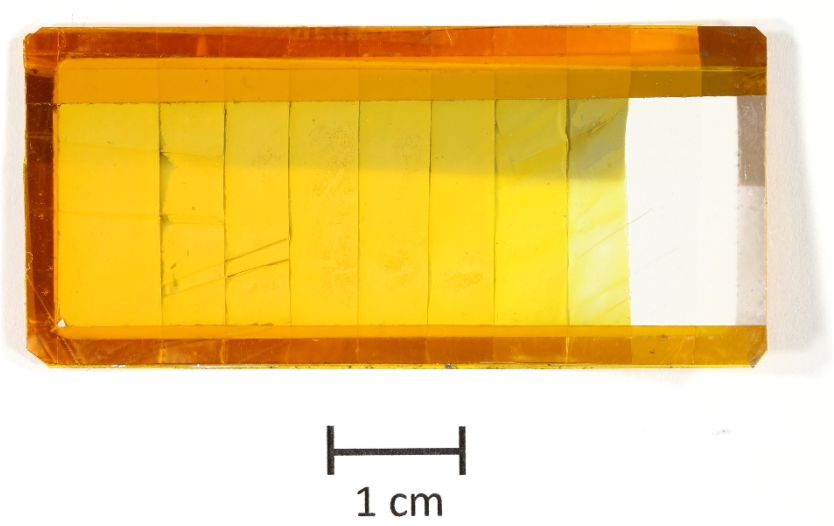

a.

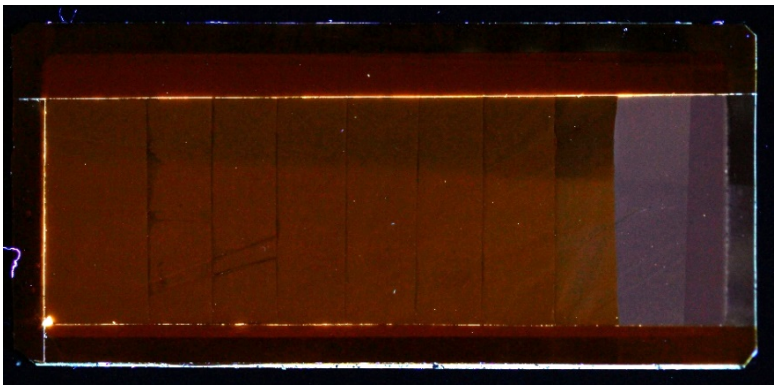

b.

Figure 37. Post-flight photographs of M10R-R1 F. (a) Visible light image, and (b) UV light (365 nm) image.

to be $<1.73 \times 10^{19}$ atoms/cm^2 based on partial erosion of the 720 Å thick carbon film. This is consistent with the AO fluence for the nadir Kapton H witness sample, which is 6.94×10^{18} atoms/cm^2.

Table 6 provides a list of the MISSE-10 PCE-2 Photographic AO Fluence Monitors along with the sample material (Kapton H or carbon) and material thickness used to compute AO fluence, the Kapton H or carbon LEO E_y, and the computed MISSE-10 ram, zenith and nadir AO fluences. As stated previously, the LEO E_y for the carbon film was assumed to be the same as the MISSE 2 E_y for pyrolytic graphite (4.15×10^{-25} cm^3/atom).[2,17]

More accurate AO fluence values could be determined for the MISSE-10 Photographic AO Fluence Monitors using erosion depth techniques. But, these additional analyses were not conducted because dehydrated mass loss based AO fluence values were determined for these missions from the Kapton H witness samples.

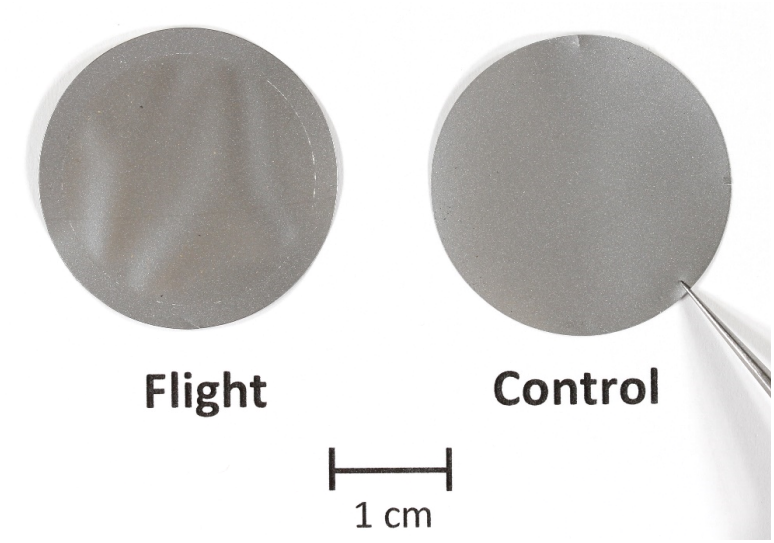

a.

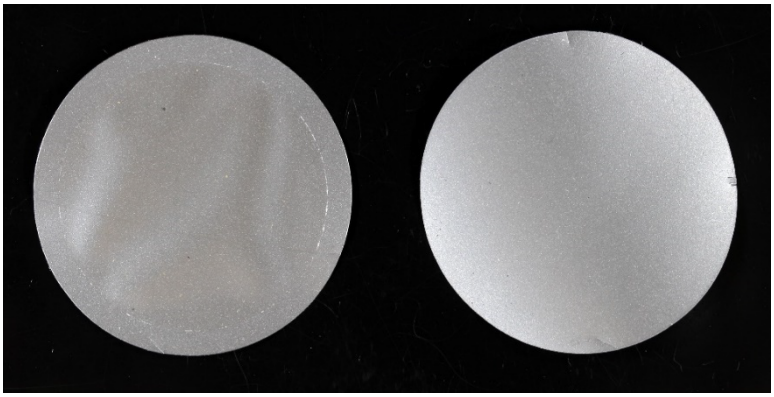

b.

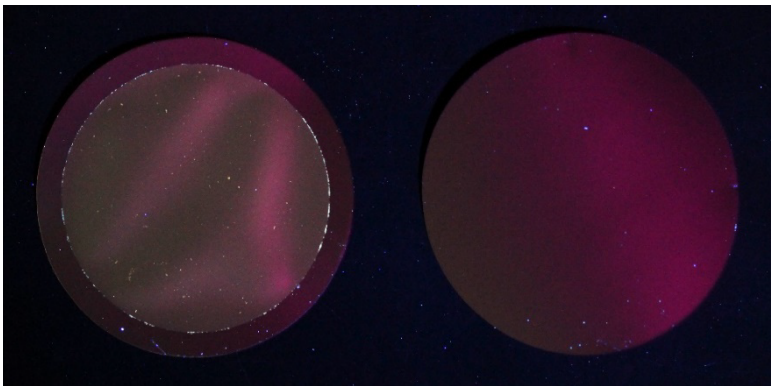

c.

Figure 38. Post-flight photographs of M10Z-C2 F and M10Z-C2 B. (a) Samples on a white background, (b) Visible light image of samples on a dark background (M10Z-C2 F on the left and M10Z-C2 B on the right), and (c) UV light (365 nm) image with M10Z-C2 F on the left and M10Z-C2 B on the right.

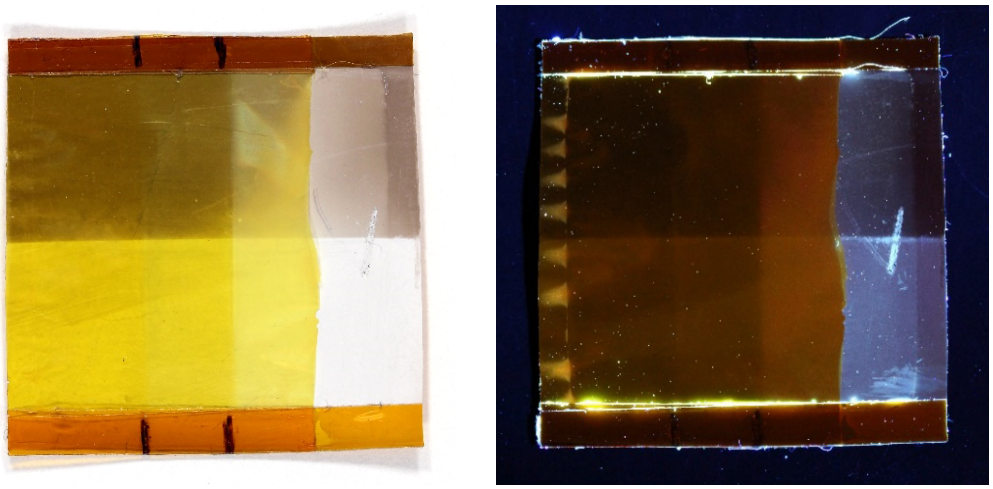

a. b.

Figure 39. Post-flight photographs of M10N-S1 F. (a) Visible light image, and (b) UV light (365 nm) image.

Table 6. MISSE-10 PCE-2 Photographic AO Fluence Monitors

Flight Orientation	Sample ID	Material	Material and Thickness Analyzed	LEO AO *Ey* (cm^3/atom)	MISSE-10 AO Fluence (atoms/cm^2)
Ram	M10R-R1 F	AO Photo Monitor (0.3 mil Kapton H)	0.00038 inch Kapton H	3.00E-24	3.22E+20 - 6.43+20
Zenith	M10Z-C2 F	Carbon (720 Å) coated White Tedlar	720 Å Carbon	4.15E-25*	<<1.73E+19
Nadir	M10N-S1 F	AO Photo Monitor (≈0.1 mil Kapton H)	720 Å Carbon	4.15E-25*	<1.73E+19

*E_y for carbon based on MISSE-2 pyrolytic graphite (PG) E_y

9.3 MISSE-12 PCE-3

Two Kapton H AO fluence witness samples were flown as part of the MISSE-12 PCE-3: M12R-C1 F in ram and M12W-C1 F in wake. A zenith Kapton H AO fluence witness sample was not included. The PCE-3 also included three Photographic AO Fluence Monitors: M12R-S1 F and M12R-S2 F were flown in ram and M12Z-S1 F was flown in zenith.

9.3.1 Kapton H AO Fluence Witness Samples

The ram Kapton H sample (M12R-C1 F) had two 5 mil thick (0.0127 cm) layers stacked together for flight: Part A and Part B. Erosion only occurred in the top layer (Part A). Because the layers were weighed separately pre-flight, only the mass loss of the Part A layer was used for computing the AO fluence for the ram flight sample. The wake Kapton H sample only had one 5 mil layer flown.

Figure 40 provides post-flight photographs of the PCE-3 ram M12R-C1 F (flight) and M12R-C1 B (control) samples. Figure 40a shows both the Part A (top) and Part B (bottom) layers. Figure 40b shows the M12R-C1 F Part A and M12R-C1 B Part A samples on a dark background. And, Figure 40c shows the Part A samples under UV light. The exposed eroded area of the M12R-C1 F Part A sample shows clearly in Figure 40b. Under 365 nm UV light the space exposed area of the flight sample is clearly defined (Figure 40c), similar to the M9R-C1 F, M9R-C19 F, M10R-C1 F samples.

As previously mentioned, the MISSE-12 wake samples were not directly exposed to the space environment during the MISSE-12 mission. The samples were re-flown and exposed to the space environment during the MISSE-15 mission. Thus, the M12W-C1 F Kapton H AO Fluence Witness sample is discussed in the *MISSE-12* and *MISSE-15 PCE-3 Wake* section.

Table 7 provides a list of the MISSE-12 PCE-3 Kapton H AO Fluence Witness samples. The table includes the ram sample film thickness, dehydrated sample mass loss, LEO exposed surface area, Kapton H density and LEO E_y, and the computed MISSE-12 ram AO fluence.

9.3.2 Photographic AO Fluence Monitors

Figure 41 provides post-flight images of the M12R-S1 F Photographic AO Fluence Monitor. As mentioned previously, this sample had a thin layer of carbon (780 Å) along with three layers of 0.38 mil Kapton H. As can be seen in Figure 41a, the carbon film is completely removed. This visible light image also indicates that the first (bottom) Kapton H layer appears to be completely eroded away (0.38 mil), and the second layer is textured but intact. The 365 nm UV light image (Figure 41b) was interesting as it appears to show traces of ultra-thin Kapton H still present from the first layer, which is not visible in Figure 41a. The AO fluence for this sample was based on the visual Kapton erosion. The AO fluence for erosion of 0.38 mil Kapton H (9.652 μm) is 3.22×10^{20} atoms/cm^2. But, since the UV light image indicates a trace amount of Kapton H is remaining, the AO fluence is slightly less than 3.22×10^{20} atoms/cm^2. Thus, the AO fluence for this sample based on visual erosion of the first Kapton H layer is probably $\approx 3.0 \times 10^{20}$ atoms/cm^2, but is reported as $< 3.22 \times 10^{20}$ atoms/cm^2. The AO fluence for the ram Kapton H witness sample was 2.97×10^{20} atoms/cm^2, which is consistent.

Figure 42 provides post-flight images of the M12R-S2 F Photographic AO Fluence Monitor. As mentioned previously, this sample had a thin layer of carbon (780 Å) along with three layers of 0.57 mil Kapton H. As can be seen in Figure 42a, the carbon film is completely removed and the first (bottom) Kapton H layer appears to be textured but still intact. The 365 nm UV light image (Figure 42b) also indicates that the first layer of Kapton H is still present. Based on visual erosion, the AO fluence would be $< 4.83 \times 10^{20}$ atoms/cm^2, the AO fluence to erode 0.57 mil (14.478 μm) of Kapton H.

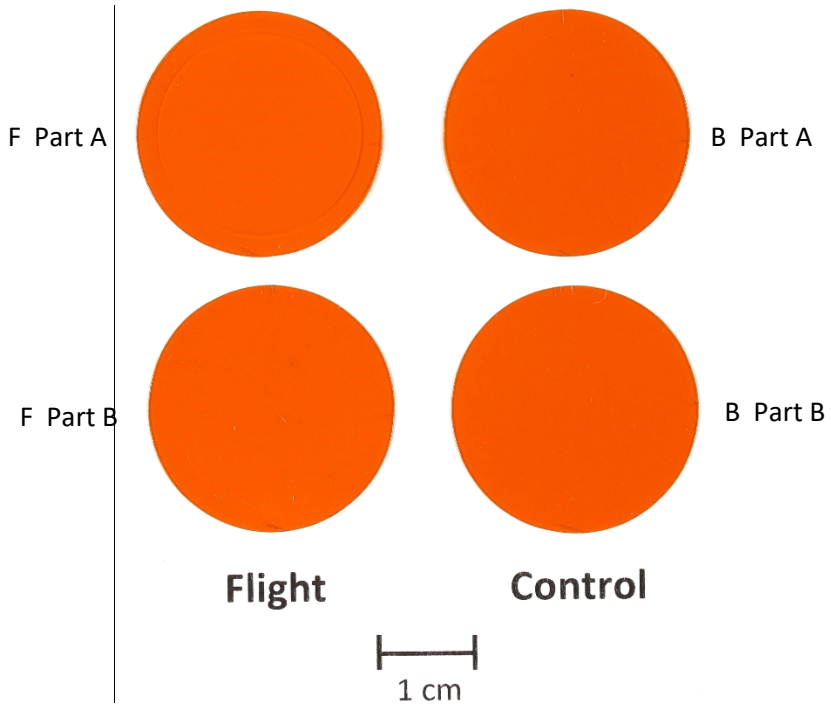

a.

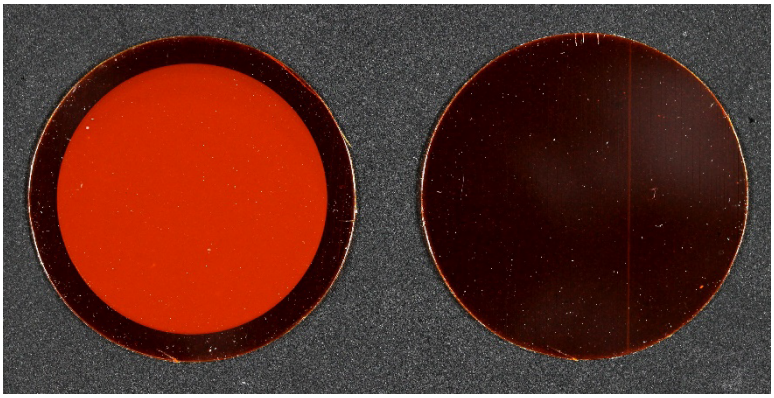

b.

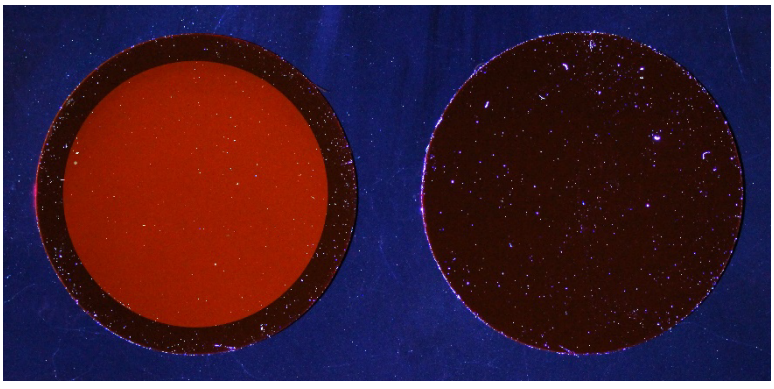

c.

Figure 40. Post-flight photographs of M12R-C1 F and M12R-C1 B. (a) Visible light image with both Part A (top layer) and Part B (bottom layer), (b) Visible light image (M12R-C1 F Part A on left and M12R-C1 B Part A on the right), and (c) UV light (365 nm) image with M12R-C1 F Part A on left and M12R-C1 B Part A on the right.

Table 7. MISSE-12 PCE-3 Kapton H AO Fluence Witness Samples

Flight Orientation	Sample ID	Thickness (inch)	Mass Loss (g)	Surface Area (cm^2)	Density (g/cm^3)	LEO AO E_y (cm^3/atom)	MISSE-12 AO Fluence (atoms/cm^2)
Ram	M12R-C1 F	0.005	0.004451	3.498	1.4273	3.00E-24	2.97E+20
Wake	M12W-C1 F	0.005	***Not exposed during MISSE-12 - Re-flown on MISSE-15***				

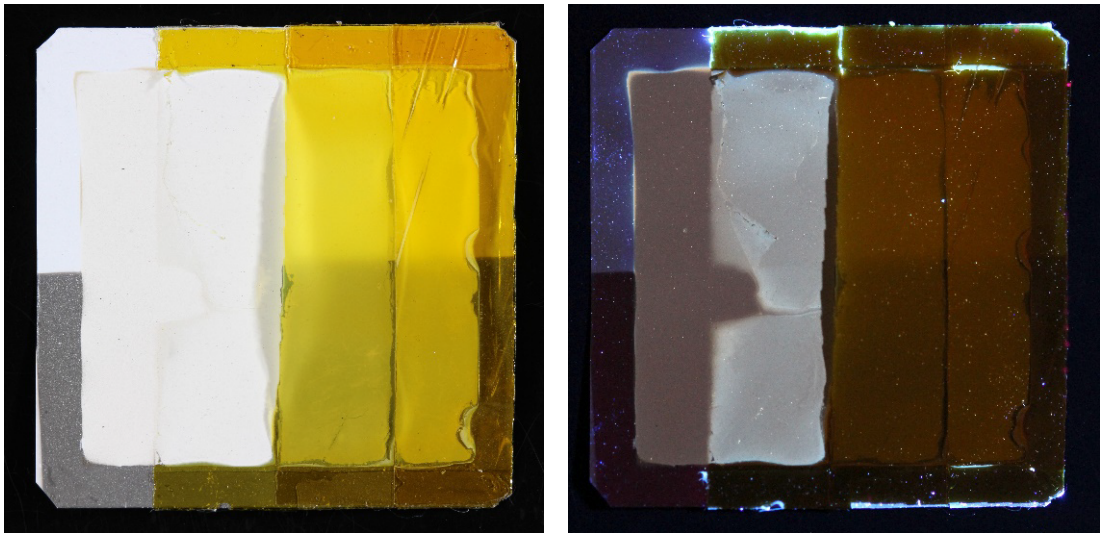

a. b.

Figure 41. Post-flight photographs of M12R-S1 F. (a) Visible light image, and (b) UV light (365 nm) image.

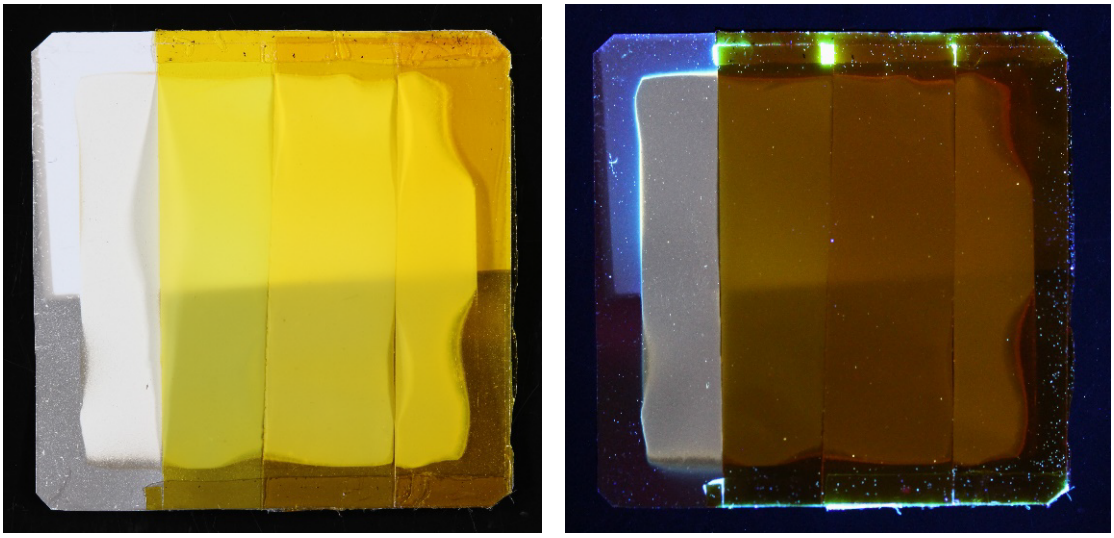

a. b.

Figure 42. Post-flight photographs of M12R-S2 F. (a) Visible light image, and (b) UV light (365 nm) image.

The M12R-S2 F Photographic AO Fluence Monitor was imaged with a Zygo Nexview™ NX2 3D Optical Profiler to get erosion depth (recession depth) based AO fluence measurements. A total of three scans at the exposed/protected Kapton border were used to compute erosion depth based AO fluence. An example of one of the scans (Scan 2) is provided in Figure 43. The scans were adjusted to avoid the deep perimeter trench. It is common for samples to have a somewhat deeper eroded "trench" at the perimeter of the sample due to scattering effects from the holder's 45° chamfer edge.[34] The Zygo data is provided in Table 8. The average AO fluence for the three fluence values is 3.13×10^{20} atoms/cm^2. This AO fluence is a little higher than the mass loss based AO fluence determined with the Kapton H witness sample which was 2.97×10^{20} atoms/cm^2. This may be due to edge effects.

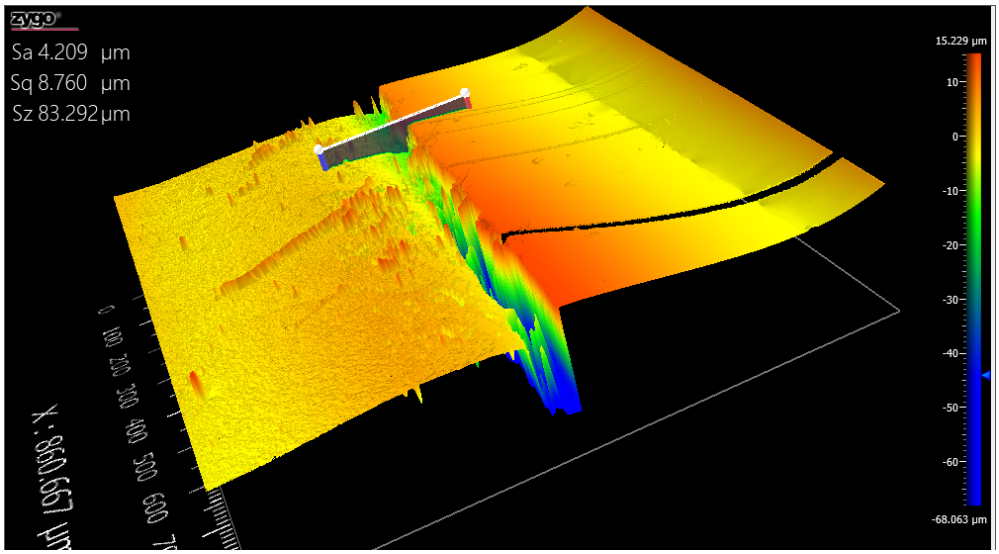

a.

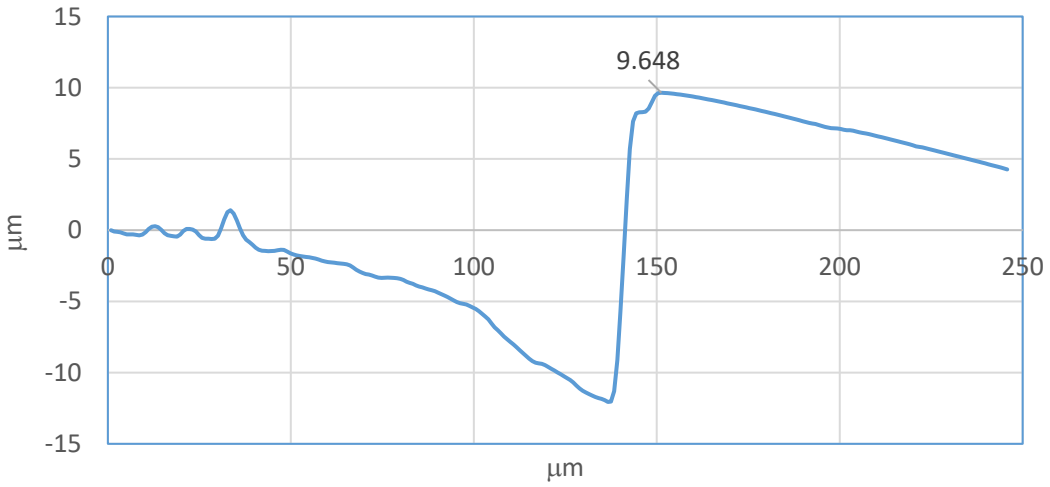

b.

Figure 43. Zygo optical image and corresponding line profile scan of M12R-S2 F at a protected-eroded Kapton H edge. (a) 3D optical image, and (b) Line profile of the section highlighted in the SD image.

Table 8. M12R-S2 F Zygo Optical Step-Height Based AO Fluence

Zygo Scan #	Zygo Step-Height (μm)	Zygo Step-Height (cm)	Kapton LEO AO E_y (cm^3/atom)	MISSE-12 AO Fluence (atoms/cm^2)
Scan 1	8.892	0.000889	3.00E-24	2.96E+20
Scan 2	9.648	0.000965	3.00E-24	3.22E+20
Scan 3	9.615	0.000962	3.00E-24	3.21E+20

The M12R-S2 F Photographic AO Fluence Monitor was also imaged using the Tescan MAIA3 FESEM. The sample was coated with a 10 nm Pt conductive coating prior to imaging. Images were taken at 0°, 30° and 45° tilt angles to show the AO erosion texture of the top Kapton H layer. Figure 44 provides images of the protected and exposed regions of M12R-S2 F. Figure 44a is a 0° tilt image (80kX effective pixel magnification) of the protected region showing a smooth surface with no texture. Figure 44b is a 0° tilt image (80kX effective pixel magnification) of the exposed region showing the erosion texture. Figures 44c and 44d are 30° tilt and 45° tilt images, respectively, showing the Kapton H ram erosion texture. These high aspect ratio erosion "cones" are typical of the erosion texture of Kapton exposed to LEO ram AO.

Figure 45 provides post-flight images of the M12Z-S1 F Photographic AO Fluence Monitor. This sample had a thin layer of carbon (780 Å) along with three layers of 0.38 mil Kapton H. As can be seen in Figure 45a, both the carbon film and the first layer of Kapton H appear intact. The most noticeable change is discoloration of the white Tedlar in the exposed region. The 365 nm UV light image (Figure 45b) also shows a change in the white Tedlar appearance. The AO fluence for erosion of the 780 Å thick carbon film would be 1.88×10^{19} atoms/cm^2. Thus, the AO fluence based on visual observations would be $<1.88 \times 10^{19}$ atoms/cm^2. Because a Kapton H AO Fluence witness sample was not flown in the MISSE-12 zenith direction, additional analyses were conducted on this sample to get a more accurate AO fluence value.

The M12Z-S1 F Photographic AO Fluence Monitor was imaged with a Zygo Nexview™ NX2 3D Optical Profiler, but step-height measurements were not obtained. The sample was then imaged using a Tescan MAIA3 Field Emission Scanning Electron Microscope (FESEM). The sample was coated with a 5 nm Pt conductive film. The erosion texture of the Kapton H layers was found to be very fine and "step-height" measurements were not able to be obtained with the FESEM.

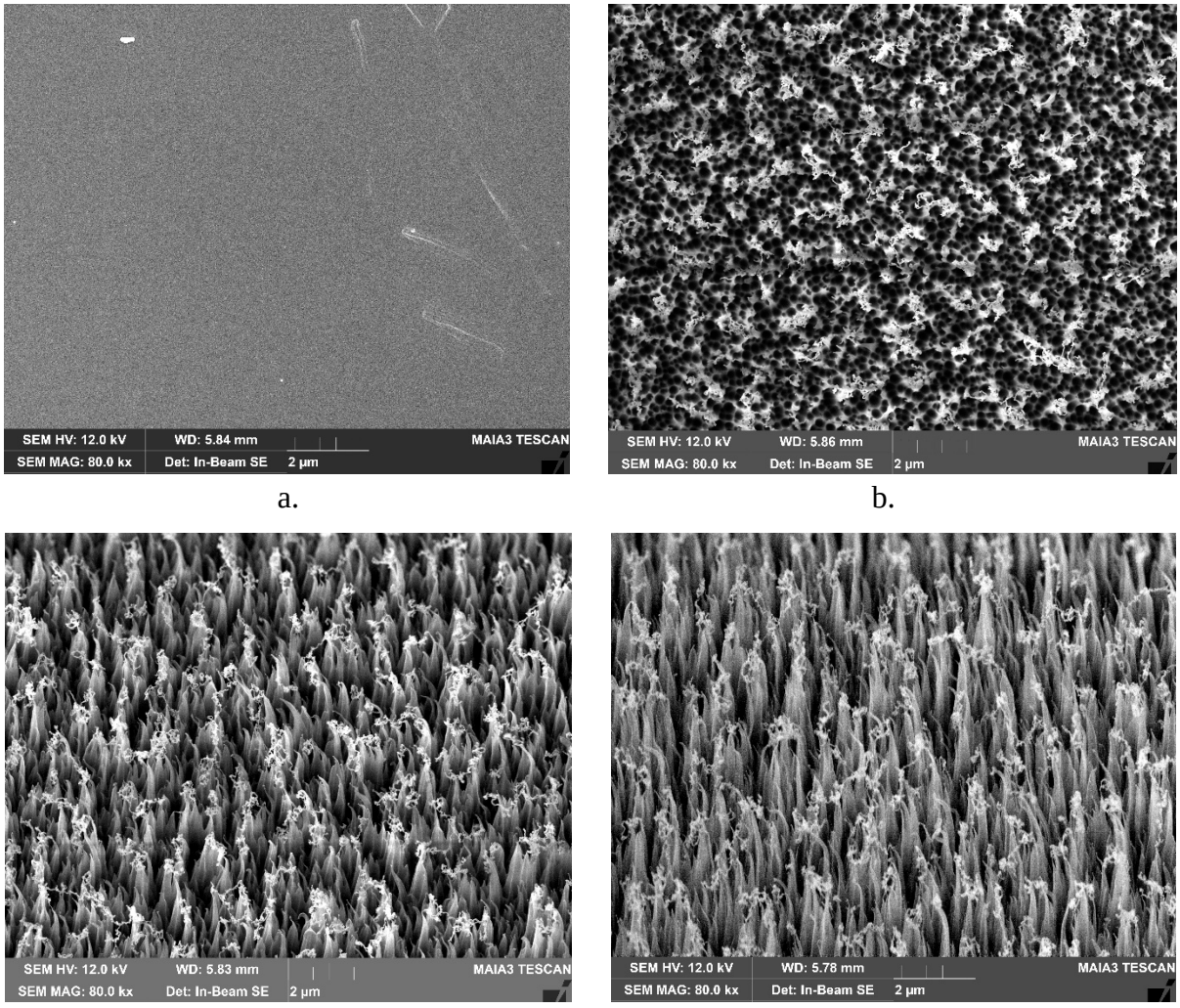

Figure 44. FESEM images the Kapton H layer of the M12R-R2 F AO Photo Monitor. (a) Protected region at 0° tilt (80kX), (b) Exposed region at 0° tilt (80kX), (c) Exposed region at 30° tilt (80kX), and (d) Exposed region at 45° tilt (80kX).

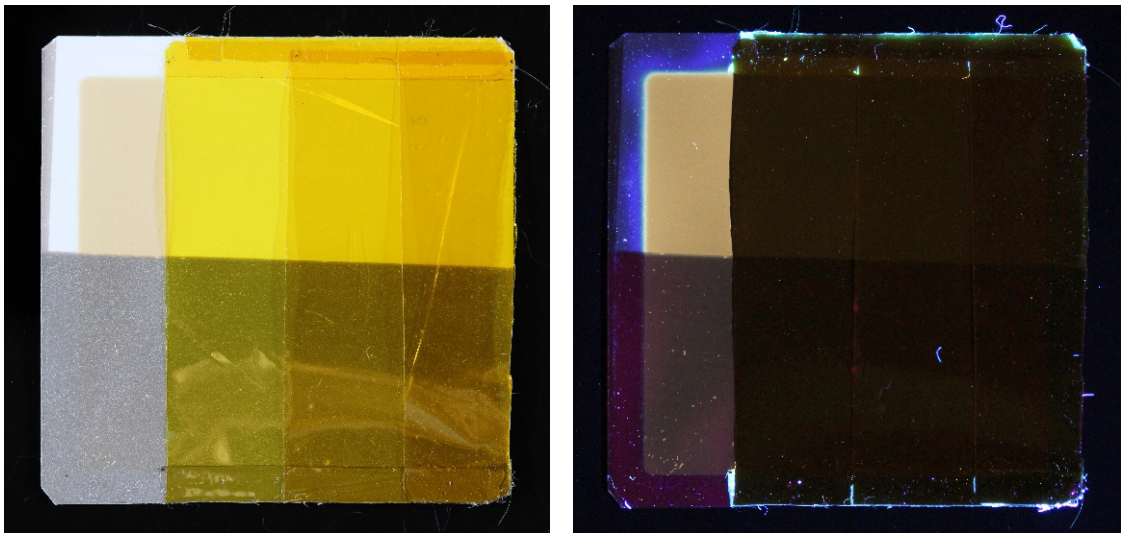

a. b.

Figure 45. Post-flight photographs of M12Z-S1 F. (a) Visible light image, and (b) UV light (365 nm) image.

Figure 46 provides FESEM images of the Kapton layers of M12Z-S1 F. Figure 46a is a low magnification image at the exposed/protected border of the top Kapton H layer. This image shows that some erosion texturing occurred in the exposed region (right side of image). Figure 46b and Figure 46c provide high magnification images (300kX effective pixel magnification) of the protected and exposed areas, respectively. A very fine erosion texture is observed in the exposed area, as shown in Figure 46c. Based on this fine texture, the erosion depth was estimated to be ≈50 nm, about the size of the texture "islands". Based on 50 nm erosion of Kapton H, the AO fluence for this sample is estimated to be $\approx 1.67 \times 10^{18}$ atoms/cm^2.

Table 9 provides a list of the MISSE-12 PCE-3 Photographic AO Fluence Monitors along with the sample material (Kapton H) and material thickness used to compute AO fluence, as described above, the Kapton H LEO E_y, and the computed MISSE-12 ram and zenith AO fluences.

9.4 MISSE-13 PCE-4

Two Kapton H AO fluence witness samples were flown as part of the MISSE-13 PCE-4: M13W-C1 F in wake and M13Z-C1 F in zenith. There were no PCE-4 ram samples. The PCE-4 also included two Photographic AO Fluence Monitors: M13W-S1 F flown in the wake direction and M13Z-S1 F flown in the zenith direction.

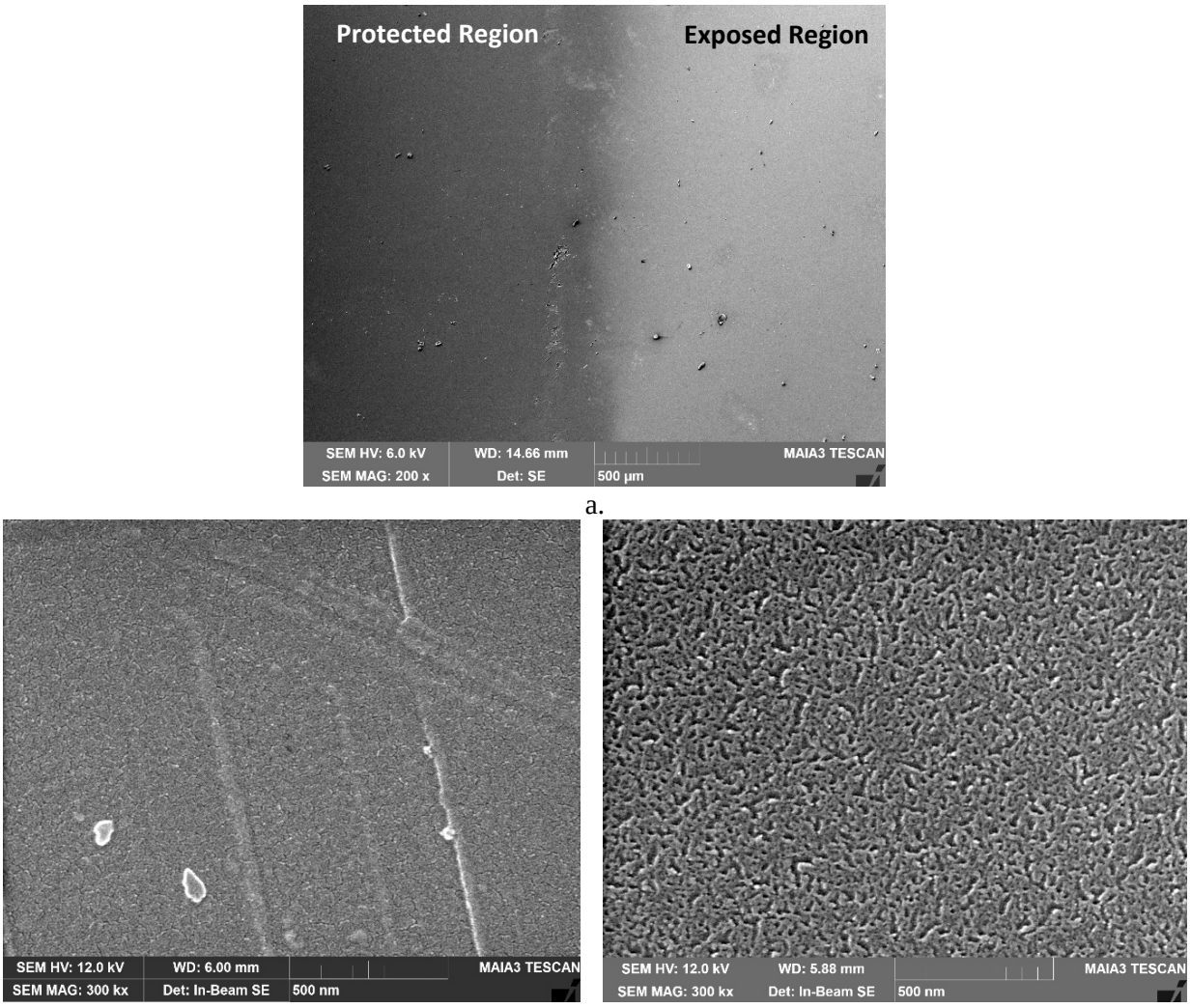

Figure 46. FESEM images the Kapton H layer of the M12Z-Z1 F AO Photo Monitor. (a) 200X at the exposed-protected border, (b) 300kX in the protected region, and (c) 300kX in the exposed region.

Table 9. MISSE-12 PCE-3 Photographic AO Fluence Monitors

Flight Orientation	MISSE-FF Sample ID	Material	Material and Thickness Analyzed	LEO AO E_y (cm^3/atom)	MISSE-12 AO Fluence (atoms/cm^2)
Ram	M12R-S1 F	AO Photo Monitor 1 (0.3 mil Kapton H)	0.00038 inch Kapton H	3.00E-24	<3.22E+20 (≈3.0E+20)
Ram	M12R-S2 F	AO Photo Monitor 2 (0.5 mil Kapton H)	0.00057 inch Kapton H	3.00E-24	3.13E+20
Zenith	M12Z-S1 F	AO Photo Monitor (0.3 mil Kapton H)	0.00038 inch Kapton H	3.00E-24	≈1.67E+18

9.4.1 Kapton H AO Fluence Witness Samples

Figure 47 provides post-flight photographs of the PCE-4 wake M13W-C1 F (flight) and M13W-C1 B (control) samples. Figure 47a shows the samples on a white background. Figure 47b shows the samples on a dark background (M13W-C1 F on the left and M13W-C1 B on the right). And, Figure 47c shows the samples under UV light. There was no visual erosion or texturing of the flight sample. The only visible effects on the flight sample are holder marks on the perimeter. This is noticeable in the image on the dark background (Figure 47b). Under 365 nm UV light, and with increased image brightness, the space exposed area of the flight sample is enhanced as shown in Figure 47c, even though there was no visible erosion or texturing of the flight sample.

Figure 48 provides post-flight photographs of the PCE-4 zenith M13Z-C1 F (flight) and M13Z-C1 B (control) samples. Figure 48a shows the samples on a white background. Figure 48b shows the samples on a dark background (M13Z-C1 F on the left and M13Z-C1 B on the right). And, Figure 48c shows the samples under UV light. There was no visual erosion or texturing of the flight sample. The only visible effects on the flight sample are holder marks on the perimeter. This is noticeable in the image on the dark background (Figure 48b). Under 365 nm UV light the space exposed area of the flight sample is enhanced as shown in Figure 48c, even though there was no visible erosion or texturing of the flight sample. The UV enhancement appeared more pronounced than for the M13W-C1 F wake sample.

Table 10 provides a list of the MISSE-13 PCE-4 Kapton H AO Fluence Witness samples. The table includes the sample film thickness, dehydrated sample mass loss, LEO exposed surface area, Kapton H density and LEO E_y, and the computed MISSE-13 AO fluence for the wake and zenith directions.

9.4.2 Photographic AO Fluence Monitors

Figure 49 provides post-flight images of the M13W-S1 F and M13W-S1 B Photographic AO Fluence Monitors. These samples had a thin layer of carbon (716 Å) along with one layer of 0.38 mil Kapton H. As can be seen in Figure 49a, both the carbon film and the Kapton H layer appears intact in the flight sample (left). The flight sample appears to have two finger rubbed areas in the carbon area and the white Tedlar is discolored a brownish-tan color, similar to the MISSE-12 zenith Photographic AO Fluence Monitor (M12Z-S1 F). Also, the exposed carbon area appears slightly discolored. The 365 nm UV light image (Figure 49b) shows a change in the white Tedlar appearance (much brighter), similar to the M12Z-S1 F sample. The AO fluence for erosion of a 716 Å thick carbon film would be 1.73×10^{19} atoms/cm^2. So, the AO fluence based on visual observations would be $<<1.73 \times 10^{19}$ atoms/cm^2. The AO fluence for the MISSE-13 wake Kapton H witness sample (M13W-C1 F) was 2.65×10^{18} atoms/cm^2, which is consistent.

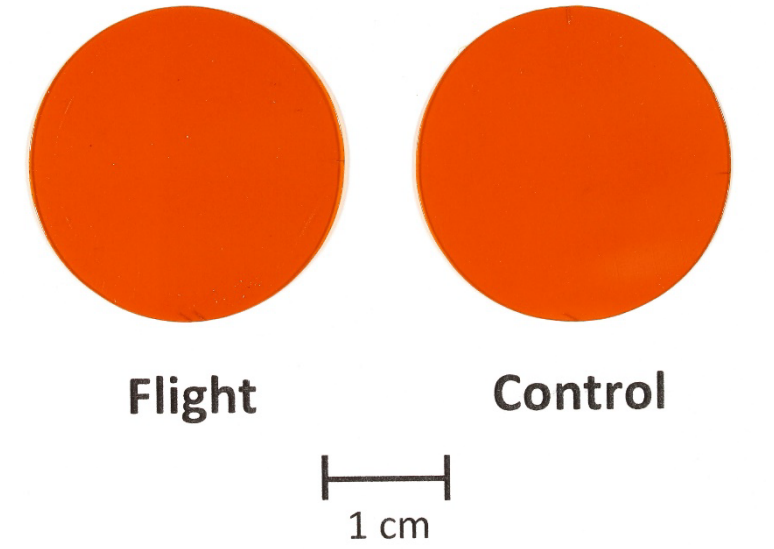

a.

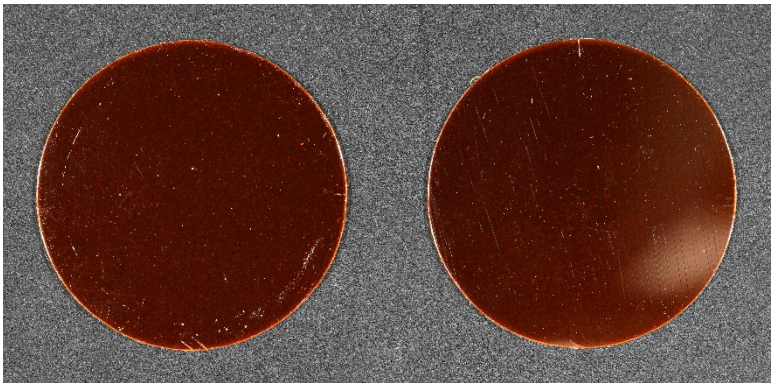

b.

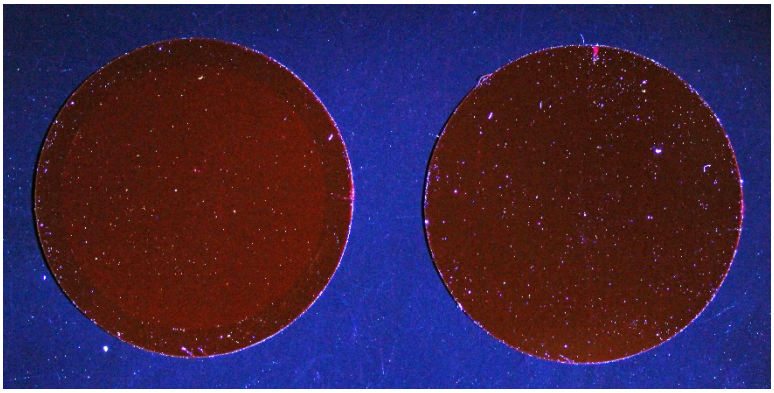

c.

Figure 47. Post-flight photographs of M13W-C1 F and M13W-C1 B. (a) Samples on a white background, (b) Visible light image of samples on a dark background (M13W-C1 F on the left and M13W-C1 B on the right), and (c) UV light (365 nm) image with M13W-C1 F on the left and M13W-C1 B on the right.

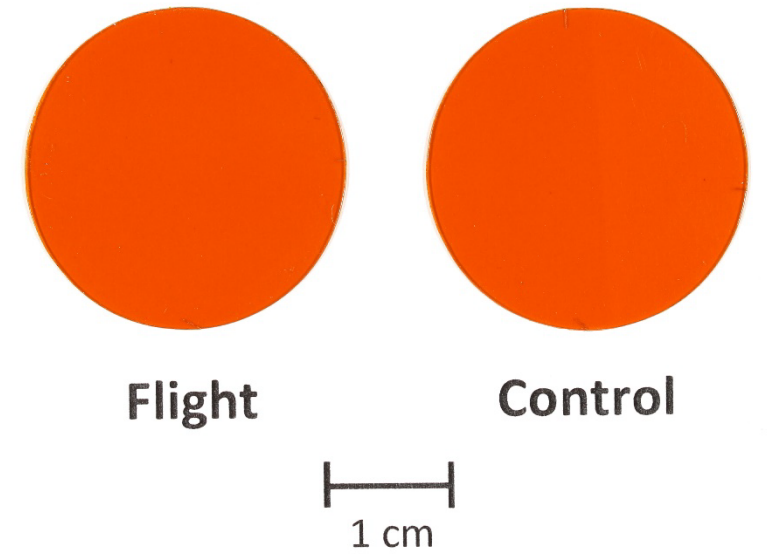

a.

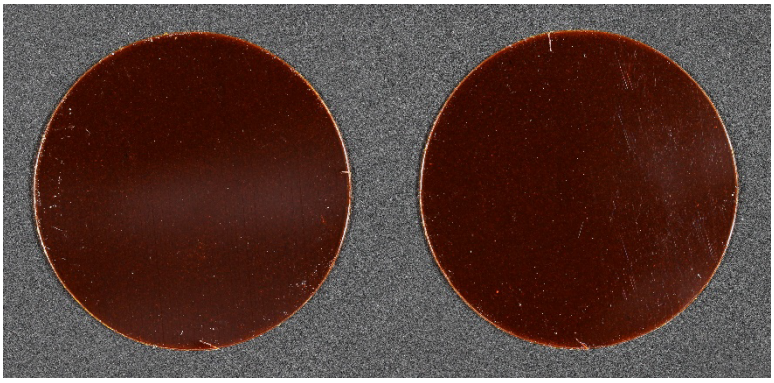

b.

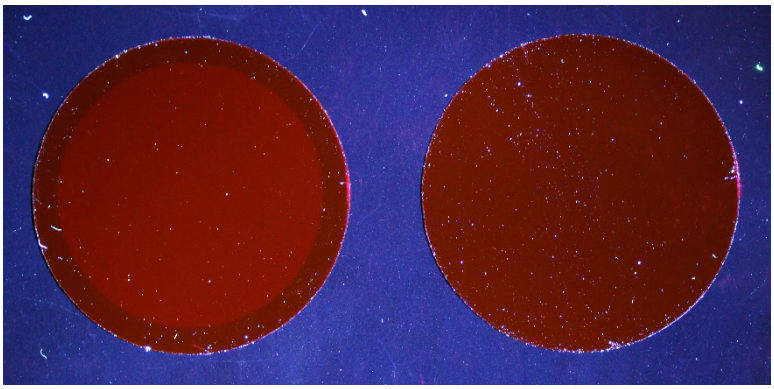

c.

Figure 48. Post-flight photographs of M13Z-C1 F and M13Z-C1 B. (a). Samples on a white background, (b). Visible light image of samples on a dark background (M13Z-C1 F on the left and M13Z-C1 B on the right), and (c). UV light (365 nm) image with M13Z-C1 F on the left and M13Z-C1 B on the right.

Table 10. MISSE-13 PCE-4 Kapton H AO Fluence Witness Samples

Flight Orientation	Sample ID	Thickness (inch)	Mass Loss (g)	Surface Area (cm^2)	Density (g/cm^3)	LEO AO E_y (cm^3/atom)	MISSE-13 AO Fluence (atoms/cm^2)
Wake	M13W-C1 F	0.005	0.000040	3.528	1.4273	3.00E-24	2.65E+18
Zenith	M13Z-C1 F	0.005	0.000034	3.538	1.4273	3.00E-24	2.24E+18

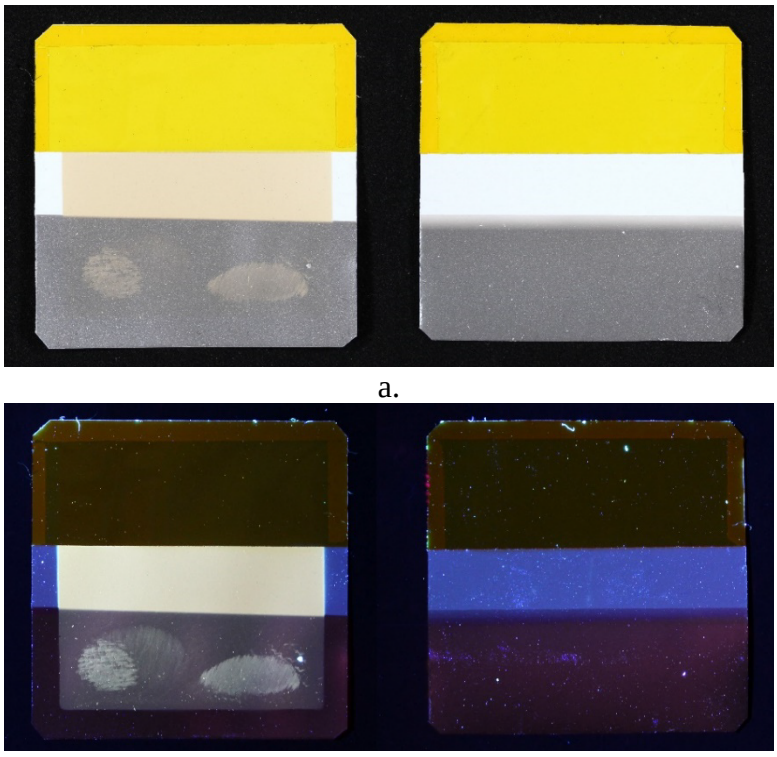

a.

b.

Figure 49. Post-flight photographs of M13W-S1 F (left) and M13W-S1 B (right). (a) Visible light image, and (b) UV light (365 nm) image.

Figure 50 provides post-flight images of the M13Z-S1 F and M13Z-S1 B zenith Photographic AO Fluence Monitors. These samples had a thin layer of carbon (716 Å) along with one layer of 0.38 mil Kapton H, similar to the wake Photographic AO Fluence Monitors. As can be seen in Figure 50a, both the carbon film and the Kapton H layer appears intact in the flight sample (left). The white Tedlar is discolored a brownish color, similar to the MISSE-12 zenith (M12Z-S1 F) samples and a little darker than the MISSE-13 wake (M13W-S1 F) sample. The exposed carbon area appears discolored also. The 365 nm UV light image (Figure 50b) also shows a change in the white Tedlar appearance (brighter), also similar to the M12Z-S1 F and M13W-S1 F samples. It also shows the exposed carbon area is a little brighter than the protected area. As stated previously, the AO fluence for erosion of the 716 Å thick carbon film would be 1.73×10^{19} atoms/cm^2. So, the AO fluence for the M13Z-S1 F sample based on visual observations would be $<<1.73 \times 10^{19}$ atoms/cm^2. The AO fluence for the MISSE-13 zenith Kapton H witness sample (M13Z-C1 F) was 2.24×10^{18} atoms/cm^2, which is consistent.

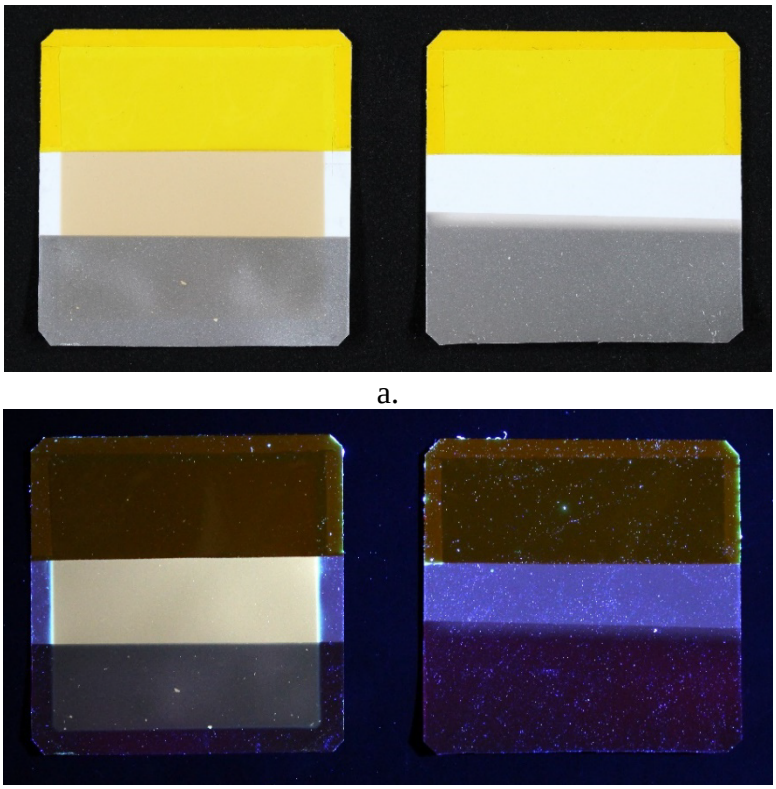

a.

b.

Figure 50. Post-flight photographs of M13Z-S1 F (left) and M13Z-S1 B (right). (a) Visible light image, and (b) UV light (365 nm) image.

Because the white Tedlar material in several of the PCE mission wake and zenith Photographic AO Fluence Monitors discolored significantly, the center white Tedlar section of the M13Z-S1 F flight and M13Z-S1 B control samples was analyzed using X-ray Photoelectron Spectroscopy (XPS). X-ray Photoelectron Spectroscopy is a surface sensitive technique that allows for the identification and quantification of elements and trace contaminants found on a surface. The XPS measurements were performed on a PHI 5000 Versaprobe (ULVAC-PHI) using monochromatic microfocused Al x-rays (200 µm, 50 W) with a photoelectron takeoff angle of 45°. Survey scans using a 117.4 eV pass energy were initially taken to identify all components, followed by higher resolution individual region scans using a pass energy of 93.9 eV. Atomic concentrations were calculated based on the individual peaks. Sputtering was then done on each sample using a 3 kV Ar+ beam to remove 10 nm of material. For the control samples, this was done to remove any adventitious carbon that comes from normal air exposure. For both the flight and control samples, sputtering was also done in one minute increments (removing 10 nm) until a clean substrate surface was obtained. This way it was possible to determine the thickness of the contamination layer on the flight exposed surfaces.

Table 11 provides the XPS atomic concentrations (at.%) for the M13Z-S1 F (flight) and M13Z-S1 B (control) samples. Figure 51 provides the XPS binding energy graphs for the M13Z-S1 F (blue line) and M13Z-S1 B sample (red line). The XPS data indicates several

chemistry changes to the flight sample. Most notable are the decrease in F (22.8 to 3 at.%) and increase in O (7.3 to 31.8 at.%), indicating oxidation of the white Tedlar material, which is crystalline polyvinyl fluoride (PVF) with white pigment (TiO_2). The other notable change is the presence of Si (3.5 at.%) on the flight sample, indicating silicone contamination. There is a very small amount of Si present on the control sample (0.2 at.% after 1 minute of ion sputtering). The sputter data indicates that the oxidized Si layer is still present on the flight sample after 50 nm of ion sputtering.

Table 11. XPS Atomic Concentrations Data for
MISSE-13 Zenith Photographic AO Fluence Monitors

MISSE-13	Material	Atomic Concentrations (at.%)										
		C	O	F	Si	Ca	Zn	Ba	N	Ti	Al	Sn
M13Z-S1-B (Control) AO Photo Monitor	Tedlar - white	68.5	7.3	22.8		0.2			1			
Sput 1 min (10 nm)		83.1	3	13	0.2	0.3	0.2	<0.1	0.1		0.1	
M13Z-S1-F (Flight) AO Photo Monitor	Tedlar - white	**58.3**	**31.8**	**3**	**3.5**	**0.7**	0.4	0.1	1.5	<0.1	0.4	0.3
Sput 1 min (10 nm)		80.6	10	4.7	1.7	1.1	0.3	0.2	0.6	0.1	0.7	0.1
Sput 2 min (20 nm)		82.2	9	5	1.2	1.1	0.2	0.2	0.2	0.2	0.6	0.1
Sput 5 min (50 nm)		84.8	6.8	5.2	0.9	1.1	0.1	0.1		0.6	0.4	

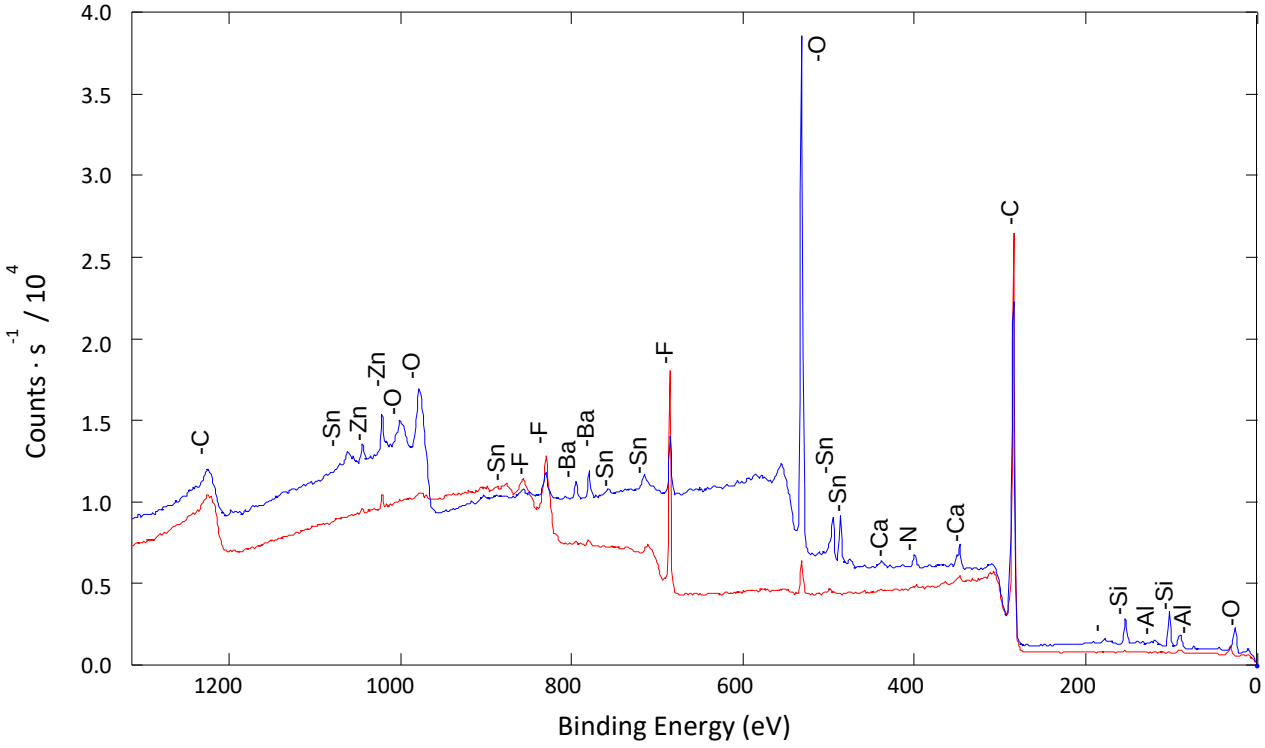

Figure 51. XPS binding energy graphs for M13Z-S1 F (blue line) and M13Z-S1 B control sample (red line).

Table 12. MISSE-13 PCE-4 Photographic AO Fluence Monitors

Flight Orientation	MISSE-FF Sample ID	Material	Material and Thickness Analyzed	LEO AO E_y (cm^3/atom)	MISSE-13 AO Fluence (atoms/cm^2)
Wake	M13W-S1 F	AO Photo Monitor (Single 0.3 mil Kapton H)	716 Å Carbon	4.15E-25*	<<1.73E+19
Zenith	M13Z-S1 F	AO Photo Monitor (Single 0.3 mil Kapton H)	716 Å Carbon	4.15E-25*	<<1.73E+19

**E_y for carbon based on MISSE-2 pyrolytic graphite (PG) E_y*[2,17]

Silicone contamination can be a serious spacecraft concern as the silicone contamination can be oxidized and fixed on a spacecraft surface with AO exposure and then darkened with UV radiation. Examples of brown silicone contamination on white spacecraft components on the Russian space station Mir has been reported by de Groh.[35] Additional discussion on silicone contamination of these flight samples is provided in the *Contamination Samples* section below.

Table 12 provides a list of the MISSE-13 PCE-4 Photographic AO Fluence Monitors along with the sample material and thickness (716 Å carbon) used to compute AO fluence, the MISSE 2 carbon LEO E_y, and the computed MISSE-13 AO fluences.

9.5 MISSE-12 and MISSE-15 PCE-3 Wake

One Kapton H AO fluence witness samples was flown as part of the MISSE-12 PCE-3 in the wake direction: M12W-C1 F. The PCE-3 also included one wake Photographic AO Fluence Monitor: M12W-S11 F. These samples, along with all the PCE-3 wake samples (42 in total), were re-flown and exposed to the LEO wake space environment during the MISSE-15 mission.

9.5.1 Kapton H AO Fluence Witness Sample

Figure 52 provides post-flight photographs of the PCE-3 wake M12W-C1 F (flight) and M12W-C1 B (control) samples. Figure 52a shows the samples on a white background. Figure 52b shows the samples on a dark background (M12W-C1 F on the left and M12W-C1 B on the right). And, Figure 52c shows the samples under UV light. There was no visible erosion or texturing of the flight sample, although the exposed area looks very slightly brighter in the visible light image, shown in Figure 52a, and barely noticeable in the image on the dark background (Figure 52b). Under 365 nm UV light, and with enhanced image brightness, the space exposed area of the flight sample is barely enhanced as shown in Figure 52c.

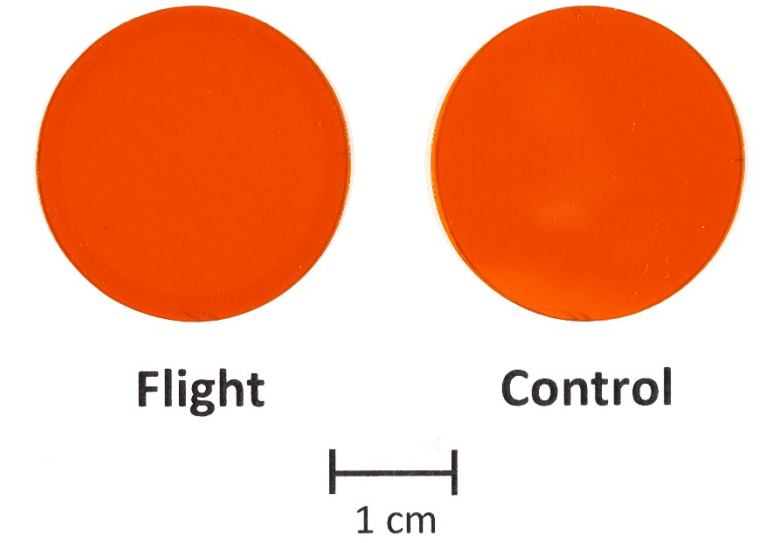

a.

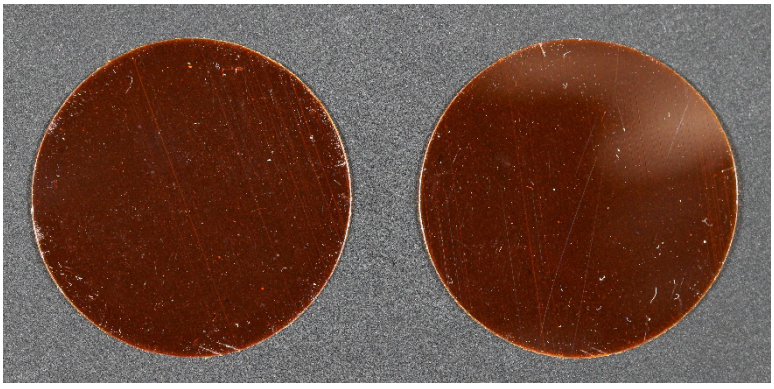

b.

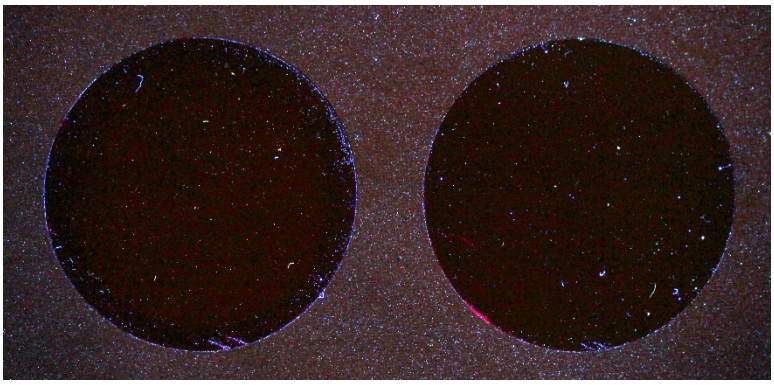

c.

Figure 52. Post-flight photographs of M12W-C1 F and M12W-C1 B. (a) Samples on a white background, (b) Visible light image of samples on a dark background (M12W-C1 F on the left and M12W-C1 B on the right), and (c) UV light (365 nm) image with M12W-C1 F on the left and M12W-C1 B on the right.

Table 13. MISSE-15 PCE-3 Wake Kapton H AO Fluence Witness Sample

Flight Orientation	Sample ID	Thickness (inch)	Mass Loss (g)	Surface Area (cm^2)	Density (g/cm^3)	LEO AO E_y (cm^3/atom)	MISSE-15 AO Fluence (atoms/cm^2)
Wake	M12W-C1 F	0.005	0.000073	3.573	1.4273	3.00E-24	4.77E+18

Table 13 provides the MISSE-15 PCE-3 wake Kapton H AO Fluence Witness sample AO fluence value. The table includes the sample film thickness, dehydrated sample mass loss, LEO exposed surface area, Kapton H density and LEO E_y, and the computed MISSE-15 wake AO fluence. Some mass loss (0.073 mg) was detected for the sample, indicating that the sample received some AO exposure. The AO fluence is very low (4.77×10^{18} atoms/cm^2) and it is possible this was the result of scattered AO from neighboring ISS payloads.

9.5.2 Photographic AO Fluence Monitor

Figure 53 provides post-flight images of the M12W-S11 F Photographic AO Fluence Monitor sample. This sample had a thin layer of carbon (780 Å) along with three layers of 0.38 mil Kapton H. As can be seen in Figure 53a and 53b, both the carbon film and the 1st layer of Kapton H appear intact. The most noticeable change is discoloration of the white Tedlar in the exposed region, similar to other wake and zenith samples. Also, the carbon area is very slightly discolored. The 365 nm UV light image (Figure 53c) also shows both the exposed white Tedlar and carbon areas to be brighter than the protected areas. The AO fluence for erosion of the 780 Å thick carbon film would be 1.88×10^{19} atoms/cm^2. So, the AO fluence based on visual observations would be $<<1.88 \times 10^{19}$ atoms/cm^2.

Table 14 provides the MISSE-15 PCE-3 wake Photographic AO Fluence Monitor values. The table includes the sample material and thickness (780 Å carbon) used to compute AO fluence, the MISSE 2 carbon LEO E_y, and the computed MISSE-15 wake AO fluence.

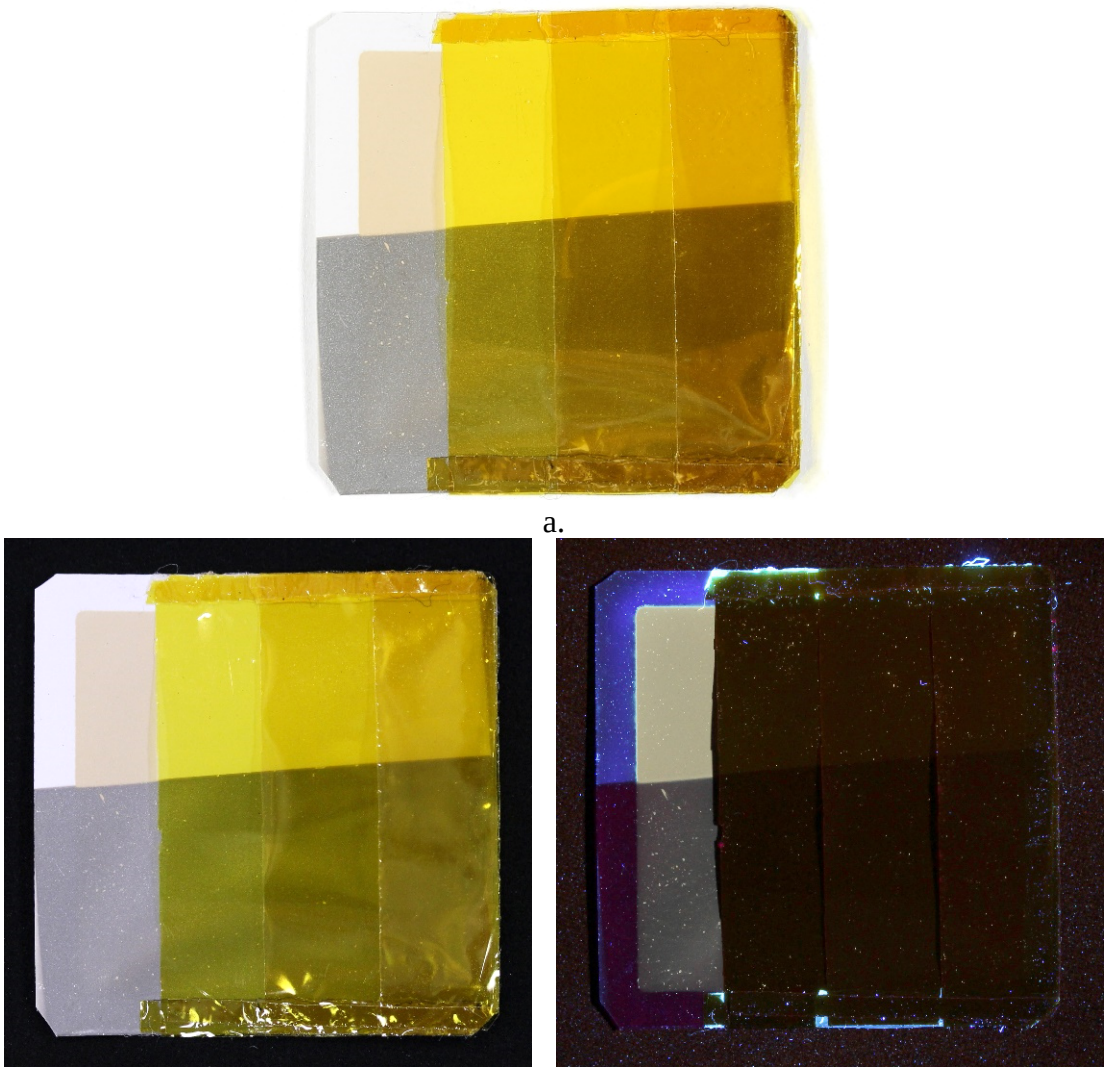

a. b. c.

Figure 53. Post-flight photographs of M1W-S11 F. (a) Visible light image with a white background, (b) Visible light image with a dark background, and (c) UV light (365 nm) image.

Table 14. MISSE-15 PCE-3 Wake Photographic AO Fluence Monitor

Flight Orientation	**MISSE-FF Sample ID**	**Material**	**Material and Thickness Analyzed**	**LEO AO E_y (cm^3/atom)**	**MISSE-15 AO Fluence (atoms/cm^2)**
Wake	M12W-S11 F	AO Photo Monitor (0.3 mil Kapton H)	780 Å Carbon	4.15E-25*	<<1.88E+19

**E_y for carbon based on MISSE-2 pyrolytic graphite (PG) E_y[2,17]*

10.0 Solar Exposure

Ultraviolet (UV) radiation sensors were flown by Aegis Aerospace as part of the MISSE-FF environmental sensor suite on each MSC so that UV Equivalent Sun Hours (ESH) exposure could be determined for each MSC. The UV sensor would, theoretically, detect periods of shadow and the effect of the solar angle on mission ESH. The UV sensors gather data when powered. The MSC decks had periods of time where the MSC was open and exposed to sunlight in the space environment, but the MSC was unpowered. In addition, other factors such as occasional communication outages also affected the availability of UV sensor data. Therefore, the total ESH for the PCE 1-4 MSCs was calculated from available UV sensor data in combination with data about MSC open/close periods.

The PCE 1-4 ESH data is provided in Table 15. These full mission ESH values were computed by Allison Goode and provided in the Aegis Aerospace "MISSE MSC UV Equivalent Sun Hours Calculation" report (MEMO-MISSE-0004 Rev C03, August 17, 2022).[36] The UV ESH was calculated by first determining a by-face exposure rate (provided in Table 16). The rate was then multiplied by the total MSC open time for the PCE 1-4 MSCs to obtain ESH for each carrier. The mission data from the MISSE-10 nadir (M10N3), MISSE-14 ram (M14R2), MISSE-14 zenith (M14Z2) and MISSE-14 wake (M14W1) MSCs were used to generate the by-face exposure rates provided in Table 16. Additional details on the ESH calculations are found in the Aegis Aerospace ESH report.[36]

Table 15. PCE 1-4 Computed Full Mission ESH[36]

MISSE-FF Expt.	Flight Direction	MISSE Sample Carrier (MSC)	Direct Space Exposure Duration (Years Open)	Full Mission ESH
MISSE-9 PCE-1	Ram	R2 (MSC 3) MS	0.77	952.3
	Wake	W3 (MSC 8) MS	0.54	634.6
	Zenith	Z3 (MSC 5) MS	0.54	555.7
MISSE-10 PCE-2	Ram	R1 (MSC 11) MS	1.17	1445.4
	Zenith	Z2 (MSC 10) MS	0.69	702.0
	Nadir	N3 (MSC 13) MS	0.48	102.3
MISSE-12 PCE-3	Ram	R2 (MSC 4) SS	0.89	1104.0
	Wake	W3 (MSC 6) MS	0	0
	Zenith	Z1 (MSC 18) MS	0.45	465.4
MISSE-13 PCE-4	Wake	W1 (MSC 5) MS & SS	0.44	515.6
	Zenith	Z2 (MSC 19) MS	0.46	467.9
MISSE-15 PCE-3 Wake Re-flight	Wake	W1 (MSC 10) MS	0.44	511.7

Table 16. ESH Rates by Face[36]

Face	ESH/ Hour Open	ESH/ Year Open
Ram	0.1414	1239.1
Wake	0.1335	1170.6
Zenith	0.1168	1024.2
Nadir	0.0245	214.7

11.0 On-Orbit Temperatures

Each of the MISSE-FF MSCs are equipped with temperature sensors that measure the anodized aluminum deck on-orbit. Under ideal circumstances, the MSC temperature was measured daily at 1 second intervals. A significant amount of temperature data is available for the MISSE-9 MSCs, the MISSE-10 ram and nadir MSCs, the MISSE-12 ram and zenith MSCs, and the MISSE-15 wake MSC. Limited data is available for the other MSCs. No data is available for the MISSE-12 wake MSC. Typical temperature ranges for the MISSE-FF MSCs are listed below.

- Ram: -30 to 45 °C
- Zenith: -20 to 50 °C
- Wake: -26 to 45 °C
- Nadir: -7 to 40 °C

These ranges were provided by Aegis Aerospace.[37] The temperatures can vary during each mission depending on the Sun's Beta angle and ISS orientation. It should also be noted that all MSC decks loaded with flight samples underwent a pre-flight thermal vacuum bake-out at Aegis Aerospace. The thermal vacuum bake-out was conducted at 60 °C for 24 hours while under vacuum (approximately 3×10^{-5} torr).

12.0 PCE 1-4 Environmental Exposure Summary

Table 17 provides the mission environmental exposure summary table for the PCE 1-4 experiment samples. The table provides the MISSE mission, specific experiment, on-orbit flight direction (also referred to as flight orientation), MSC details including mount or swing side deck, launch and return missions, and the dates of MSC installation onto the MISSE-FF along with the MSC retrieval dates from the MISSE-FF. The table also provides for each MSC the direct space vacuum duration, direct space exposure duration (total time the MSC was open and exposed to the space environment), the computed AO fluence and the Aegis Aerospace provided total mission ESH. As discussed in the sections above, the AO fluence reported for each MSC was computed from Kapton H AO Fluence Witness sample dehydrated mass loss, except for MISSE-12 zenith where the AO fluence was based on the erosion morphology of the M12Z-S1 F Photographic AO Fluence Monitor.

Table 17. Polymers and Composites Experiment 1-4 (PCE 1-4) Mission Exposure Summary

MISSE Mission and Experiment	Flight Direction	MISSE Sample Carrier (MSC)	Launch Mission	Installed on MISSE-FF	Retrieved from MISSE-FF	Return Mission	Space Vacuum Duration (Years)	Time on MISSE-FF (Years)	Direct Space Exposure Duration (Years)	Atomic Oxygen Fluence (atoms/cm^2)^	Mission Equivalent Sun Hours (ESH)^^
MISSE-9 PCE-1	Ram	R2 (MSC 3) MS	SpaceX-14 April 2, 2018	April 18, 2018	Nov. 11, 2019	SpaceX-19 Jan. 7, 2020	1.59	1.57	0.77	3.44E+20	952.3
	Wake	W3 (MSC 8) MS		April 18, 2018	April 26, 2019	SpaceX-17 June 3, 2019	1.07	1.02	0.54	4.46E+16	634.6
	Zenith	Z3 (MSC 5) MS		April 19, 2018			1.07	1.02	0.54	3.19E+18	555.7
MISSE-10 PCE-2	Ram	R1 (MSC 11) MS	NG-10 Nov. 17, 2018	Jan. 4, 2019	Nov. 25, 2020	SpaceX-21 Jan. 13, 2021*	1.93	1.90	1.17	3.93E+20	1445.4
	Zenith	Z2 (MSC 10) MS			March 18, 2020	SpaceX-20 April 7, 2020	1.25	1.20	0.69	4.84E+18	702.0
	Nadir	N3 (MSC 13) MS					1.25	1.20	0.48	6.94E+18	102.3
MISSE-12 PCE-3	Ram	R2 (MSC 4) SS	NG-12 Nov. 2, 2019	Nov. 11, 2019	Nov. 25, 2020	SpaceX-21 Jan. 13, 2021*	1.07	1.04	0.89	2.97E+20	1104.0
	Wake	W3 (MSC 6) MS			Nov. 27, 2020		1.07	1.05	0**	0	0
	Zenith	Z1 (MSC 18) MS			Nov. 26, 2020		1.07	1.05	0.45	*≈1.67E+18*	465.4
MISSE-13 PCE-4	Wake	W1 (MSC 5) MS/SS	SpaceX-20 March 6, 2020	March 18, 2020	Nov. 27, 2020	SpaceX-21 Jan. 13, 2021*	0.72	0.70	0.44	2.65E+18	515.6
	Zenith	Z2 (MSC 19) MS			Nov. 26, 2020		0.72	0.70	0.46	2.24E+18	467.9
MISSE-15 PCE-3 Wake Re-flight**	Wake	W1 (MSC 10) MS	SpaceX-23 Aug. 29, 2021	Dec. 28, 2021	Aug. 2, 2022	SpaceX-25 Aug. 20, 2022	0.71	0.60	0.44	4.77E+18	511.7

MS: Mount side deck; SS: Swing side deck

*January 13, 2021 EST (January 14, 2021 UTC)

**The PCE-3 wake samples were re-flown as part of the MISSE-15 mission

^ AO fluence was computed from dehydrated Kapton H mass loss, except for MISSE-12 zenith which was based on erosion morphology of the M12Z-S1 Photographic AO Fluence Monitor

^^ Mission Equivalent Sun Hours (ESH) from Aegis Aerospace's "MISSE MSC UV Equivalent Sun Hours Calculation" Report (A. Goode, MEMO-MISSE-0004 Rev C03, August 17, 2022)

13.0 Contamination Samples

Each of the PCE 1-4 experiments included passive contamination witness samples in each flight direction for post-flight molecular contamination and optical property analyses. A total of 13 contamination flight samples were flown. The post-flight analyses of the PCE 1-4 contamination samples included X-ray Photoelectron Spectroscopy (XPS) analyses (surface and ion sputter depth analyses) and optical properties (total reflectance, total transmittance and solar absorptance) of flight and corresponding control samples. The majority of the contamination samples were alumina (sapphire) slides (Al_2O_3) as alumina does not erode with AO exposure and silicone contamination can be detected. A NiTi shape memory alloy (SMA) sample was used for XPS analyses for the MISSE-12 zenith direction. Back-surface aluminized-Teflon fluorinated ethylene propylene (FEP/Al) samples were used for contamination detection for the MISSE-13 mission. Details on the contamination witness samples along with all the XPS and optical property procedures and results are provided by de Groh in Reference 38.

As stated previously, one of the more serious on-orbit contamination concerns is silicone contamination. Silicones are used as adhesives, potting compounds and lubricants in various spacecraft components, such as solar cell adhesives. Although spacecraft designers generally use silicones that meet outgas requirements, silicone fragments can still be evolved in the vacuum environment in LEO and the process is enhanced with AO and/or radiation-induced bond breaking.[6] Silicone fragments that deposit on surfaces with accompanying AO exposure are oxidized, lose hydrocarbons, and convert to a hardened, often crazed, silica-based oxide layer.[39,40] In addition, UV can react with silicone fragments causing a polymerized contaminant layer to build up. If the silicone deposition is also accompanied by hydrocarbon deposition, a much more optically absorbing coating can result.[6] Examples of darkened silicone contamination have been reported on the Long Duration Exposure Facility,[41] the Russian space station Mir[35] and the ISS.

Table 18 provides the surface Si atomic concentrations (at.%) for the PCE 1-4 contamination witness samples.[38] The Si atomic concentration varied from 1.5 to 15.1 at.%. None of the corresponding control samples had any detectable Si, with the exception of M10N-C5 B (Al_2O_3) which had <0.1 at.% Si. The higher levels of Si contamination could certainly impact the erosion and other properties of the MISSE spaceflight samples. The MISSE-12 and MISSE-12/MISSE-15 missions appear to have received significant amounts of Si (15.1 at.% for ram and wake directions).

It is difficult to know for sure if the silicone contamination occurred on the ground prior to flight (i.e., during pre-flight vacuum back-out) or while on-orbit. The PCE 1-4 contamination samples indicate that Si molecular contamination occurred on-orbit because all missions have some level of Si contamination. There is also some consistency for each mission between the varying direct exposure durations and the amount of Si, which would also indicate on-orbit contamination. The exceptions are for MISSE-10 nadir (which is close to other ISS components and had a high Si atomic % for the duration) and the re-flown MISSE-12/MISSE-15 samples.

Table 18. Silicon Atomic Concentrations for the PCE 1-4 Contamination Witness Samples[38]

Sample ID	Flight Orientation	Material	Time on MISSE-FF (Years)	Direct Space Exposure Duration (Years)	Si Atomic Concentration (at.%)
MISSE-9					
M9R-C6-F	Ram	Al_2O_3	1.57	0.77	6.0
M9W-C3-F	Wake	Al_2O_3	1.02	0.54	1.7
M9Z-C3-F	Zenith	Al_2O_3	1.02	0.54	1.5
MISSE-10					
M10R-C4 F	Ram	Al_2O_3	1.9	1.17	8.4
M10Z-C5 F	Zenith	Al_2O_3	1.2	0.69	6.6
M10N-C5 F	Nadir	Al_2O_3	1.2	0.48	8.1
MISSE-12					
M12R-C3 F	Ram	Al_2O_3	1.04	0.89	15.1
M12W-C3 F	Wake	Al_2O_3	1.05	0*	N/A
M12Z-S2 F	Zenith	NiTi	1.05	0.45	6.2
MISSE-13					
M13W-C4 F	Wake	FEP/Al	0.7	0.44	1.6
M13Z-C4 F	Zenith	FEP/Al	0.7	0.46	2.2
MISSE-12 & MISSE-15 Re-flight*					
M12W-C3 F	Wake	Al_2O_3	1.05 + 0.6	0.44	15.1

14.0 Discussion

The AO ram fluence for the MISSE-FF missions is low as compared to the MISSE 1-8 missions of equivalent space exposure duration. Tables 19 and 20 provide the average ram AO fluence per year for the MISSE 2-8 missions, and the MISSE-9, -10 and -12 missions, respectively. As can be seen, the average ram AO fluence per year for the MISSE 2-8 missions ranges from 1.36 to 2.83×10^{21} atoms/cm^2, while the average ram AO fluence per year for the MISSE-9, -10 and -12 missions ranges from 3.34 to 4.46×10^{20} atoms/cm^2. Thus, the MISSE 2-8 missions received 3.0 to 8.5X the ram AO fluence for an equivalent exposure duration as the MISSE 9-12 missions.

Table 19. Average Ram AO Fluence per Year for the MISSE 2-8 missions

MISSE Mission	Space Exposure Duration	Direct Space Exposure Duration (Years)	AO Fluence (atoms/cm^2)	AO Fluence/ Exposure Duration (atoms/cm^2/year)	Si Atomic Concentration (at.%)	Solar Cycle
MISSE 2 Ram*	8/16/2001 - 7/30/2005	3.95	8.43E+21	2.13E+21*	5.4-5.5[19]	Solar max & decreasing
MISSE 4 Ram*	8/3/2006 - 8/18/2007	1.04	2.15E+21	2.07E+21*	-	Nearing solar min
MISSE 6 Ram^	3/22/2008 - 9/1/2009	1.45	1.97E+21	1.36E+21^	-	Solar min
MISSE 7 Ram	11/23/2009 - 5/20/2011	1.49	4.22E+21	2.83E+21	-	Increasing to solar max
MISSE 8 Ram	7/12/2011 - 7/9/2013	2.00	4.62E+21	2.31E+21	-	Solar max

* Quest Airlock
^ Columbus Laboratory

Table 20. Average Ram AO Fluence per Year for the MISSE-9, -10 and -12 missions

MISSE-FF Expt.	Space Exposure Duration	Direct Space Exposure Duration (Years)	AO Fluence (atoms/cm^2)	AO Fluence/ Exposure Duration (atoms/cm^2/year)	Si Atomic Concentration (at.%)	Solar Cycle
MISSE-9 Ram	4/19/2018 - 10/2/2019	0.77	3.44E+20	4.46E+20	6.0	Solar min
MISSE-10 Ram	4/26/2019 - 11/25/2020	1.17	3.93E+20	3.36E+20	8.4	Solar min & increasing
MISSE-12 Ram	12/3/2019 - 11/25/2020	0.89	2.97E+20	3.34E+20	15.1	Solar min & increasing

One of the contributing factors to the AO fluence is the variation in AO flux with the 11-year solar cycle. Figure 54 provides solar cycle sunspot numbers from 1996 to 2023.[42] Figure 55 shows the effect of the 11-year solar cycle on yearly AO fluence from 2015 to 2026.[2] As shown in Figure 55, for the time period shown the AO fluence per year can vary up to 4.7X from solar max (3.27×10^{21} atoms/cm^{21}) to solar min (6.97×10^{20} atoms/cm^{2}). Thus, the solar cycle could account for some of the difference in AO fluence for the MISSE 2-8 missions as compared to the MISSE 9-12 missions. The MISSE-9, MISSE-10 and MISSE-12 missions (April 2018 to November 2020) were during low sunspot periods (i.e., solar min), and hence the low AO fluence portion of the solar cycle. The MISSE mission durations have been added to the solar cycle graph shown in Figure 54. The MISSE-2, MISSE-7, and MISSE-8 missions occurred during higher solar activity including solar max periods.

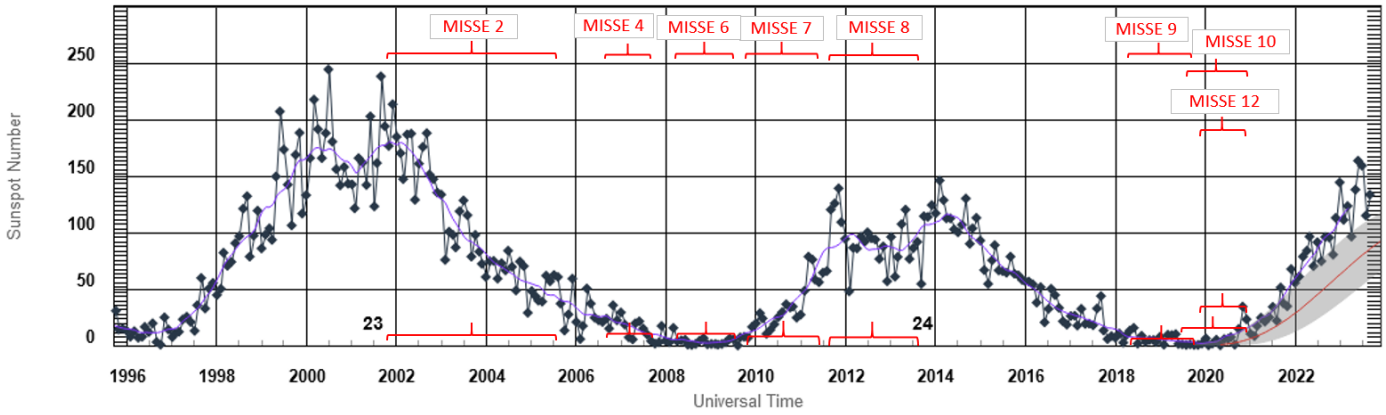

Figure 54. International Space Environmental Services (ISES) Solar Cycle Sunspot Number Progression.[42]

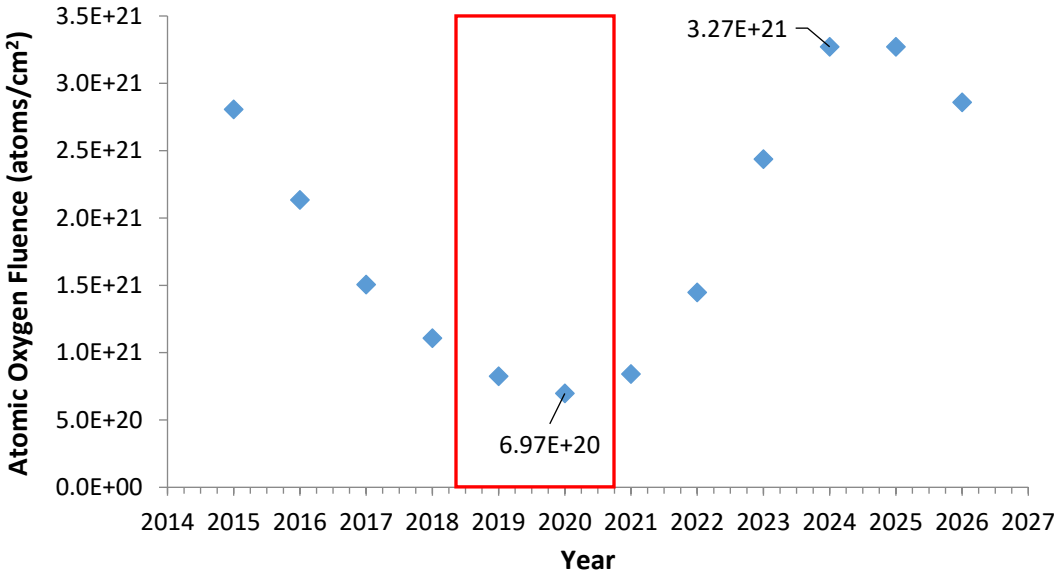

Figure 55. Atomic oxygen fluence per year based on the 11-year solar cycle. The red box highlights the MISSE-9 and MISSE-10 mission (April 2018 to November 2020).[2]

The MISSE-4 and MISSE-6 missions occurred during solar min periods, and they still had higher equivalent AO fluence than the MISSE 9-12 missions. The MISSE-4 and MISSE-6 missions (and MISSE 2) were located in different locations on the ISS. The MISSE-4 ram tray was on the Quest Airlock and the MISSE-6 ram tray was on the ISS Columbus Laboratory. So, perhaps the ISS location contributed to the AO fluence variation. The MISSE-7 and MISSE-8 missions were located in the same ELC-2 Site 3 location on ISS as the MISSE-FF.[10,16] Thus, for similar ISS locations, the AO fluence ratios vary from 5.2X to 8.5X. The majority of the difference is likely the effect of the 11-year solar cycle.

An additional factor that would impact the AO fluence is the MISSE-FF 8° "pitch up" rotation. With this facility rotation, the ram surface is off-set 8° from true ram. An 8° off-set from the ram direction would result is a slightly lower AO flux, which is estimated to be 0.99% of the direct ram flux.[2] This is only a small difference in the AO flux and hence AO fluence, but is worth noting.

Another potential contributor to a lower AO fluence for the MISSE-FF missions would be on-orbit contamination effects. Tables 19 and 20 include the atomic concentration of Si, as determined by XPS analyses, and as discussed previously. It is interesting to see for the MISSE-9, MISSE-10 and MISSE-12 missions the higher the Si at.% the lower the average ram AO fluence per year. This data helps to verify that Si contamination can affect the AO fluence. Dever reported XPS analyses for sapphire (Al_2O_3) contamination witness slides for the MISSE-2 mission.[19] The ram samples had 5.4 to 5.5 at.% of Si on the surface. Thus, the MISSE-2 mission has somewhat lower Si contamination than the MISSE-9, MISSE-10 and MISSE-12 missions.

The Stratospheric Aerosol and Gas Experiment (SAGE) III is a solar and lunar occultation instrument mounted externally on the ISS measuring Earth's stratospheric ozone, aerosols, water vapor and other trace gases.[43] The SAGE III payload is located on ISS's ELC-4 and is the first instrument on ISS to be built with two Contamination Monitoring Packages (CMPs) to monitor environmental conditions and manage contamination events as they arise.[43] The CMP1 and CMP2 have multiple sensors containing quartz crystals that vibrate at frequencies dependent on the amount of contamination deposited onto them.[43] After more than four years of collecting and studying CMP data, the SAGE III team determined that the ram surface had large amounts of accumulated contamination, as shown in Figure 56.[43] They determine that visiting vehicles have been the largest source of on-orbit contamination.[43] And, the SAGE III team found that Cargo Dragon vehicles consistently had the highest rates of contamination on the CMP sensors that could not be burned off and removed, also known as chemisorption.[43] Thus, it appears accumulated on-orbit contamination is a concern on ISS, and thus the MISSE-FF possibly effecting AO fluence.

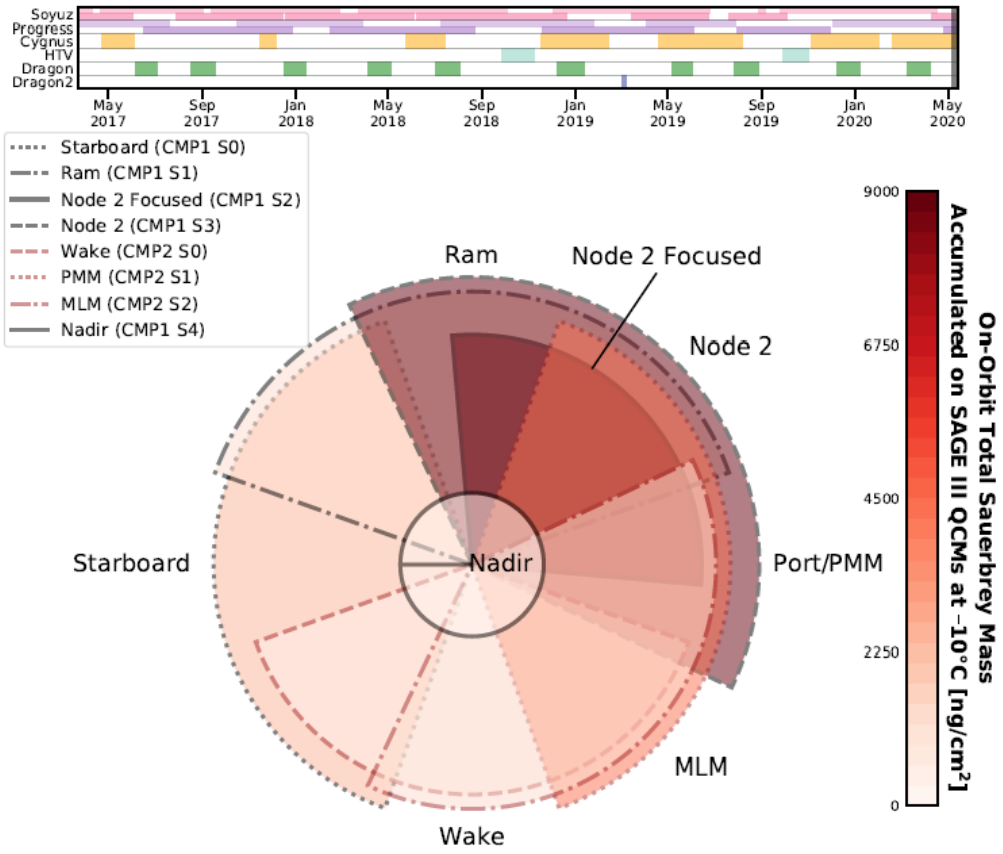

Figure 56. Contamination Deposition Map of the SAGE III Sensors from Reference 43.

15.0 Summary

NASA Glenn Research Center's Polymers and Composites Experiment 1-4 (PCE 1-4) with 365 flight samples have been exposed to the space environment on the ISS's external MISSE-Flight Facility (MISSE-FF). The PCE-1 was flown as part of the MISSE-9 mission, the PCE-2 was flown as part of the MISSE-10 mission, the PCE-3 was flown as part of the MISSE-12 and MISSE-15 missions and the PCE-4 was flown as part of the MISSE-13 mission. This paper provides details on the space environmental exposure of Glenn's PCE 1-4 flight samples, data necessary for the flight experiment data interpretation.

Passive samples were flown in each flight orientation for AO fluence determination and on-orbit contamination analyses. The AO fluence samples included Kapton H samples for dehydrated mass loss based AO fluence and Photographic AO Fluence Monitors that were designed to obtain incremental AO fluence overtime based on on-orbit images. The environment exposure details include the total space vacuum duration, time on the MISSE-FF, the direct space exposure duration, the AO fluence and the computed mission Equivalent Sun Hours (ESH) solar exposure. Typical on-orbit temperatures are also provided along with a summary of analyses of PCE 1-4 contamination witness samples. In addition, the AO fluence values are compared with the prior MISSE missions.

The PCE 1-4 samples direct space exposure durations were substantially less than the time on the MISSE-FF. This is due to numerous MSC closures, in an effort to prevent contamination during visiting vehicles and EVAs and for "exposure protection" for ISS flight configuration changes. Depending on the MISSE mission and specific MSC, the time on the MISSE-FF ranged from 0.60 to 1.90 years, while the direct space exposure ranged from 0.44 to 1.17 years. The estimated solar exposure ranged from 102.3 ESH for the MISSE-10 nadir samples (0.48 years of direct space exposure) to 1445.5 ESH for the MISSE-10 ram samples with the longest direct space exposure duration (1.17 years). The AO fluence varied substantially with flight orientation, with the ram surfaces receiving the highest AO fluence as expected. The ram AO fluence ranged from 2.97×10^{20} atoms/cm^2 for the MISSE-12 ram samples (0.89 years of direct space exposure) to 3.93×10^{20} atoms/cm^2 for the MISSE-10 ram samples (1.17 years of direct space exposure). Also as expected, the wake and zenith samples received essentially no AO (4.46×10^{16} atoms/cm^2 for the MISSE-9 wake samples) or very small amounts of AO (1.67 to 6.94×10^{18} atoms/cm^2). Because of the 8° pitch-up off-set of the MISSE-FF, the MISSE-10 nadir samples received a slightly higher AO fluence (6.94×10^{18} atoms/cm^2) than the MISSE-10 zenith samples with the same exposure duration (4.84×10^{18} atoms/cm^2).

The ram AO fluence for the MISSE-FF missions was found to be low as compared to the MISSE 1-8 missions of equivalent space exposure duration. One significant contributing factor to the AO fluence is the variation in AO flux with the 11-year solar cycle. Another factor could be the difference in the ISS location for some of the MISSE missions. In addition, the PCE 1-4 contamination sample data indicates that molecular contamination may also have had some level of impact on the AO fluence for some the MISSE-FF MSCs.

References

1. Dickerson, R.E., Gray, H.B., and Haight, G P., *Chemical Principles 3rd Edition*. Menlo Park, CA, Benjamin Cummings Publishing Co. Inc. p. 457, 1979.
2. de Groh, K.K., Banks, B.A. and McCarthy, C.E., Spacecraft Polymers Atomic Oxygen Durability Handbook, NASA–HDBK–6024, Revalidated: 2022-12-16.
3. National Aeronautics and Space Administration: U.S. Standard Atmosphere, 1976. NASA TM–X–74335, 1976.
4. Gregory, J.C., "Interaction of Hyperthermal Atoms on Surfaces in Orbit: The University of Alabama Experiment," David E. Brinza, Ed., *Proceedings of the NASA Workshop on Atomic Oxygen Effects, Nov. 10–11, 1986*. JPL 87–14, pp. 29–30.
5. Dever, J.A., "Low Earth Orbital Atomic Oxygen and Ultraviolet Radiation Effects on Polymers," NASA TM 103711, February 1991.
6. de Groh, K.K., Banks, B.A., Miller, S.K.R., and Dever, J.A., Degradation of Spacecraft Materials (Chapter 28), Handbook of Environmental Degradation of Materials, Myer Kutz (editor), William Andrew Publishing, pp. 601–645, 2018.
7. O'Neal, R.L., Levine, A.S. and Kiser, C.C., *Photographic Survey of the LDEF Mission*. NASA SP-531. NASA LaRC: Hampton, VA (1996).

8. de Groh, K. K., “Materials Spaceflight Experiments,” Encyclopedia of Aerospace Engineering, R. Blockley and W. Shyy (eds). John Wiley & Sons Ltd, Chichester, UK, pp. 2535–2552 (2010).
9. American Society for Testing and Materials: 2000 ASTM Standard Extraterrestrial Spectrum Reference E–490–00, 2000. (https://www.nrel.gov/grid/solar-resource/spectra-astm-e490.html)
10. de Groh, K. K., Banks, B. A., Yi, G. T., Haloua, A., Imka, E. C., Mitchell, G. G., Asmar, O. C., Leneghan, H.A. and Sechkar, E. A., “Erosion Results of the MISSE 7 Polymers Experiment and Zenith Polymers Experiment After 1.5 Years of Space Exposure,” NASA-TM-2016-219167 (March 2017)
11. Hansen, P. A., Townsend, J. A., Yoshikawa, Y., Castro, D. J., Triolo, J. J., and Peters, W. C., SAMPE International Symposium, 43, (1998) 570.
12. Townsend, J. A., Hansen, P. A., Dever, J. A., de Groh, K. K., Banks, B. A., Wang, L., and He, C. C., “Hubble Space Telescope Metallized Teflon FEP Thermal Control Materials: On-Orbit Degradation and Post-Retrieval Analysis,” *High Performance Polymers 11 (1999) 81–99.*
13. de Groh, K. K, Perry, B. A., Mohammed, J. A. and Banks, B.A., “Analyses of Hubble Space Telescope Aluminized-Teflon Multilayer Insulation Blankets Retrieved After 19 Years of Space Exposure,” NASA TM-2015-218476, February 2015.
14. Yang, J. C. and de Groh, K. K., “Materials Issues in the Space Environment,” MRS Bulletin, Vol. 35, January 2010, pp. 12-19.
15. de Groh, K. K., Banks, B. A., Dever, J. A., Jaworske, D. J., Miller, S. K., Sechkar, E. A. and Panko, S. R., “NASA Glenn Research Center’s Materials International Space Station Experiments (MISSE 1-7),” Proceedings of the International Symposium on “SM/MPAC&SEED Experiment,” Tsukuba, Japan, March 10-11, 2008, JAXA-SP-08-015E, March 2009, pp. 91 – 119; also NASA TM-2008-215482, December 2008.
16. de Groh, K. K. and Banks, B. A., “Atomic Oxygen Erosion Data from the MISSE 2-8 Missions,” NASA/TM-2019-219982, May 2019.
17. de Groh, K. K., Banks, B. A., McCarthy, C. E., Rucker, R. N., Roberts L. M. and Berger, L. A., “MISSE 2 PEACE Polymers Atomic Oxygen Erosion Experiment on the International Space Station,” *High Performance Polymers*, 20 (2008) 388–409.
18. de Groh, K. K, Perry, B. A. and Banks, B. A., “Effect of 1.5 Years of Space Exposure on Tensile Properties of Teflon,” Journal of Spacecraft and Rockets (Special Issue on Materials in a Space Environment), Vol. 53., No. 6, November-December 2016, 1002-1011.
19. Dever, J. A., Miller, S. K., Sechkar, E. A. and Wittberg, T. N., “Space Environment Exposure of Polymer Films on the Materials International Space Station Experiment: Results from MISSE 1 and MISSE 2,” *High Performance Polymers*, 20 (2008), pp. 371- 387.
20. Miller, S. K. R. and Dever, J. A., “Materials International Space Station Experiment 5 (MISSE 5) Polymer Film Thermal Control Experiment”, *Journal of Spacecraft and Rockets*, Volume 48, No. 2., March-April 2011. pp 240-245.
21. de Groh, K. K. and Banks, B. A., “MISSE-Flight Facility Polymers and Composites Experiment 1-4 (PCE 1-4),” NASA TM-20205008863 (February 2021).

22. de Groh, K. K., Banks, B. A. and Demko, R., "Techniques for Measuring Low Earth Orbital Atomic Oxygen Erosion of Polymers," Proceedings of the SAMPE 2002 Conference, Long Beach, CA May 6-10, 2002, pp. 1279-1292; also NASA TM-2002-211479, March 2002.
23. Banks, B. A., Mirtich, M. J., Rutledge, S. K., and Swec, D. M., "Sputtered Coatings for Protection of Spacecraft Polymers," *Thin Solid Films*, vol. 127, 1985, pp. 107–114; also NASA TM–83706, 1984.
24. Visentine, J. T., Leger, L. J., Kuminecz, J. F. and Spiker, I. K., "STS–8 Atomic Oxygen Effects Experiment," AIAA-85-0415, 1985.
25. Koontz, S. L., Lubert, J. L., Visentine, J. T., Hunton, D. E., Cross, J. B. and Hakes, C. L., "EOIM–III Mass Spectrometry and Polymer Chemistry: STS 46, July–August 1992," *Journal of Spacecraft and Rockets*, Vol. 32, No. 3, 1995, pp. 483–495.
26. Gregory, J. C., "On the Linearity of Fast Atomic Oxygen Effects," NASA CP 3257, 1994, 193-198.
27. Young, P. R., St. Claire, A. K., and Slemp, W. S., "Response of Selected High Performance Polymers Films to LEO Exposure," Technical Proceedings of the 38th International SAMPE Symposium, May 1993, 664-678.
28. Silverman, E. M., "Space Environmental Effects on Spacecraft: LEO Materials Selection Guide," NASA CR–4661, Part 1, August 1995.
29. de Groh, K. K., McCarthy, C. E., Girish, K. M., Banks, B. A., Kaminski, C., Youngstrom, E. E., Lillis, M., Youngstrom, C. A., Hammerstrom, A. M., Hope, S. and Marx, L. M., "Rehydration Data for the Materials International Space Station Experiment (MISSE) Polymer Films," NASA TM-2019-220063, February 2019.
30. Bourassa, R. J. and Gillis, J. R., "Atomic Oxygen Exposure of LDEF Experiment Trays," NASA CR 189627, May 1992
31. U.S. Standard Atmosphere, 1976, NASA-TM-X-74-335 (NOAA NASA, USAF, 1976)
32. de Groh, K. K., Banks, B. A., "MISSE 2 PEACE Polymers Erosion Morphology Studies," Proceedings of the International Symposium on Materials in a Space Environment (ISMSE-11), September 15-18, 2009, Aix-en-Provence, France, 2009.
33. Aegis Aerospace - Commercial Space (2023): https://aegisaero.com/commercial-space-services/.
34. Banks, B. A., de Groh, K. K., Miller, S. K. and D. K. Waters, "Lessons Learned from Atomic Oxygen Interaction with Spacecraft Materials in Low Earth Orbit," Proceedings of the 9th International Conference "Protection of Materials and Structures from Space Environment," (May 19–23, 2008 in Toronto, Canada) Ed. J.I. Kleiman, AIP Conference Proceedings 1087, pp. 312–328, 2009; also NASA/TM—2008-215264, July 2008.
35. de Groh, K. K. and McCue, T. R., "Analyses of Contaminated Solar Array Handrail Samples Retrieved from Mir," Proceedings of the IECEC-99 Conference, August 1999, Vancouver Canada (99IECEC-25, SAE 1999-01-2694); also NASA TM-1999-209399, October 1999.
36. Aegis Aerospace "MISSE MSC UV Equivalent Sun Hours Calculation" Report (A. Goode, MEMO-MISSE-0004 Rev C03, August 17, 2022)
37. Personal Communication with Jeffrey Buell, Aegis Aerospace (May 2023)

38. de Groh, K. K., Lukco, D., Crowell, S. F., Gregor, S. J. and Banks, B.A., “Analyses of the MISSE 9-15 Polymers and Composites Experiment 1-4 (PCE 1-4) Contamination Samples,” NASA TM-20240000941, February 2024.
39. de Groh, K. K. and McCollum, T. A., “Low Earth Orbit Durability of Protected Silicone for Refractive Photovoltaic Concentrator Arrays,” *Journal of Spacecraft and Rockets*, Vol. 32, No. 1, Jan-Feb 1995, pp. 103-109.
40. de Groh, K. K., Banks, B. A. and Ma, D., “Ground-to-Space Effective Atomic Oxygen Fluence Correlation for DC 93-500 Silicone,” *Journal of Spacecraft and Rockets*, Vol. 43, No. 2, March-April 2006, 414-420.
41. Banks, B. A., de Groh, K. K., Rutledge, S. K. and Haytas, C. A., “Consequences of Atomic Oxygen Interaction with Silicones and Silicone Contamination on Surfaces in Low Earth Orbit,” Proceedings of SPIE, Vol. 3784, Rough Surface Scattering and Contamination, 1999; also NASA TM-1999-209179.
42. International Space Environmental Services (ISES) Solar Cycle Sunspot Number Progression (Solar Cycle Progression), Space Weather Prediction Center, National Oceanic and Atmospheric Administration (NOAA). https://www.swpc.noaa.gov/products/solar-cycle-progression (Nov. 2023)
43. Dawson, T. T., Hill, C. A., Rowell, A. F., Leavor, K. R. and Hawley, S.A., “SAGE III/ISS Contamination Monitoring Package: Observations in Orbit,” NASA/TM-20205001963, June 2020.